RIO

PUC

Tese de Doutorado

A Business-Oriented Optimization Model for Low-Voltage Virtual Power Plants Integrating Economic Aspects and Ancillary Services via MINLP

Arthur Massari Filho

Pontifícia Universidade Católica do Rio de Janeiro
Centro Técnico Científico
Departamento de Engenharia Elétrica

Rio de Janeiro, 24 de setembro de 2025

Pontifícia
Universidade
Católica do
Rio de Janeiro

Tese de Doutorado

A Business-Oriented Optimization Model for Low-Voltage Virtual Power Plants Integrating Economic Aspects and Ancillary Services via MINLP

Arthur Massari Filho

Orientação: Delberis Araujo Lima

Tese apresentada como requisito parcial para a obtenção do grau de Doutor em Engenharia Elétrica pelo programa de Pós-Graduação em Engenharia Elétrica, no Departamento Engenharia Elétrica.

Rio de Janeiro, 24 de setembro de 2025

Pontifícia
Universidade
Católica do
Rio de Janeiro

A Business-Oriented Optimization Model for Low-Voltage Virtual Power Plants Integrating Economic Aspects and Ancillary Services via MINLP

Arthur Massari Filho

Tese apresentada como requisito parcial para a obtenção do grau de Doutor em Engenharia Elétrica pelo programa de Pós-Graduação em Engenharia Elétrica, no Departamento Engenharia Elétrica.

Professor Delberis Araujo Lima
Orientador
Departamento de Engenharia Elétrica – PUC-Rio

Professor André Milhorance de Castro
Departamento de Engenharia Elétrica – PUC-Rio

Professora Luana Medeiros Marangon Lima
Marangon Consultoria e Engenharia

Professor Osvaldo Ronald Saavedra Mendez
Universidade Federal do Maranhão

Professor Renan Silva Maciel
Universidade Tecnológica Federal do Paraná

Rio de Janeiro, 24 de setembro de 2025

Pontifícia
Universidade
Católica do
Rio de Janeiro

Arthur Massari Filho

Graduado em Engenharia Elétrica pela Universidade Federal Fluminense (UFF) em 2016. Mestre em Engenharia Elétrica em 2021 pelo programa de pós-graduação em Engenharia Elétrica da Pontifica Universidade Católica do Rio de Janeiro (PUC-Rio).

Ficha Catalográfica

Massari Filho, Arthur

A business-oriented optimization model for low-voltage virtual power plants integrating economic aspects and ancillary services via MINLP / Arthur Massari Filho ; advisor: Delberis Araujo Lima. – 2025.
127 f. : il. color. ; 30 cm

Tese (doutorado)–Pontifícia Universidade Católica do Rio de Janeiro, Departamento de Engenharia Elétrica, 2025.

Inclui bibliografia

1. Engenharia Elétrica – Teses. 2. Usina virtual de energia. 3. Recursos energéticos distribuídos. 4. Sistema de armazenamentos de energia por bateria. 5. Geração distribuída. 6. Modelo de otimização não linear inteira mista. I. Lima, Delberis Araujo. II. Pontifícia Universidade Católica do Rio de Janeiro. Departamento de Engenharia Elétrica. III. Título.

CDD: 621.3

I dedicate this work to my Wife, Mother and Father, with all my love

Acknowledgement

First, I would like to thank God for granting me the strength and perseverance to reach this point.

To my wife, Michele Guarany Guimarães Massari, whose unwavering support and presence have been a constant source of strength through both challenging and joyful moments.

To my mother for always being by my side, giving me all the emotional support I needed to keep going.

To my late father, who nurtured my love for learning and made sure I never went without care, support, or opportunity.

To my advisor, Delberis Lima, whose professional excellence I deeply admire, and whose guidance has been instrumental throughout this journey.

To my lab colleagues, Rafael Saadi, Vanessa Gonzalez, and Karina Mosqueira who accompanied me through every step of the doctoral journey, sharing both insights and laughter.

To all my professors at PUC-Rio, and all the other professors who have ever come into my life, I also thank PUC-Rio for the infrastructure it provided me with to carry out this work.

To all my friends, which provided me with moments of joy, laughter, conversations, and several others of relaxation that helped me to relieve daily stress and make this period less exhausting.

This work was financed in part by the Energisa Group, through the R&D Project ANEEL 2205

This study was financed in part by the Coordenação de Aperfeiçoamento de Pessoal de Nível Superior - Brasil (CAPES) - Finance Code 001.

Abstract

Massari Filho, Arthur; Lima, Delberis Araujo (Advisor). **A Business-Oriented Optimization Model for Low-Voltage Virtual Power Plants Integrating Economic Aspects and Ancillary Services via MINLP.** Rio de Janeiro, 2025. 127p. Tese de Doutorado – Departamento de Engenharia Elétrica, Pontifícia Universidade Católica do Rio de Janeiro.

After the enactment of Law 14,300/2022 in Brazil, which allowed micro and mini generators to be charged for the use of the distribution network, commercial incentives for installing Distributed Energy Resources (DERs) have been significantly reduced. As a result, investors have been seeking alternatives to compensate for these economic losses. In this context, this thesis proposes a transactional energy model that incorporates a Virtual Power Plant (VPP) composed of Photovoltaic (PV), batteries, and hybrid systems (i.e., combinations of PV panels and batteries). The main objective is to assess the efficiency of DERs from a business perspective while addressing technical challenges of distribution networks, including energy losses, voltage regulation, substation peak demand, and transformer lifespan and replacement.

These technical issues are mitigated through optimized control of battery charging/discharging and DER inverter operation. The relationships between DER power injections (active and reactive) and the aforementioned network impacts are linearized for inclusion in a Mixed-Integer Nonlinear Programming (MINLP) model. Simulations were conducted using a real Brazilian distribution network from Energisa Tocantins and results demonstrate the effectiveness of leveraging battery flexibility and reactive power control via DER inverters to optimize both economic and technical outcomes. The model was implemented in Python (v3.9.13) using Pyomo (v6.4.4), with Gurobi (v10.0.1) as the solver and results were validated using OpenDSSDirect (v0.7.0).

Keywords

Virtual Power Plants, Distributed Energy Resources, Battery Energy Storage Systems, Distributed Generation, Mixed Integer Nonlinear Optimization Model

Resumo

Massari Filho, Arthur; Lima, Delberis Araújo. **Um Modelo de Otimização Orientado a Negócios para Usinas Virtuais de Baixa Tensão Integrando Aspectos Econômicos e Serviços Ancilares Através de MINLP,** Rio de Janeiro, 2025. 127p. Tese de Doutorado – Departamento de Engenharia Elétrica, Pontifícia Universidade Católica do Rio de Janeiro.

Após a promulgação da lei 14.300/2022 no Brasil, que permitiu a tarifação do uso da rede de distribuição pelos microgeradores e minigeradores, os incentivos comerciais, para a instalação de recursos energéticos distribuídos (REDs), foram reduzidos. Diante dessa realidade, os investidores têm buscado alternativas para compensar essas perdas econômicas. Nesse contexto, essa tese propõe um modelo energia transacional, que incorpora uma Usina Virtual de Energia (UVE), composta por unidades de painéis fotovoltaicos (UFV), baterias e sistemas híbridos (combinação entre painéis e baterias). O objetivo principal é avaliar a coordenação de REDs para fins comerciais, ao mesmo tempo em que aborda questões técnicas relacionadas à rede elétrica, incluindo perdas elétricas, controle de tensão, redução de demanda na subestação e vida útil do e troca do transformador.

Esses problemas técnicos são mitigados através do controle otimizado do carregamento/descarregamento de baterias e operação dos inversores dos REDs. A relação entre injeção potência (ativa ou reativa) e os impactos acima mencionados são linearizados para serem incluídos no modelo de Programação Não Linear Inteira Mista. As simulações foram conduzidas usina uma rede real brasileira da Energisa Tocantins e os resultados demonstram a eficácia de aproveitar a flexibilidade da bateria e o controle de potência reativa por meio dos inversores dos REDs para otimizar os resultados econômicos e técnicos. O modelo foi implementado no Python (v3.9.13) usando a Pyomo (v6.4.4), com Gurobi (v10.0.1) como o solucionador e os resultados foram validados usando OpenDSSDirect (v0.7.0).

Palavras-chave

Usina Virtual de Energia, Recursos Energéticos Distribuídos, Sistema de Armazenamentos de Energia por Bateria, Geração Distribuída, Modelo de Otimização Não Linear Inteira Mista

Table of Contents

List of Figures

List of Tables

List of Acronyms and Abbreviations

Index

b	Index of DER buses.
d	Index of days.
h	Index of hours.
p	Index of phases.
T	Index of transformer

Sets

B	Set of DER buses.
D	Set of days.
H	Set of hours.
P	Set of phases
TR	Set of transformers

Constants and Data

$\alpha^{+}_{b,h}, \alpha^{-}_{b,h}$	Voltage magnitude sensitivity to active power injection $(+)$ and extraction $(-)$ coefficients at bus b and hour h
$\alpha^{inj}_{kvar,b,h}, \alpha^{ext}_{kvar,b,h}$	Voltage magnitude sensitivity to reactive power capacitive (cap) and inductive (ind) coefficients at bus b and hour h
$a^{L}_{i,b,d,h}, b^{L}_{i,b,d,h}$	Linear coefficients for multilinear contribution of power injection/extraction on bus b for the power loss on day d and hour h
$a^{Xfmr}_{i,T,d,h}, b^{Xfmr}_{i,T,d,h}$	Angular coefficient for determining the variation of power flow in the transformer
α_h	Contract percentage for different on-peak tariffs
β_h	Contract percentage for different off-peak tariffs
BT	DER association parameter with the transformer T
CAP^{Xfmr}_{T}	Transformer maximum capacity (in kVA) for transformer T
$C^{labor}_{T'}$	Labor cost for transformer T'
$C^{equip}_{T'}$	Equipment cost for transformer T'
d^{UD}	Distribution system usage discount rate [%]
DOD_b	Battery Depth of Discharge [%]
DUT	Distribution usage tariff [R$/kW]
E^{bat}_{b}	Battery Energy [kWh]
ef_b	Battery efficiency [%]
$f_{d,h}$	Main substation power import on day d and hour h [kW]
$f^{Xfmr}_{T,d,h}$	Power flow at transformer T, for day d and hour h
$G^{p}_{b,d,\mathrm{h}}$	Photovoltaic energy generated on-peak at bus b, for day d and hour h [pu]
$G^{op}_{b,d,\mathrm{h}}$	Photovoltaic energy generated off-peak at bus b, for day d and hour h [pu]

$G_{b,d,\mathrm{h}}^{mid}$	Photovoltaic energy generated mid-peak at bus b, for day d and hour h [pu]
M	Big-M
n_b^{bess}	Number of BESS installed on bus b
N_f	Number of phases at bus b
P_b^{bess}	Battery Power [kW]
P_b^{PV}	PV system power installed on bus b [kW]
$T_E^{p\,(G)}$	On-peak green energy tariff [R$/kWh]
$T_E^{op\,(G)}$	Off-peak green energy tariff [R$/kWh]
$T_E^{p\,(W)}$	On-peak white energy tariff [R$/kWh]
$T_E^{op\,(W)}$	Off-peak white energy tariff [R$/kWh]
$T_E^{mid\,(W)}$	Mid-peak white energy tariff [R$/kWh]
$T_E^{(C)}$	Conventional energy tariff [R$/kWh]
$V_{b,p,d,h}^0$	Voltage magnitude at bus b and phase p on day d and hour h, without DER installation
V_b^{min}, V_b^{max}	Voltage magnitude minimum and maximum limits for bus b
ΔV	Voltage variation due to power extracion or injection at bus with a DER
V_{base}	Voltage at bus with DER in the base case (without DER operation)
$V_{ext/inj}$	Voltage at bus with DER, corresponding to different power extraction or injection levels
$P_v(hours)$	Loss of transformer lifespan, in percentage
B	Adjusted Arrhenius constant (6,987.15)
A	Empirical constant, which depends on transformers temperature class
$T_e(K)$	Hotspot temperatur of the winding in Kelvin
$S(kW)$	Active power flow through transformer
T_{r_i}	Rated capacity in kVA
T^{max}	Maximum top-oil temperature, depending on transfomer class
V_{DER}	Voltage at the DER-connected bus after the optimization model, in p.u.
ΔV_{exc}	Deviation from theupper or lower voltage limit
ΔQ	Reactive power adjustiment needed to maintain the voltage within prescribed limits
I	Initial investment
CF_n	Cash Flow in year n
k	Discount rate
N	Project lifetime, in years
R_n^a	Revenue or any cost associated with ancillary service
CM	Customer Margin
FR	Frustration Rate
ΔP	Power variation between base case and VPP operation
EI	Eletric Inflation
$NPV_{project}$	Net Present Value for the project

C_{INV}	Initial investment on the project brought to a present value
$R_{annualized}$	Revenue os cost annualized
$R_{dataset}$	Revenue or cost from all days in dataset
$N_{dataset}$	Quantity of days in the dataset

Variables

C_{ϕ}^{p}	Cost of on-peak losses [R$]
C_{ϕ}^{op}	Cost of off-peak losses [R$]
C_{ϕ}^{mid}	Cost of mid-peak losses [R$]
$E_{d,h}^{C(G),p}$	On-peak green tariff energy contracts for day d and hour h [kWh]
$E_{d,h}^{C(W),p}$	On-peak white tariff energy contracts for day d and hour h [kWh]
$E_{d,h}^{C(W),op}$	Off-peak white tariff energy contracts for day d and hour h [kWh]
$E_{d,h}^{C(C),op}$	Off-peak conventional tariff energy contracts for day d and hour h [kWh]
$E_{d,h}^{C(W),mid}$	Mid-peak white tariff energy contracts for day d and hour h [kWh]
$E_{b,d,h}^{G,p}$	On-peak energy credit at bus b, for day d and hour h [kWh]
$E_{b,d,h}^{G,op}$	Off-peak energy credit at bus b, for day d and hour h [kWh]
$E_{b,d,h}^{G,mid}$	Mid-peak energy credit at bus b, for day d and hour h [kWh]
$E_{b,d,h}^{D,p}$	On-peak energy debit at bus b, for day d and hour h [kWh]
$E_{b,d,h}^{D,op}$	Off-peak energy debit at bus b, for day d and hour h [kWh]
$E_{b,d,h}^{D,mid}$	Mid-peak energy debit at bus b, for day d and hour h [kWh]
$P_{b,d,h}$	Net injected power at bus b, day d and hour h
$P_{b,d,h}^{-}$	Consumed power at bus b, day d and hour h
$P_{b,d,h}^{+}$	Injected power at bus b, day d and hour h
$P_{b,d,h}^{L}$	Power loss contribution due to a power injection at bus b, day d and hour h
ΔP^{max}	Demand contract at main substation [kW]
R_{annual}	Annual revenue from all contracts discounting electrical losses and demand contracting at the substation [R$]
R_{E}^{p}	Revenue from on-peak contracts [R$]
R_{E}^{op}	Revenue from off-peak contracts [R$]
R_{E}^{mid}	Revenue from mid-peak contracts [R$]
$V_{b,p,d,h}$	Voltage magnitude at bus b, phase p, day d and hour h
$\gamma_{b,d,h}^{ov}$	Voltage magnitude deviation over maximum limit at bus b, day d and hour h
$\gamma_{b,d,h}^{uv}$	Voltage magnitude deviation under minimum limit at bus b, day d and hour h
$x_{h,b}$	Battery charging operation at bus b and day d
$y_{h,b}$	Battery discharging operation at bus b and day d

$\theta^{+}_{b,d,h}, \theta^{-}_{b,d,h}$	Boolean variables to indicate power injection $(+)$ or consumption $(-)$ at bus b, day d and hour h
$C^{Xfmr}_{T,d,h}$	Lifespan transformer cost at transformer T, day d and hour h
C^{rep}_{T}	Replacement transformer cost at transformer T
ω_T	Boolean variable to indicate transformer replacement
$\Delta \mathrm{P}^{\mathrm{Xfmr},+}_{T,d,h}$	Positive Power Flow Variation at transformer T for each day d and hour h
$\Delta \mathrm{P}^{\mathrm{Xfmr},-}_{T,d,h}$	Negative Power Flow Variation at transformer T for each day d and hour h
$\Delta \mathrm{P}^{\mathrm{Xfmr}}_{T,d,h}$	Power Flow Variation at transformer T for each day d and hour h
$\gamma^{Xfmr}_{T,d,h}$	Power Flow magnitude deviation at transformer over maximum limit at Transformer T, day d and hour h

Abbreviations

DER	Distributed Energy Resources
DSO	Distribution System Operator
VPP	Virtual Power Plant
PV	Photovoltaic
BESS	Battery Energy Storage System
DG	Distributed Generation
OPF	Optimum Power Flow
EV	Electrical Vehicles
MINLP	Mixed Integer Nonlinear Programming
XFMR	Transformer

1
Introduction

1.1.
General Considerations

In recent years, distribution systems have undergone significant changes due to the integration of Distributed Energy Resources (DERs). In Brazil, the regulatory resolution REN482/12 (ANEEL, 2012) encouraged investment in DERs, particularly in Photovoltaic (PV) systems at the distribution system level. According to this resolution, micro and mini generation, with power limits of 100 kW and from 100 kW to 1 MW, respectively, are eligible to participate in the energy compensation system. Furthermore, (ANEEL, 2012) imposes a low tax on prosumers, maintained at this low by subsidies paid by other consumers, serving as a powerful incentive to expand distributed generation in Brazil.

In 2016, REN482/2012 was updated, resulting in REN687/2016 (ANEEL, 2016), which changed the upper limits for micro and mini generation to 75 kW and 3 MW, respectively. This new resolution also introduced new modalities for Distributed Generation (DG) associated with energy credit sharing. The modalities include enterprises with multiple consumer units, where different consumers can use the energy credits form a DG; remote consumption, allowing different consumers to share energy credits from a remote DG installation, provided by the same utility company. It is important to notice that, according to the rules, the energy credits can be used until 60 months after the injection of energy generated.

The main outcome of implementing REN687/2016 was a significant increase in installed DG, particularly from photovoltaic (PV) systems. Installed PV capacity grew from just 3 MW in 2013 to 36 GW in 2024, with projections reaching 64 GW in 2029, according to (Energy Research Company - EPE, 2025).

Recently, Law 14.300/2022 (Brazilian Chamber of Deputies, 2022) was enacted, which, on one hand, tends to increase investor confidence, but on the other

hand, may reduce some of the investments that initially boosted DG in Brazil. The most notable change was the partial deduction of tariffs associated with grid usage cost, which represents approximately 30% of total energy tariff for low voltage consumers. According to (Brazilian Chamber of Deputies, 2022), this new structure will take place gradually from 2023 to 2028. The expected result is slower growth in DG investment, prompting a search for new ways to add value to the business model, especially for remote DG installations. Another important aspect that this law brings is the possibility of contracting ancillary services from micro and mini generators by distribution companies, however, there is no specific regulatory about the valuation and form of the contracting for these services implemented and consolidated by ANEEL.

The main goal of this thesis is to present an alternative business model for VPP in Brazil following the enactment of Law 14,300/2022, enabling contribution as a future proposal for valuing ancillary services by DERs. A distribution feeder, located in Palmas, Tocantins, Brazil (also known as ETO) was used to validation of this model, in partnership with the Energisa Group, considering the integration of PV systems, Battery Energy Storage Systems (BESS), and hybrid systems (PV and BESS). This integration will form a Virtual Power Plant (VPP), which, in addition to generating energy credits, will provide ancillary services to enhance the overall value of the business model, which is mathematically modeled as a mixed integer nonlinear programming (MINLP). The VPP is a system that groups and manages a remote set of DERs.

1.2. Objective

As mentioned previously, the main objective of this thesis is to integrate economic and technical aspects of a VPP, specifically adapted to operate in low-voltage grid. The focus on technical aspects is voltage control, mitigating the impact on electric losses, reducing peak demand at the substation, decrease transformer overload, and extending transformers lifespan.

Voltage control is conducted in two steps, optimizing BESS operation and using inverters to inject or absorb reactive power after the optimization process. Furthermore, a piecewise linearization is used to capture the nonlinear behavior of

electric losses associated with active power injection/absorption by DERs. Finally, the power flow reduction at substation is integrated into the linear model, along with the reduction of power flow at transformers and extension of the transformer lifespan.

The main contribution of this thesis consists of the proposition of a comprehensive business model tailored for an energy aggregator. The model integrates commercial and technical aspects of the grid while aligning with regulatory frameworks in Brazil. The distinguishing characteristics of this work, compared to existing literature, cover a synergistic combination of the following components: (i) the proposal of a comprehensive business model for an energy aggregator; (ii) the mitigation of voltage issues in low-voltage systems through the optimal charge/discharge operation of BESS; (iii) the reduction of DER-related impacts on energy losses, peak demand at the substation, transformers overload and transformers lifespan by leveraging VPPs with various DERs distributed across the grid; and (iv) the valuation of ancillary services in grid systems as a by-product, taking into account the benefits provided by VPP operation.

1.3. Thesis Structure

This thesis is structured into five chapters and five appendices. The first chapter is the contextualization of the presented work, the main objective of this thesis, the structure of the thesis, and the publications associated with this work. Chapter two provides a review of the works related to this thesis presenting the differences among the proposed work and other projects presented in literature.

Chapter three introduces the business model, the Brazilian market structure, the transactive energy model, the computation of sensitivity parameters, operation optimization, voltage control in the post-optimization process and framework analysis applied in the proposed model. For didactic reasons, sensitivity parameters were computed in IEEE 13 Bus.

Chapter four provides results were presented from the proposed model business with a real system data located at Tocantins city, in Brazil, which has

ENERGISA as the utility for the (RE)Energisa aggregator. The data grid is also called ENERGISA-Tocantins 2023 (ETO-2023).

Chapter five provides the main conclusions derived from the research conducted along with recommendations for future work.

1.4. Publications

This research has produced, directly or indirectly, several articles in conferences and journal as follows:

1. LIMA, DELBERIS A.; MASSARI FILHO, A.; CASTRO, A. M.; GOULART, GUSTAVO M.; VALENTE, K. M.; TEIXEIRA, R. S. D. Avaliação abrangente de novos modelos de negócios com Recursos Energéticos Distribuídos no Brasil após a Lei 14.300/2022. In: SENDI - Seminário Nacional de Distribuição de Energia Elétrica, 2023, Espírito Santo. Seminário Nacional de Distribuição de Energia Elétrica, 2023.
2. LIMA, DELBERIS A.; TEIXEIRA, RAFAEL S. D.; FILHO, ARTHUR M.; VALENTE, KARINA M.; MILHORANCE, ANDRÉ; TEIXEIRA, WENDELL W.; GOULART, GUSTAVO M.; TEIXEIRA, ALEXANDRE M. Toward a New Transactive Energy System with Distributed Energy Resources in Brazil: A Real Case Application. In: 2023 IEEE PES Innovative Smart Grid Technologies Latin America (ISGTLA), 2023, San Juan. 2023 IEEE PES Innovative Smart Grid Technologies Latin America (ISGT-LA), 2023. p.235.
3. LIMA, DELBERIS A.; FILHO, ARTHUR M.; TEIXEIRA, RAFAEL S.D.; MILHORANCE, ANDRÉ. Transactive energy based on virtual power plant and ancillary services: A real case application in Brazil after the Law 14.300/2022. JOURNAL OF ENERGY STORAGE, v. 90, p. 111761, 2024.
4. Lima, D. A.; MASSARI FILHO, A.; SAADI, R.; ATENCIA, V.; CASTRO, A. M.; Valoração de Serviços Ancilares em Sistemas de Distribuição para Usina Virtual de Energia. In: CBRED - Congresso Brasileiro de Recursos Energéticos Distribuídos, 2024, Uberlândia. CBRED - Congresso Brasileiro de Recursos Energéticos Distribuídos, 2024.

5. Lima, D. A.; MASSARI FILHO, A.; SAADI, R.; ATENCIA, V.; CASTRO, A. M.; LIÇÕES APRENDIDAS COM A IMPLEMENTAÇÃO DE UMA USINA VIRTUAL NA ENERGISA TOCANTINS: MODELO DE NEGÓCIOS, RESULTADOS PRÁTICOS E PRÓXIMOS PASSOS; In: XXVIII SNPTEE - Seminário Nacional de Produção e Transmissão de Energia Elétrica, Recife - PE, 2025 – Paper approved for presentation

2
Literature Review

This chapter reviews the existing literature on VPP, as a business model and BESS for ancillary services provision in low-voltage distribution grids. It presents a range of studies employing diverse methodologies, highlighting the variety of approaches used in this field. Furthermore, the chapter situates the present work within the context of the current state of research, identifying its contributions relative to existing studies.

Several alternatives business models for VPPs have emerged to implement a transactive energy strategy. However, effective coordination between the Distribution System Operator (DSO) and VPPs is crucial for the sustainable growth of DERs in distribution systems. At this context, in (Renani, Ehsan, & Shahidehpour, 2018), it is proposed that the DSO can reduce energy supply costs and increase the return on investment within a transactive market structure for a distribution area. Furthermore, in (Molzahn, 2017), distributed algorithms are analyzed for offline solutions to Optimal Power Flow (OPF), as well as algorithms for real-time, online OPF solutions. In (Scott, Gordon, Franklin, Jones, & S. Thiebaux, 2019), a method for coordinating DERs with grid constraints in distribution systems is presented to reduce the need of conventional methods and expensive management, as a diesel generator in higher feeder demand. In (Apostolopoulou, Bahramirad, & Khodaei, 2016), a DSO scheme is proposed that leverages efficient DERs to improve the system reliability and resilience while reducing greenhouse gas emissions through diversification. Therefore, in the references discussed in this paragraph there are a deeper understanding of the agreements necessary to achieve the best results in terms of cost-benefit through the integration of DERs, DSO and distribution.

In (Naval & Yusta, 2021), a set of VPP models is presented, including their classification and a detailed analysis with several types of energy markets. In this

case, the methods approach for VPP business are separated into two different sets: optimization and heuristic. The optimization problems include linear programming, mixed-integer linear programming (MILP), and nonlinear programming, mixed-integer nonlinear programming, while heuristic methods include particle swarm, genetic algorithms, big bang crunch and imperialist competitive. In reference (Burger & Luke, 2017), it is providing an empirical analysis of the most common business model for the implementation of the DERs, which classifies the revenue streams, customers segments, electricity services provided, and resources for 144 business models. This assessment is made to identify a set of archetypes in each category. In article (Guerrero, Gebbran, Mhanna, Chapman, & Verbič, 2020), it is made a review approach that facilitates the integration of DERs on a small scale in low- and medium-voltage grids within the context of transactive energy, with the aim to provide the information needed in DERs integration to select a tailored approach to their specific power network and system integrations. Therefore, the articles mentioned in this paragraph explore VPP business model, considering various electricity markets and the implications of different regulatory frameworks.

Building on the work (Guerrero, Gebbran, Mhanna, Chapman, & Verbič, 2020), the business model for DER is categorized into three main types: uncoordinated model, which focuses solely on Home Energy Management System (HEMS); coordinated models, which integrates the responsibility of multiplies users to address optimal energy management problems, and peer-to-peer energy trading models, which establishes decentralized energy markets.

Recently, in article (Zhang, Wang, & Luo, 2024), it is proposed an internal aggregation optimization model of VPP, which explicitly accounts for the uncertainty associated with energy output. The objective of the proposed model is to minimize the total operational cost, incorporating costs related to energy generation.

The study made in (Zhao, Yi, Xu, Zhao, & Wang, 2024), summarizes the trading framework for VPP composed of energy storage in the power market and proposes an optimization model for VPP. This model is proposed on a distributed power marketing clearing based on Alternating Direction Method of Multipliers.

It is also possible to incorporate user-side resources into the control of a VPP though demand response mechanisms. In this context, the author of the article (Qu, Tang, Ni, Zhang, & Yan, 2024) analyses the operational structure of a VPP and proposes a user-side distributed optimal control method for VPP with demand response through an improved particle swarm optimization algorithm. The user's load response is based on the time-of-using price.

The use of BESS to provide ancillary services in low-voltage grids was also explored in many projects. In article (Alpízar-Castillo, Linders, Slaifstein, Ramírez-Elizondo, & Bauer, 2024), the conditions that can make attractive, from a cost perspective for individual prosumers to participate in low-voltage ancillary services are investigated, with a particular focus on curtailment and peak shaving.

On the other hand, in article (Alyami, Wang, Wang, Zhao, & Zhao, 2014), a model is proposed to limit power injections and prevent overvoltage by adjusting PV inverters limits in real time. In (Mamun, et al., 2022), the bidirectional power flow caused by using electrical vehicles (EVs) in distribution systems is studied, and its association with voltage issues. It is important to highlight that in both cases, the voltage violation is the most critical issue. In (Chaudhary & Rizwan, 2018), the problem of overvoltage of PV penetration is also mentioned, as well other issues, such as electrical losses, and energy phase balance.

In (Chand, et al., 2020), different types of DERs are presented in microgrid, showing that the main challenges in microgrids are the voltage stability and frequency regulation. In reference (Islam, Prakash, Mamun, Lallu, & Mudliar, 2016), a new type of control for PV system is proposed, that can track maximum power but may lead to curtailment and increase in electrical losses.

Furthermore, in (Prakash, et al., 2022) is provided an in-depth review of BESS applications in ancillary services for distribution networks. According to this reference, the types of DER ancillary services can offer include voltage support, peak shaving congestion relief, power smoothing, black start, and frequency regulation.

One of the main contributions of BESS is the capacity to reduce peak demand in power systems. This can be achieved, typically by charging during off-peak periods and discharging during peak hours (Akhil, Boyes, Butler, & Doughty,

2010), providing peak shaving in both periods. In this context, in reference (Chua, Lim, & Morris, 2016), proposed a strategy to optimize peak reduction using BESS. In (Lima & Rodrigues, 2022), a stochastic model is proposed based on mixed integer linear programming (MILP), which integrates PV and BESS, utilizing generations and load scenarios under a time-of-use model. In the article (Lakshmi & Ganguly, 2019), it is proposed a strategy for the allocation of PVs and BESS to reduce the peak loads in distributions networks. Therefore, the studies cited in this section present methods that utilize BESS to reduce peak demand.

In (Prakash, et al., 2022), three distinct types of voltage control are presented using BESS: centralized, decentralized or localized. The definitions of centralized and decentralized are provided in (Antoniadou-Plytaria, Kouveliotis-Lysikatos, Georgilakis, & Hatziargyriou, 2017), while the definition of localized control is given in (Farivar, Zho, & Chen, 2015). The three types of control are defined as follows: centralized, with all measurements are collected in a control center, where a central controller takes all decisions related to voltage issues in distribution systems; decentralized, in which the controllers collect local measurements, process them, and apply actions to mitigate voltage issues and; localized, where the inverter performs voltage control with the DER (through volt/var control) by reactive power injection/extraction.

The study presented in (Wang, Bai, Yan, & Saha, 2018), evaluated centralized operation in the coordination between PV and BESS on medium voltage levels. In (Hashemi & Østergaard, 2018), the centralized methodology aimed at reducing voltage violations in low-voltage distributions networks by combining BESS operation with reactive power from DERs.

Another type of ancillary service that BESS can provide is related to transformers, specifically by extending their lifespan and avoiding their replacement due to overload, caused by the consumption and the largest PV penetration (which leads to a reverse power flow). In (Majeed & Nwulu, 2022), is presented the impact of PV penetration in low-voltage transformers, demonstrating that natural loading and PV injection have overloaded transformers.

Several studies in literature reinforce this aspect. For instance, (Affonso & Kezunovic, 2019) presents a smart charging method designed to minimize

electricity consumption cost while preventing transformer overloading. This approach considers the integration of charging stations with PV systems and BESS units. In (Mamede, et al., 2023) different BESS dispatches are analyzed, and one of the reported benefits is the reduction in distribution transformers loading, thereby increasing the system's capacity. In reference (Okubo, et al., 2020), proposed a charging/discharging strategy for BESS specifically to prevent transformers overloading in low-voltage networks. Additionally, in (Kumar & Krishan, 2021), it is introduced a nonlinear autoregressive model introduced with exogenous input for short-term load forecasting; based on its results, a day-ahead BESS dispatch plan is defined to minimize the transformers degradation.

In the context of ancillary services for renewable energy integration into power systems, recent studies have proposed a cost allocation mechanism for inertia and frequency response. In (Matamala, Badesa, Moreno, & G. Strbac, 2024) and (Badesa, Matamala, & Strbac, 2023), the authors explore cost allocation approaches based on cooperative game theory and shadow pricing, respectively, to distribute payments for frequency control among all generators or loads that create the need for these services. Furthermore, in (Liang, Mieth, & Dvorkin, 2023), it is formulated a chance-constrained stochastic commitment model with inertia requirements and computes equilibrium energy, reserve, and inertia prices using convex duality.

The integration of DERs has introduced several challenges in distributions systems, particularly related to voltage, often leading to values outside the appropriate range. Numerous studies have explored technical solutions, such as the injection or extraction of reactive power by the inverters connected to DERs. In (Almeida, Pasupuleti, & Ekanayake, 2021), the main strategy used by inverters (PV) to mitigate voltage rise in low-voltage systems is highlighted. In this reference, two voltage control strategies using smarter inverter are analyzed. The first one is limiting the active power injection, which reduces PV generations gains, and the second is oversizing the inverter, which allows it to operate at maximum capacity. Additionally, in this article, it is identified that the reactive power compensation by inverters is a promising and economically viable solution for voltage management in the grid.

Another method used to ensure adequate voltage levels within an established limit is through power factor control, performed by inverters. In (Ishimaru, Komami, & Tamach, 2014), voltage control is achieved through a leading power factor. Meanwhile, in (Gokmen, Hu, & Chen, 2017), is proposed a dynamic achieved control based on solar radiation. In reference (Chirapongsananurak & Hooncharеon, 2017), reactive power absorption is suggested by the inverter using a constant power factor. Therefore, all references propose voltage control methods based on power factor adjustment, which can be configured in most inverters.

Volt/Var control is another technique used by inverters, which allows the inverter to monitor the voltage at specific points of the grid and inject or absorb reactive power in case a voltage violation is detected (Smith, Sunderman, Dugan, & Seal, 2011). In this same article, local voltage control is proposed using Volt/Var. Another article in this theme is (Almeida D. , Pasupuleti, Ekanayake, & Karunarathne, 2020), which analyzes the Volt/Var function of the smart inverters to mitigate overvoltage issues. In (Rahimi, Tbaileh, Broadwater, Woyak, & Dilek, 2017), the authors compare voltage control using power factor adjustment and Volt/Var control, in low-voltage grid.

A crucial factor for voltage control through active or reactive power is the X/R ratio. If this ratio is greater than one, the voltage variation at a specific point in the grid will be more sensitive to reactive power injection/extraction than to active power, as well as, if the X/R ratio is less than one, the voltage variation at a specific point in the grid will be more sensitive to active power injection/extraction than to reactive power (Almeida, Pasupuleti, & Ekanayake, 2021).

In this thesis, in addition to the focus on economic aspects, there is a focus on the analysis of ancillary services, approaching issues related to voltage violations, energy losses, peak demand, transformer overload and transformer lifespan, providing a comprehensive assessment of these services.

Table 1 shows the contributions of the references cited in this section, along with those of the present thesis, which are summarized. Within the VPPs context, the proposed model in this thesis stands out itself by integrating both network operation (linked to the coordinated management of DERs) and commercial

aspects, particularly energy credits derived from the net metering system. Additionally, the proposed approach incorporates a broader and more comprehensive set of ancillary services into the optimization framework when compared to the models discussed in the literature. Transformer is abbreviated to XFMR.

Table 1 - Contributions of the thesis presented in this section

Works	VPP					Ancillary Services					
	On-Grid	Off-Grid	HEMS	OPF	Energy credit	Loss	Peak Shaving	Response Demand	Voltage Control	Frequency	XFMR
(Renani, 2018)	x										
(Molzahn, 2017)	x			x		x			x	x	
(Scott, 2019)	x			x					x	x	
(Apostolopoulou, 2016)	x			x			x		x	x	
(Naval, 2021)	x				x					x	
(Burger, 2017)	x						x		x	x	
(Guerrero, 2020)	x		x								
(Zhang, 2024)	x			x	x						
(Zhao, 2024)	x			x	x						
(Qu, 2024)	x		x	x				x			
(Alpízar-Castillo, 2024)	x		x				x	x	x		
(Prakash., 2022)	x						x		x	x	
(Alyami, 2014)	x								x		
(Mamun, 2022)		x							x		
(Chaudhary, 2018)	x			x			x		x		
(Chand, 2020)	x						x		x		
(Islam, 2016)		x				x			x		
(Akhil, 2010)	x						x				
(Chua, 2016)	x						x		x	x	
(Lima 2022)	x				x						
(Lakshmi 2019)	x					x	x		x		
(Farivar, 2015)	x			x					x		
(Wang, 2018)	x								x		
(Hashemi 2016)	x								x		
(Matamala, 2024)	x									x	
(Badesa, 2022)	x									x	
(Liang, 2023)	x										
(Dilini, 2021)	x								x		
(Gómez-González, 2018)	x								x		
(Ishimaru, 2013)	x								x	x	
(Gokmen, 2017)	x								x		
(Chirapongsananurak, 2017)	x								x		
(Smith, 2011)	x								x		
(Almeida, 2020)	x								x		
(Rahimi, 2017)	x								x	x	
(Majeed, 2022)	x										x
(Affonso, 2019)	x			x			x				x
(Mamede, 2023)	x						x		x		x
(Okubo, 2020)	x										x
(Kumar, 2021)	x										x
(Lima, 2023)	x				x	x	x				
This Thesis	x			x	x	x	x		x		x

3
VPP Business Model

3.1.
Brazilian Market Structure

In Brazil, there are two types of electricity contracting environments: The regulated and free electricity markets (ANEEL, 2021). The regulated market is the Brazilian segment of the electricity sector, which the commercialization of electrical energy occurs through the distribution companies, with rules defined by government and by ANEEL, while the free electricity market is the Brazilian segment of the electricity sector, which the commercialization of electrical energy occurs in a directly negotiated manner between generators, energy traders and eligible consumers, without tariff intermediation by the distribution companies. Until 2023, the free electricity market was only accessible to high/medium-voltage consumers with demand contracts exceeding 500 kW. However, in 2024 the scenario changed significantly, allowing all group A consumers to migrate for the Free Electricity Markets.

This thesis aims an application of a business model in the regulated market, where consumers connected to high or medium voltage, categorized as group A, or low voltage, categorized as group B have the option to choose among four tariff modalities: green, or blue (for group A consumers), white, or conventional (for group B consumers) (ANEEL, 2021). Table 2 presents the tariff modality difference between these two groups.

Table 2 - Tariff modality for each group of consumers

Group A (High or medium Voltage)	Group B (Low voltage)
Green	Conventional
Blue	White

The main difference in these modalities for consumers in group A is related with contracted peak demand, while for energy contract, both modalities provide different energy tariff values for peak and off-peak periods. In contrast, consumers connected to low-voltage grid, categorized as Group B (which includes residential consumers), have two tariff options: conventional or white. The conventional tariff applies to a single rate, whereas the white tariff consists of three rates: peak, off-peak, and mid-peak periods. These tariffs modalities play a significant role in determining energy costs and billing structures for consumers in the regulated market who use the net metering system. In this context, the proposed business model is designed to integrate DERs into a transactive energy system for consumers, both at group A and B, in the regulated market.

3.2. VPP Business Model

The proposed VPP business model proposed in this thesis can be divided into two parts: commercial and ancillary services. In a commercial context, Figure 1 illustrates three stages of the proposed transactional structure, which is presented in Section 4.1. Stage 1 is the energy credit generation originating from the PVs in off-peak times. These credits are used to charge the BESS in stage 1 (hybrid systems) and in stage 2, then the energy credits are offered for consumers in white and green tariff, for peak times, concluding stage 3.

The proposed VPP business model aims to maximize revenue through selling energy generated by PVs and BESS on grid. Excess accumulated energy credit during off-peak and mid-peak periods, as well the energy credits generated on peak periods, should be transferred as credits to different consumers. The mathematical model for energy transactions, presented in Figure 1, will be detailed in the optimization model.

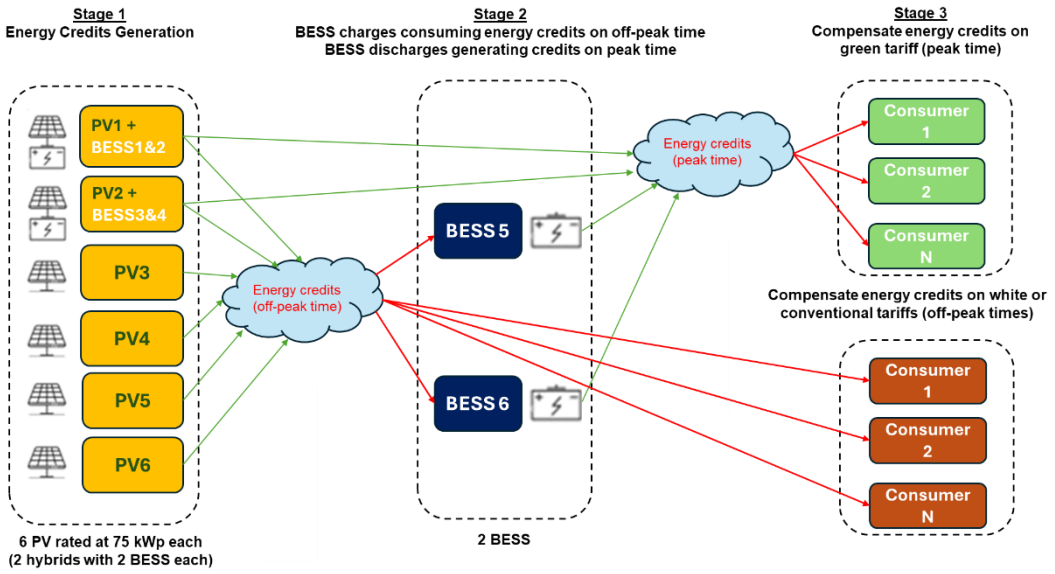

Figure 1 - Business model in three stages which considers Brazilian rules

Source: (Lima, et al., 2023)

The model also proposes to consider ancillary services, including voltage control, minimizing the impact of energy losses, peak demand reduction at substation, overload management to reduce transformers replacements, and increase transformers lifespan. The proposed approach aims to use ancillary services as additional income to VPP, and the complete model is presented below:

$$\max_{\Theta} \left(R_E^p + R_E^{op} + R_E^{mid}\right) - \left(C_\phi^p + C_\phi^{op} + C_\phi^{mid}\right) - \Delta P^{max} \cdot DUT - \sum_{d\in D}\sum_{h\in H}\sum_{b\in B} M \cdot \left(\gamma_{b,d,h}^{ov} + \gamma_{b,d,h}^{uv}\right) - \sum_{T\in Tr}\sum_{d\in D}\sum_{h\in H} \left(C_{T,d,h}^{Xfmr}\right) - \sum_{T\in Tr}\left(C_T^{rep}\right) \quad (1)$$

$$\Theta = \{x_{hb}, y_{hb}, \theta_{bdh}^{+}, \theta_{bdh}^{-}, E_{dh}^{C(G),p}, E_{dh}^{C(W),mid}, E_{dh}^{C(C),op}, \omega_T\} \quad (2)$$

s.t.:

$$E_{b,d,h}^{G,p} = P_b^{pv} \cdot G_{b,d,h}^{p} + y_{h,b} \cdot n_b^{bess} \cdot DOD_b \cdot P_b^{bess} \cdot ef_b - x_{h,b} \cdot n_b^{bess} \cdot DOD_b \cdot \left(P_b^{bess}\right) + E_{b,d,h}^{D,p} \quad \forall\, d \in D,\ h \in H^p,\ b \in B \quad (3)$$

$$E_{b,d,h}^{G,op} = P_b^{pv} \cdot G_{b,d,h}^{op} + y_{h,b} \cdot n_b^{bess} \cdot DOD_b \cdot \left(P_b^{bess}\right) \cdot ef_b - x_{h,b} \cdot n_b^{bess} \cdot DOD_b \cdot P_b^{bess} + E_{b,d,h}^{D,op} \quad \forall\, d \in D,\ h \in H^{op},\ b \in B \quad (4)$$

$$E_{b,d,h}^{G,mid} = P_b^{pv} \cdot G_{b,d,h}^{mid} + y_{h,b} \cdot n_b^{bess} \cdot DOD_b \cdot \left(P_b^{bess}\right) \cdot ef_b - x_{h,b} \cdot n_b^{bess} \cdot DOD_b \cdot \left(P_b^{bess}\right) + E_{b,d,h}^{D,mid} \quad \forall\, d \in D,\ h \in H^{mid},\ b \in B \quad (5)$$

$$E_{b,d,h}^{G,p} \geq 0 \quad \forall\, d \in D,\ h \in H^p,\ b \in B \quad (6)$$

$$E_{b,d,h}^{G,op} \geq 0 \quad \forall\, d \in D,\ h \in H^{op},\ b \in B \quad (7)$$

$$E_{b,d,h}^{G,mid} \geq 0 \quad \forall\, d \in D,\ h \in H^{int},\ b \in B \quad (8)$$

$$E_{b,d,h}^{D,op} \geq 0 \quad \forall\, d \in D,\ h \in H^{op},\ b \in B \quad (9)$$

$$E_{b,d,h}^{D,mid} \geq 0 \quad \forall\, d \in D,\ h \in H^{mid},\ b \in B \quad (10)$$

$$E_{b,d,h}^{D,p} \geq 0 \quad \forall\, d \in D,\ h \in H^p,\ b \in B \quad (11)$$

$$P_{b,d,h} = P_b^{pv} \cdot G_{b,d,h}^{p} + y_{b,h} \cdot n_b^{bess} \cdot DOD_b \cdot P_b^{bess} \cdot ef_b - x_{b,h} \cdot n_b^{bess} \cdot DOD_b \cdot P_b^{bess} \quad \forall\, d \in D,\ h \in H,\ b \in B \quad (12)$$

$$\Delta P^{max} \geq f_{d,h} - \sum_{b \in B} P_{b,d,h} \quad d \in D, h \in H \tag{13}$$

$$P_{L_{b,d,h}} \geq a^{L}_{1\,b,d,h} \cdot P_{b,d,h} + b^{L}_{1\,b,d,h} \quad \forall\, d \in D,\ h \in H,\ b \in B \tag{14}$$

$$P_{L_{b,d,h}} \geq a^{L}_{2\,b,d,h} \cdot P_{b,d,h} + b^{L}_{2\,b,d,h} \quad \forall\, d \in D,\ h \in H,\ b \in B \tag{15}$$

$$P_{L_{b,d,h}} \geq a^{L}_{3\,b,d,h} \cdot P_{b,d,h} + b^{L}_{3\,b,d,h} \quad \forall\, d \in D,\ h \in H,\ b \in B \tag{16}$$

$$C^{p}_{\phi} = \sum_{d \in D\ h \in H^{p}\ b \in B} P_{L_{b,d,h}} \cdot T_E^{p\,(G)} \tag{17}$$

$$C^{op}_{\phi} = \sum_{d \in D\ h \in H^{op}\ b \in B} P_{L_{b,d,h}} \cdot T_E^{op\,(G)} \tag{18}$$

$$C^{mid}_{\phi} = \sum_{d \in D\ h \in H^{mid}\ b \in B} P_{L_{b,d,h}} \cdot T_E^{mid(G)} \tag{19}$$

$$R_E^{p} = \sum_{d \in D\ h \in H^{p}} \left(E^{C(G),p}_{d,h} - \alpha \cdot \sum_{b \in B} E^{D,p}_{b,d,h} \right) \cdot T_E^{p\,(G)} + \left[E^{C(W),p}_{d,h} - (1-\alpha) \cdot \sum_{b \in B} E^{D,p}_{b,d,h} \right] \cdot T_E^{p\,(W)} \tag{20}$$

$$R_E^{op} = \sum_{d \in D\ h \in H^{op}} \left(E^{C(W),op}_{d,h} - \beta \cdot \sum_{b \in B} E^{D,op}_{b,d,h} \right) \cdot T_E^{op\,(W)} + \left(E^{C(C),op}_{d,h} - (1-\beta) \cdot \sum_{b \in B} E^{D,op}_{b,d,h} \right) \cdot T_E^{(C)} \tag{21}$$

$$R_E^{mid} = \sum_{d \in D\ h \in H^{mid}} \left(E^{C(W),mid}_{d,h} - \sum_{b \in B} E^{D,mid}_{b,d,h} \right) \cdot T_E^{mid(W)} \tag{22}$$

$$\sum_{d \in D\ h \in H^{p}\ b \in B} (\alpha) \cdot (d^{UD} \cdot E^{G,p}_{b,d,h} - E^{D,p}_{b,d,h}) \geq \sum_{d \in D\ h \in H^{p}} E^{C(G),p}_{d,h} \tag{23}$$

$$\sum_{d \in D\ h \in H^{p}\ b \in B} (1-\alpha) \cdot (d^{UD} \cdot E^{G,p}_{b,d,h} - E^{D,p}_{b,d,h}) \geq \sum_{d \in D\ h \in H^{p}} E^{C(W),p}_{d,h} \tag{24}$$

$$\sum_{d \in D\ h \in H^{op}\ b \in B} \beta \cdot (d^{UD} \cdot E^{G,op}_{b,d,h} - E^{D,\,op}_{b,d,h}) \geq E^{C(W),op}_{d,h} \tag{25}$$

$$\sum_{d \in D\ h \in H^{mid}\ b \in B} (d^{UD} \cdot E^{G,mid}_{b,d,h} - E^{D,\,mid}_{b,d,h}) \geq \sum_{d \in D\ h \in H^{int}} E^{C(W),mid}_{d,h} \tag{26}$$

$$\sum_{d \in D\ h \in H^{op}\ b \in B} (1-\beta) \cdot (d^{UD} \cdot E^{G,op}_{b,d,h} - E^{D,op}_{b,d,h}) \geq \sum_{d \in D\ h \in H^{op}} E^{C(C),op}_{d,h} \tag{27}$$

$$x_{h,b} \geq 0 \quad \forall\, h \in H,\ b \in B \tag{28}$$

$$y_{h,b} \geq 0 \quad \forall\, h \in H\ ,\ b \in B \tag{29}$$

$$x_{h,b} \leq 1 \quad \forall\, h \in H,\ b \in B \tag{30}$$

$$y_{h,b} \leq 1 \quad \forall\, h \in H,\ b \in B \tag{31}$$

$$\sum_{h \in H} y_{h,b} = \sum_{h \in H} x_{h,b} \quad \forall\, b \in B \tag{32}$$

$$\sum_{h \in H} y_{h,b} \cdot n^{bat}_{b} \cdot P_{bat} \leq E_{bat} \tag{33}$$

$$V_{b,p,d,h} = V^{0}_{b,p,d,h} + a^{+}_{b,h} \cdot \frac{P^{+}_{b,d,h}}{N_f} - a^{-}_{b,h} \cdot \frac{P^{-}_{b,d,h}}{N_f} \forall\, h \in H,\ b \in B,\ d \in D \tag{34}$$

$$V_{b,p,d,h} \geq V^{min}_{b} - \gamma^{uv}_{b,p,d,h} \forall\, h \in H,\ b \in B,\ d \in D \tag{35}$$

$$V_{b,p,d,h} \leq V^{max}_{b} + \gamma^{ov}_{b,p,d,h} \forall\, h \in H,\ b \in B,\ d \in D \tag{36}$$

$$P^{+}_{b,d,h} = \theta^{+}_{b,d,h} \cdot P_{b,d,h} \quad \forall\, h \in H,\ b \in B,\ d \in D \tag{37}$$

$$P^{-}_{b,d,h} = \theta^{-}_{b,d,h} \cdot P_{b,d,h} \quad \forall\, h \in H,\ b \in B,\ d \in D \tag{38}$$

$$\theta^{+}_{b,d,h} + \theta^{-}_{b,d,h} = 1 \quad \forall\, h \in H,\ b \in B,\ d \in D \tag{39}$$

$$P^{+}_{b,d,h} \geq 0 \quad \forall\, h \in H,\ b \in B,\ d \in D \tag{40}$$

$$P^{-}_{b,d,h} \leq 0 \quad \forall\, h \in H,\ b \in B,\ d \in D \tag{41}$$

$$\Delta P^{Xfmr,+}_{T,d,h} \geq f^{Xfmr}_{T,d,h} - \sum_{b \in B} (P_{b,d,h} \cdot BT_{b,t}) \quad \forall\, T \in TR, d \in D, h \in H \tag{42}$$

$$\Delta P_{T,d,h}^{Xfmr,-} \leq f_{T,d,h}^{Xfmr} - \sum_{b \in B} (P_{b,d,h} \cdot BT_{b,T}) \quad \forall T \in TR, d \in D, h \in H \tag{43}$$

$$\Delta P_{T,d,h}^{Xfmr,+} \geq 0 \quad \forall T \in TR \tag{44}$$

$$\Delta P_{T,d,h}^{Xfmr,-} \leq 0 \quad \forall T \in TR \tag{45}$$

$$\Delta P_{T,d,h}^{Xfmr} \geq \Delta P_{T,d,h}^{Xfmr,+} \quad \forall T \in TR \tag{46}$$

$$\Delta P_{T,d,h}^{Xfmr} \geq -\Delta P_{T,d,h}^{Xfmr,-} \quad \forall T \in TR \tag{47}$$

$$\Delta P_{T,d,h}^{Xfmr} \leq Cap_T^{Xfmr} + \gamma_{T,d,h}^{Xfmr} \quad \forall d \in D, h \in H, T \in TR \tag{48}$$

$$C_{T,d,h}^{Xfmr} \geq a_1^{Xfmr} \Delta P^{Xfmr} + b_1^{Xfmr} \quad \forall d \in D, h \in H, T \in TR \tag{49}$$

$$C_{T,d,h}^{Xfmr} \geq a_2^{Xfmr} \Delta P^{Xfmr} + b_2^{Xfmr} \quad \forall d \in D, h \in H, T \in TR \tag{50}$$

$$C_{T,d,h}^{Xfmr} \geq 0 \tag{51}$$

$$\gamma_{T,d,h}^{Xfmr} \leq M \cdot \omega_T \tag{52}$$

$$C_T^{rep} \geq \left(C_{T'}^{labor} + C_{T'}^{team}\right)\omega_T \quad \forall T \in TR \tag{53}$$

The objective function (1) can be divided into six groups, each with its own characteristics to achieve the desired objective. The first group ($R_E^p + R_E^{op} + R_E^{mid}$) aims to maximize energy credit revenue of the aggregator for the peak, off-peak and mid-peak periods. The second group ($-C_\phi^p - C_\phi^{op} - C_\phi^{mid}$) aims to minimize costs related to electrical losses for each tariff period, with losses represented as deductions in objective function. The third group ($-\Delta P^{max} \cdot DUT$) focused on reducing peak demand costs at substation. The fourth group ($-\sum_{d \in D\ h \in H\ p \in P\ b \in B} M \cdot (\gamma_{b,p,d,h}^{ov} + \gamma_{b,p,d,h}^{uv})$) is directed at voltage control, using auxiliary variables that are penalized with a large value (M) to mitigate voltage violations ($\gamma_{b,p,d,h}^{ov} + \gamma_{b,p,d,h}^{uv}$). The fifth group ($-\sum_{T \in TR d \in D h \in H}\left(C_{T,d,h}^{Xfmr}\right)$) has the objective of minimizing the transformer lifespan reduction. The sixth group ($-\sum_{T \in TR d \in D h \in H}\left(C_T^{rep}\right)$) has the objective of minimizing the need for transformers replacement in case of overload.

Equation (2) presents all control variables used in this optimization model. Constraints (3), (4) and (5) compute energy credit accumulation for peak, off-peak and mid-peak periods, respectively. These constraints account for PV generation, adding the energy discharged by BESS and subtracting the energy charged into BESS across all buses, days, and hours of the availed time. The BESS cannot be completely discharged, then the constant DOD (Deep of Discharge) represents the depth of BESS discharge, where the BESS is not completely discharged due to this value. The variable $E_{b,d,h}^{D,p}$ represents the energy debit, which corresponds to the surplus energy from the available VPP energy credits used to supply the BESS.

Constraints (6) – (11) indicate that both energy credit and debit should be positive throughout analyzed period.

Constraint (12) controls the net power (generation minus consumption) for all buses during the analyzed period. It follows a structure like energy credit, allowing positive values (energy injection into grid) and negative values (energy consumption from the grid). The variable $P_{b,d,h}$ indicates the power flow direction: when it is positive, it indicates that there is an energy injection, and when it is negative, it indicates energy extraction.

To manage and optimize the distribution system, constraint (13) ensures that the ΔP^{max} is always set as the maximum difference between the substation flow and the sum of all net powers from all DERs. In this way, the model is designed so that the DER dispatch minimizes the substation peak power demand.

The power demand at substations fluctuates throughout the day. In the proposed model, a scan is realized on all active power flows previously computed at the substation within the analyzed time intervals. The model subtracts the active power from DERs at same interval as this power demand, determining the maximum substation power value. This maximum value is defined as ΔP^{max} and is used to be minimized in the objective function.

In section 3.3.1.2, it will be shown that the behavior of losses is nonlinear concerning active power injection or extraction from DERs. Therefore, three linear curves are built to linearize the loss curves for each bus, day, and hour. This linearization is described by constraints (14) – (16). Constraint (14) represents the linearization of electric losses variation when power is extracted from bus, while constraints (15) and (16) represents the linearization of loses variations when power is injected at bus, the difference between this two constraints is that in (15) the linearization is for region where the electrical losses are decreased for injection power, while the constraint (16) is for region where the electrical losses are increased. The variable $P_{L_{b,d,h}}$ will always be equal to or greater than the loss value across the three curves, acting as an epigraph. The loss costs are calculated by constraints (17) – (19), multiplying the electrical loss by the tariff in each period, where constraints (17) represents costs at peak periods, (18) represents costs at off-peak periods, and (19) represents costs at mid-peak periods. These costs are

minimized in the objective function, with the purpose of the insertion of DERs on grid losses is as small as possible.

The revenues are determined by constraints (20) – (22) for each tariff period. The total generated energy, after subtracting energy debit required for BESS charging, is multiplied by the corresponding tariff for that period. The revenue is the sum of the difference between energy credit and energy debit for each modality.

Various tariff modalities are available to energy exchange contracts. For example, during peak times (constraint (20)), contracts may involve the white or green tariff, which are commonly used in Brazil. At this point, the parameter α denotes the percentage allocated to the green tariff, while its complement is allocated to white tariff.

Similarly, during the off-peak times (constraint (21)), the parameter β indicates the percentage allocated to the white tariff, while its complement is allocated to the conventional tariff. In mid-peak times (constraint (22)) the contracts are exclusively attributed to the white tariff, which is the only tariff for this period.

Constraints (23) – (27) refer to auxiliary variables used for revenue calculation, ensuring that these variables do not exceed the total available energy limits for each tariff modality. The parameter d^{UD} represents the discount applied for the use of grid distribution through the energy credits, in accordance with law 14,300/22 (Brazilian Chamber of Deputies, 2022). Constraint (23) ensures that the energy in peak times for energy contracts in green tariff will be not greater than the total energy difference between energy credit and debit in these times. Constraint (24) is like constraint (23), the difference is in the tariff modality, which in this case is allocated for energy contracts in white tariff. Constraint (25) ensures that the energy in off-peak times for energy contracts in the white tariff will be not greater than the total difference between energy credit and energy debit in these times. Constraint (26) ensures that the energy in mid-peak times for energy contracts in the white tariff will be not greater than the total difference between energy credit and energy debit in these times, and constraint (27) ensures that the energy in off-peak times for energy contracts in the green tariff will be not greater than the total difference between energy credit and energy debit in these times.

The control variables $x_{h,b}$ and $y_{h,b}$ are defined in constraints (28) – (31), which manage the BESS charging and discharging process. These variables are limited to 0 and 1, indicating that the battery charge or discharge cannot exceed 100% or fall below 0% of its capacity. Constraint (32) ensures that the total charge and discharge must be identical for each BESS. Constraint (33) limits the total charging and discharging capacity for each battery, restricting it to values less than or equal to its maximum capacity.

The group of constraints (34) – (40) is related to voltage control. Voltage is represented in (34) through linear regression model with distinct slope coefficients, denoted as $a_{b,h}^{+}$ (used for active power injection) and $a_{b,h}^{-}$ (used for active power extraction). In this context, voltage control is linked to energy injection or extraction. Consequently, the variables $P_{b,d,h}^{+}$ and $P_{b,d,h}^{-}$, defined in (37) and (38), play a fundamental role in management and regulation of voltage levels within the model. The variable $P_{b,d,h}^{+}$ represents the positive net power multiplied by a binary auxiliary variable $\theta_{b,d,h}^{+}$, while $P_{b,d,h}^{-}$ represents the negative net power multiplied by another binary auxiliary variable $\theta_{b,d,h}^{-}$. As indicated in (39), these two auxiliary variables cannot be activated simultaneously, because they are binary variables, when one is being activated, the other will not be activated. Furthermore, constraints (40) and (41) show that $P_{b,d,h}^{+}$ cannot take on negative values and $P_{b,d,h}^{-}$ cannot take on positive values. This approach explicitly defines whether the control should increase or decrease in voltage levels. Additionally, constraint (34) considers different slope coefficients for each bus and hour, and the calculation of these parameters is detailed in Section 3.3.

Constraints (35) and (36) define minimum and maximum voltage levels, ensuring compliance with legal regulations (ANEEL, 2016). Each constraint incorporates an auxiliary variable ($\gamma_{b,d,h}^{ov}$ and $\gamma_{b,d,h}^{uv}$), which allows undervoltage or overvoltage scenarios. These variables are subject to a penalty in the objective function. This penalty helps prevent infeasible situations, and any eventual voltage violations can be addressed in the post-optimization process through power factor control, as described in section 3.4.

The group of constraints (42) – (53) are related to power flow control in transformers. The power flow is represented in constraints (42) and (43), where the

new power flow with the usage of DER is the reference power flow ($f_{T,d,h}^{Xfmr}$) minus the energy from DERs multiplied by a binary value, which indicates whether the DER is in the transformer circuit. The variable $\Delta P_{T,d,h}^{Xfmr,+}$ and $\Delta P_{T,d,h}^{Xfmr,-}$ represent positive and negative transformer power flow variables, respectively. Constraints (44) and (45) ensure that these variables are always positive and negative, respectively. Constraints (46) and (47) relate to the positive and negative power flow transformers with the total absolute variation of power in transformers. Therefore, the total power variation ($\Delta P_{T,d,h}^{Xfmr}$) should be at least equal to or greater than the positive transformer power flow. Similarly, the total power variation should be equal or greater than absolute value of the negative transformer power flow, for each transformer with a DER in its low-voltage system.

Constraint (48) allows the transformer to operate in overload if necessary. The variable $\gamma_{T,d,h}^{Xfmr}$ represents the overload for each transformer, day, and hour, while Cap_T^{Xfmr} denotes the nominal capacity for each transformer. Constraint (52) penalizes this overload.

The transformer lifespan behavior is nonlinear, as will be shown in Section 3.3.1.5. Therefore, three linear curves are constructed to linearize the lifespan curves for each transformer, day, and hour. This linearization is represented by constraints (49) – (51). The variable $C_{T,d,h}^{Xfmr}$, which represents the transformer lifespan cost, must be equal or greater than the cost value across the three curves, acting as an epigraph. Constraint (51) ensures that the lifespan cost is always positive.

Constraint (53) computes the transformer replacement cost. The auxiliary binary variable ω_T is activated when the transformer operates in overloaded conditions.

3.3. Computation of Sensitivity Parameters

The sensitivity parameters establish a relationship with the electrical grid variables without the need to compute the power flow for each simulation. This approach enables the linearization of the relationship between quantities.

Through these sensitivities, it is possible to relate the injected or extracted power in a DER with some variables, such as voltage, electric losses or power demand at the substation and transformers. The voltage variation in this thesis is related to both active and reactive power injection/extraction.

The methodology used to define the coefficients of these sensitivities are related to the injection or extraction of active power considering a base case power flow solution, in which all initial data from the low-voltage grid are recorded. After establishing the base case, active power is either injected or extracted at each bus where each DER is installed. This injection/extraction is performed in 5 kW increments due to balance between accuracy and computational time, especially to the nonlinear behavior of losses. The power variation ranges from 0 to 75 kW at buses equipped with one 75 kW BESS, and from 0 to 150 kW at buses with two 75 kW BESS units.

For each scenario, variations in voltage, system losses, and power flows at the substation and transformers are measured relative to the base case. Based on these variations, sensitivity factors are derived for each parameter in every case within the dataset. Voltage sensitivity factors are obtained applying linear regression, while electrical losses are linearized through a piecewise approach.

The computation of sensitivity factors extraction of voltage in relation to the reactive power injection/extraction applied for each DER follow the same process, but the steps are 10 kVar. These steps were chosen aggregating the best accuracy and computational time.

Figure 2 shows the flowchart of the utilized method to obtain the sensitivity factors.

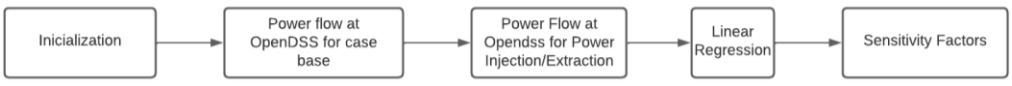

Figure 2 – Flowchart of extraction of sensitivity factors.

In the next subsections sensitivity for active power and reactive power will be presented. The sensitivity for active power will be divided into five subsections:

active voltage sensitivity, electrical losses sensitivity, flow substation sensitivity, flow transformer sensitivity and lifespan transformer. While the sensitivity for reactive power is applied only for voltage variation.

To exemplify the applications of sensitivities, a modified IEEE13-Bus system will be used to demonstrate the results from the analysis of sensitivities. This circuit is presented in Figure 3, and a new circuit is connected on the bus "634", with four buses, each one with 3 kW of load, all of them three-phase, as shown in Figure 4. The simulations are considered a typical curve for load throughout the day. The injection or extraction of power will be allocated on Bus 1, in the connected circuit.

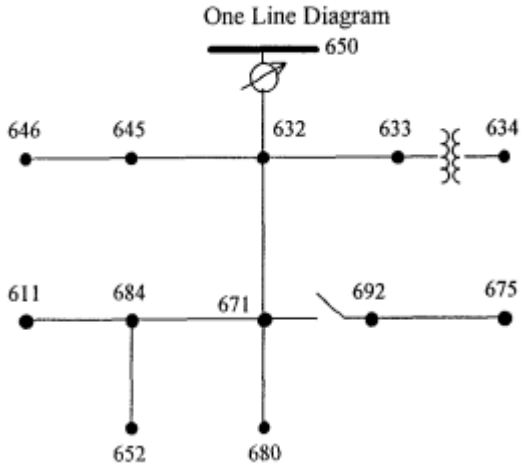

Figure 3 - IEEE 13 Bus Radial Distribution Feeder

Source: (Kersting, 2001)

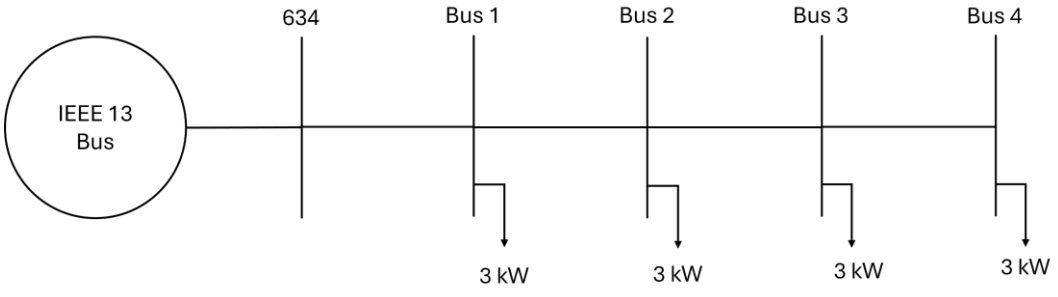

Figure 4 - Low Voltage System connected with IEEE 13 Bus

3.3.1. Active Power Sensitivity

This section presents all sensitivity factors related to active power. The sensitivity factors presented in this section are voltage, losses, power flow through the substation, power flow through the transformers, and lifespan transformers.

3.3.1.1. Active Power Voltage Sensitivity

Voltage sensitivity factors establish the relationship between active power injection or extraction and the voltage at the bus where the DERs are installed, using a first-degree linear equation ($f(x) = a \cdot x + b$).

The computation of these voltage sensitivity factors begins by recording voltage in the base case (i.e., without DERs). Then, 5 kW of active power is injected or extracted at the bus with DER, and the resulting voltage is recorded. This process is repeated in 5 kW increments, up to 75 kW (or 150 kW for buses with two BESS units), with voltage values recorded at each step.

The procedure is repeated for each bus equipped with a DER. The voltage variation is calculated using equation (54). When power is injected, the voltage increases, and the variation is positive. Conversely, when power is extracted, voltage decreases, and the variation is negative.

$$\Delta V = V_{ext/inj} - V_{base} \tag{54}$$

For power extraction cases, the BESS operates as a load, leading to a voltage dip, meaning the voltage variation is negative. Conversely, in power injection cases, the BESS works as a generator, or there is photovoltaic generation at the bus, causing a voltage rise, making voltage variation positive.

Figure 5 illustrates the voltage variation at bus 1, for phase 1 and hour 1, for a single day (considered as weekday in January) from the modified IEEE 13 Bus, when active power is injected or extracted on this bus. It is observed that the voltage variation with respect to power (within the 75kW three phase range) exhibits a linear relationship. This behavior is uniform across the entire load shape and for all three-phases. The coefficient of determination (R^2) for the linear regression, across

all data, fluctuates between 0.984 to 0.998. This linear behavior is consistent across all analyzed datasets. The legend in Figure 5 represents the month and the day of the week, which in this case is represented as a weekday in January.

When analyzing the voltage across the three phases of the same bus, it is observed that these variations are highly similar. Therefore, after linearization, a single sensitivity factor is calculated as the average of the sensitivity values across all day and phases, because voltage variation can be different throughout the hours of a day, due to active power injection of PVs. In other words, for each bus with a DER, there are twenty-four sensitivity factors for active power extraction and twenty-four for active power injection.

3.3.1.2. Electrical Losses Sensitivity

Similarly, to voltage variation, it is necessary to create a relationship between the power extracted/injected at a specific bus in the grid and the variation system losses. However, unlike voltage variation, this relationship is nonlinear, as will be demonstrated later.

The algorithm used to extract the sensitivity factors related to system losses initiates with simulations of the base case, and the corresponding loss values are recorded in all scenarios. Then, the power extracted/injected gradually increased at each bus, individually, in 5 kW steps up to a maximum of 75 kW (or 150 kW for two BESS units). For each scenario, the loss values are recorded, and the difference between the base case and the case with power extraction/injection is computed.

Figure 6 presents the relationship between extracted/injected power and loss variation in the modified IEEE 13 Bus system, at hour 1, when the extraction/injection is allocated at bus 1. For active power extraction, the correlation between loss variation and extracted power is linear. However, when analyzing the relationship for power injection, it is observed that power injection initially reduces technical losses before causing them to increase again (Figure 6). This behavior occurs due to power flow inversion in the secondary branch which the DER is installed. As the power flow increases, electrical losses also tend to rise.

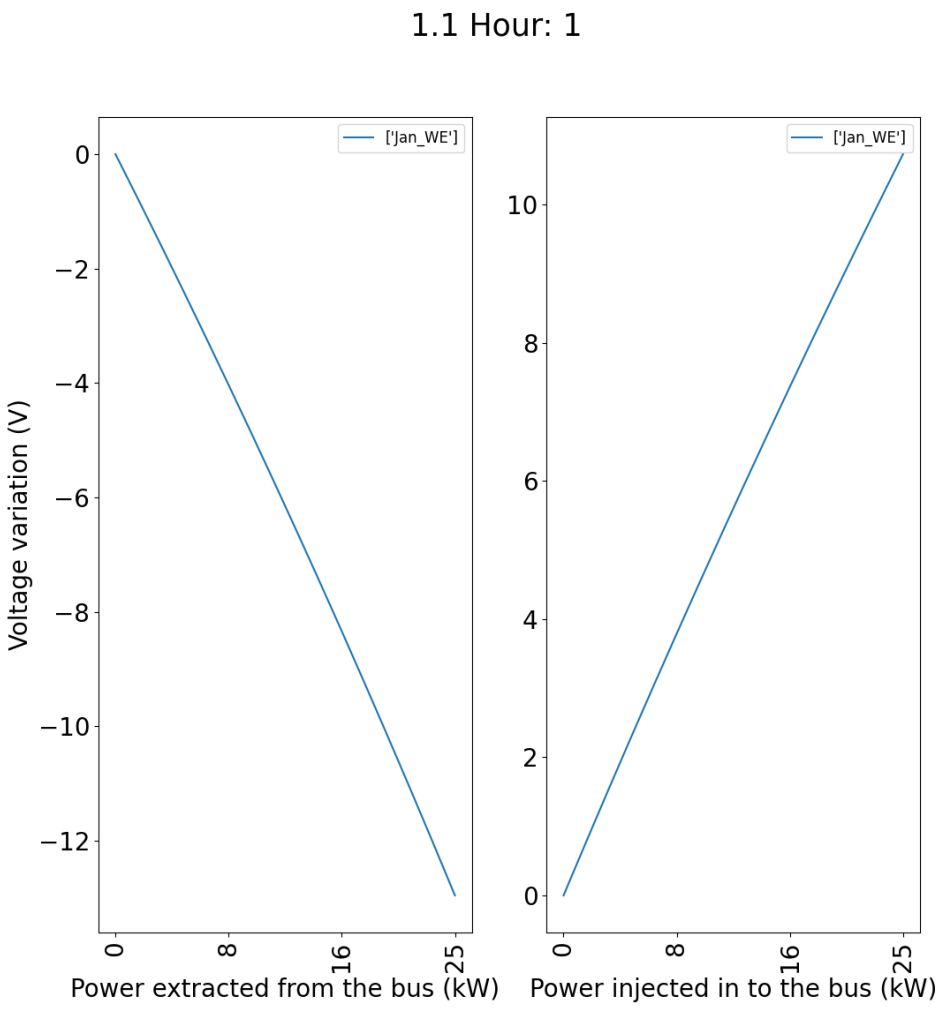

Figure 5 – Voltage variation at bus 1 and phase 1 for active power with extraction (left) and with injection (right)

The linearization of the relationship between power at a bus and electrical losses is performed using three distinct operational regions, as shown in Figure 7. First is the power extraction at the bus, second is the power injection at the bus, up to maximum loss reduction point (if such reduction occurs), and third is the power injected at the bus, from the maximum loss reduction point up to 75 kW.

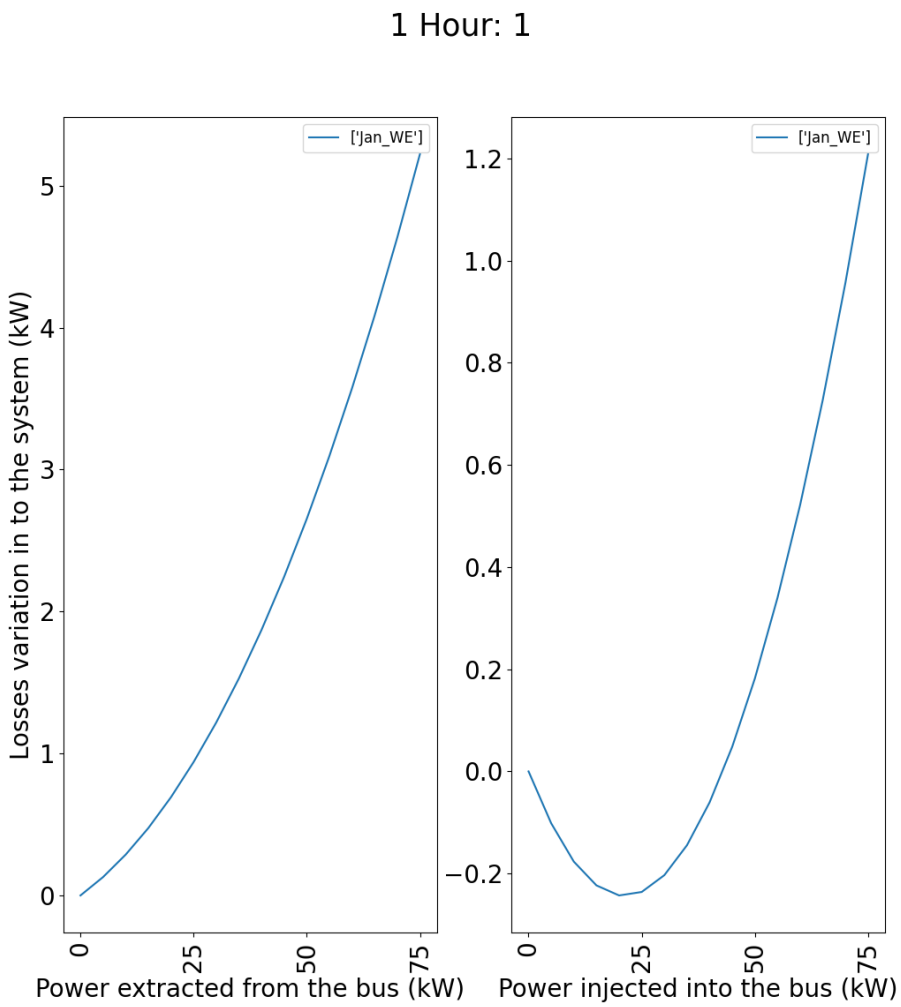

Figure 6 – Relationship between power variation at bus 1 with system loss variation at hour 1.

The piecewise linearization approach is adopted to accurately capture the impact that DER can have on system losses. If only two regions were considered (one for extraction and another for injection), as done in the voltage case, the effects of electrical loss reduction would be overlooked, which is not desirable.

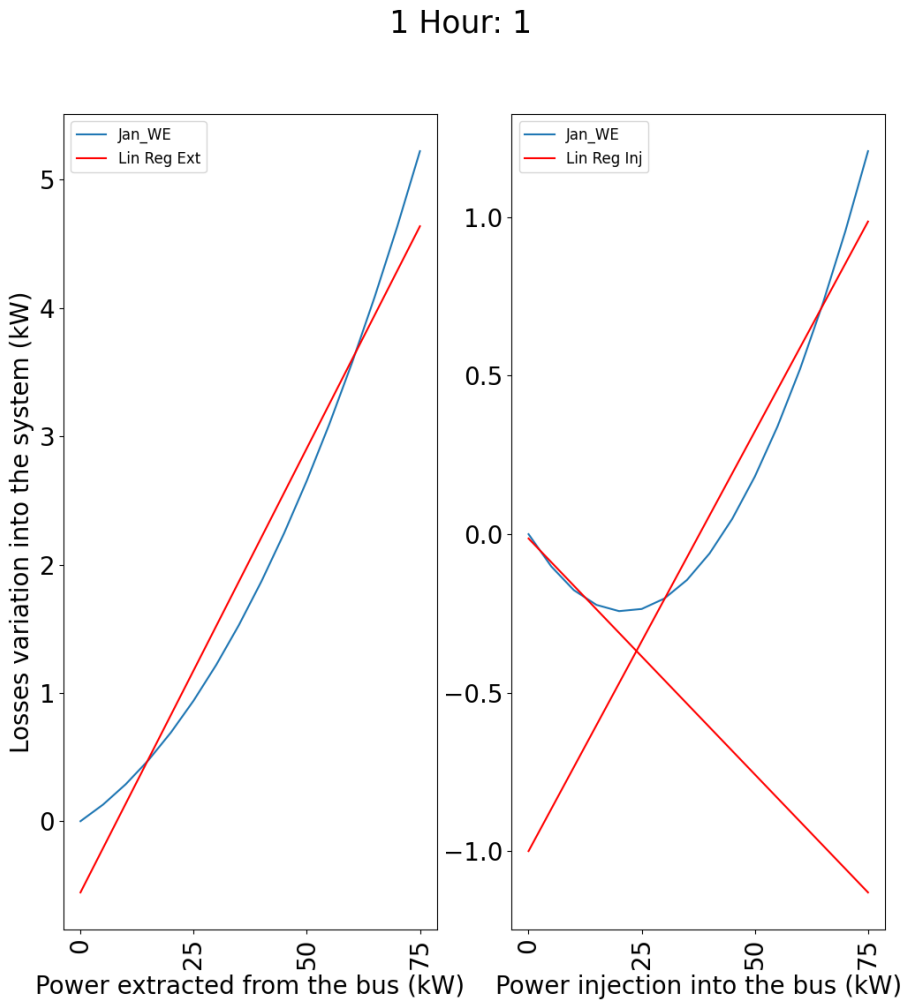

Figure 7 - Linear Regression for Three Regions.

3.3.1.3. Substation Power Flow Sensitivity

VPP can reduce the maximum active power flow at the substation during the peak hours, allowing for a potential adjustment in the contracted Distribution Usage Tariff (DUT). This relationship between the power extracted/injected by DERs and the power flow at the substation is directly proportional, meaning that any extracted/injected power results in the active power flow at the substation.

Figure 8 presents the relationship between the power variation at bus 1 and the power flow variation at the substation.

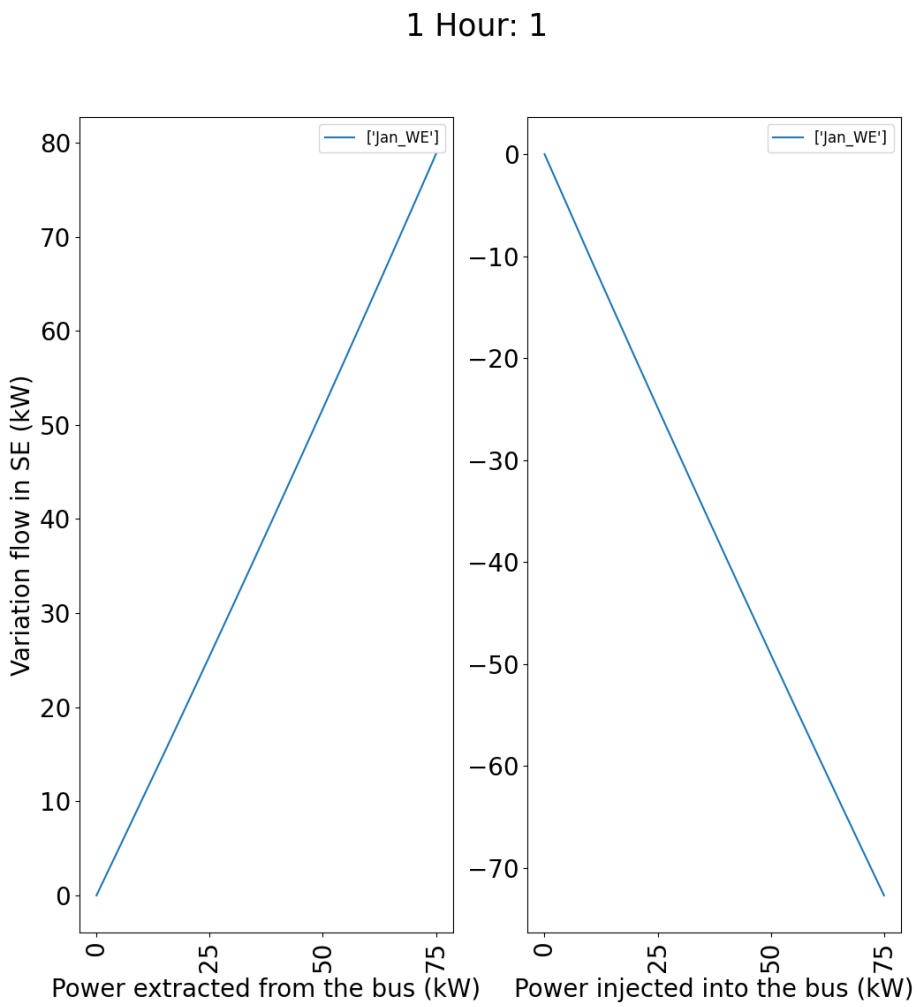

Figure 8 - Relationship between power variation at Bus 1 with power flow variation at substation.

Since the relationship between the power variation at a bus and power variation at the substations is one-to-one, practically, this direct proportionality is incorporated into the optimization model.

3.3.1.4. Transformers Power Flow Sensitivity

Similarly to substation flow sensitivity, transformer power flow sensitivity represents the relationship between the active power of the DER and the power flow at the transformer. This relationship is directly proportional, meaning that any power extracted/injected by the DER leads to an equivalent variation in the active power at the transformer.

This one-to-one relationship also applies in this context: injecting 1 kW from a DER reduces transformer load by 1 kW, while extracting 1 kW increases the transformer load by 1 kW.

Figure 9 shows this power flow variation at the transformer, connected to the circuit where Bus 1 is located, in IEEE 13 Bus modified system. This variation is linear, and when extracted or injected 75 kW at Bus 1, it is increased or reduced 75 kW of power flow at the transformer, respectively.

This relationship is applied in the optimization model to achieve two objectives: Simulate transformer overload, assessing whether the transformer operates beyond its nominal capacity due to DER; and estimate transformer lifespan, considering the impact of load variations over time

By using sensitivity factors, the optimization model eliminates the need to run a full power flow solution within the optimization process.

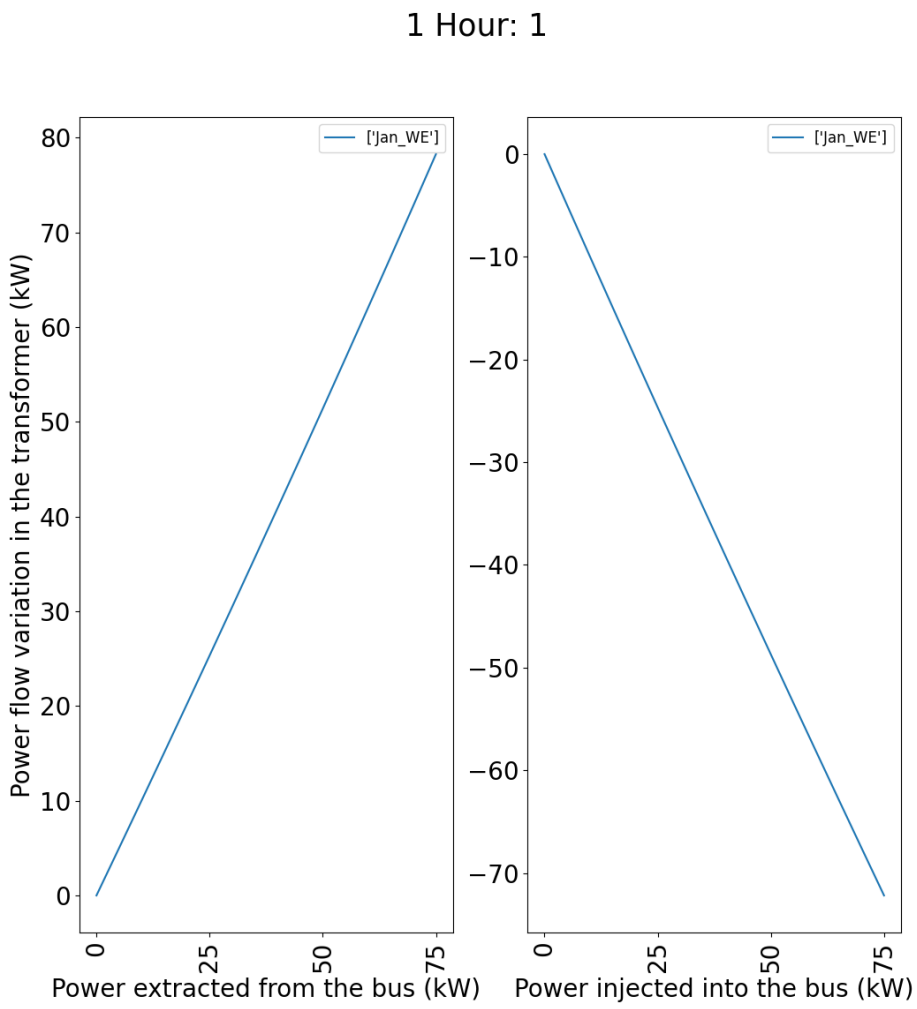

Figure 9 - Transformer power flow variation connected with circuit where Bus 1 is located.

3.3.1.5. Lifespan Transformer

Experimental evidence indicates that the deterioration of transformers through time follows an adaptation of the Arrhenius reaction rate theory.

The lifespan transformer decreases with temperature, following the expression (55), according to (Mamede J. F., 2013). In (55), the empirical constant depends on transformers temperature class: -14,133 for transformers of 55°C or -13,391 for transformers of 65°.

$$Log\ P_v(hours) = \left(A + \frac{B}{T_e(P^{(kw,t)})}\right) \cdot 100\% \quad (55)$$

$$T_e(K) = T_e(°C) + 273 \quad (56)$$

The winding hotspot temperature $T_e(°C)$ is determined based on transformers loading and its rated temperature class, as shown in equation (57) (Mamede J. F., 2013). The maximum top-oil temperature is 95°C for 55°C rated transformers or 105°C for 65°C rated transformers.

$$T_{e(°C)} = \frac{S}{T_{r_i}} \cdot T^{max} \tag{57}$$

The expected transformer lifespan is inversely proportional to its lifespan loss, which means that loss increases, the expected lifespan decreases. Can be calculated in equation (58).

$$E_v = \frac{100}{P_v} \tag{58}$$

The associated cost of a lifespan transformer, for each transformer, day, and hour, is inversely proportional to his expected lifespan transformer, as shown in equation (59).

$$C_{T,d,h}^{xfmr} = \frac{C_T^{rep}}{E_v} \tag{59}$$

Figure 10 demonstrates the hourly cost associated with the transformer lifespan, which has a capacity of 150 kVA. It can be observed that for lower power levels, the associated cost is zero. However, as the load approaches 50% of the transformer capacity, the costs start to increase, indicating a reduction in its expected lifespan.

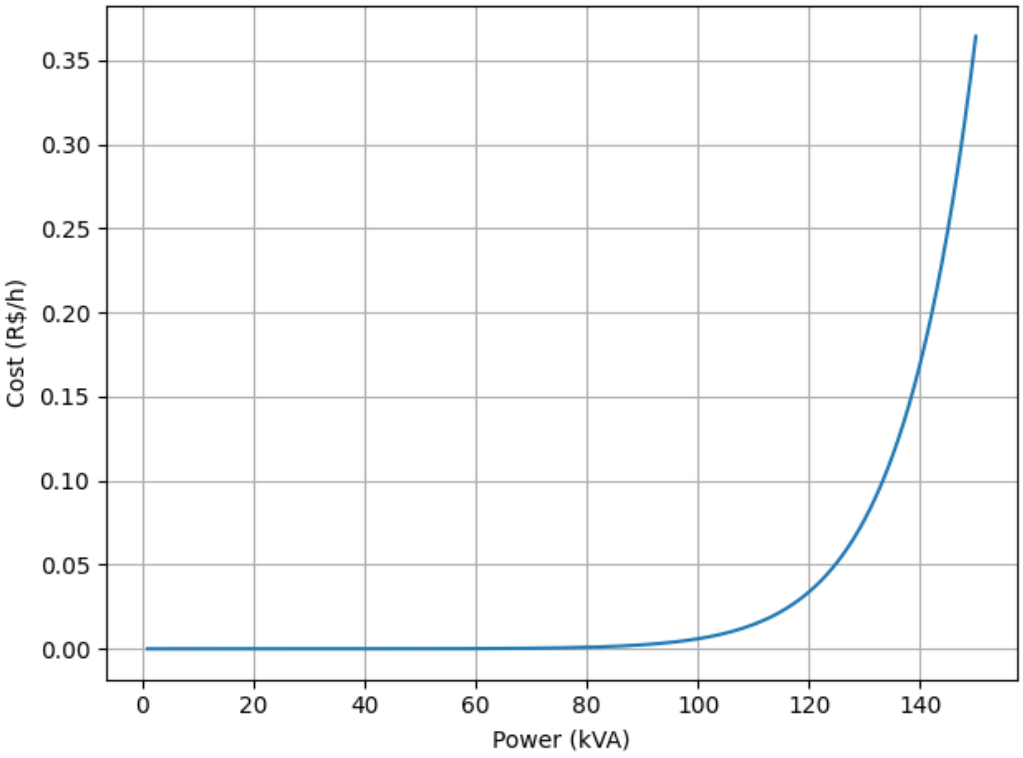

Figure 10 - Hourly cost associated with loss of transformer lifespan

After calculating the cost associated with transformers lifespan, a piecewise linearization approach is adopted to accurately capture the impact that DER can have on transformers' useful life. Two adjusted curves were considered, a range in which the cost remains zero and a range in which the cost increases significantly.

Figure 11 shows the piecewise linearization approach for bus 1 where it is observed that for lower load, the linearization approach is close to zero, and when the load is increased, the linearization approach has a greater angle.

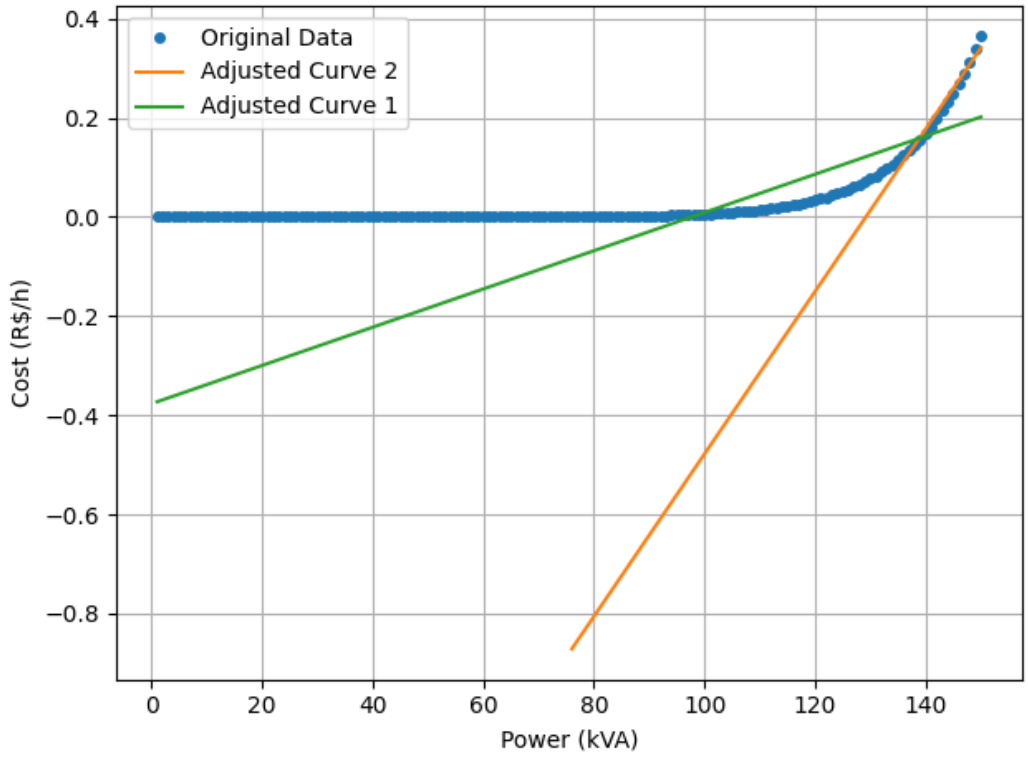

Figure 11 - Piecewise linearization for hourly cost associated with useful life transformer

3.3.2. Reactive Power Flow Sensitivity Factor

The relationship between reactive power provided by a DER and the voltage isa almost linear, like the relationship between active power and voltage. It is observed that there is no interaction between the reactive power at one bus and the other buses with DERs.

The procedure for computing reactive sensitivity factors follows a methodology analogous to that used for active power sensitivity analysis. In the base case, simulations are performed using the OpenDSS computational tool. Subsequently, reactive power is either injected (capacitive) or extracted (inductive) individually on each bus designed to host a DER. The reactive power variation ranges from 0 to 120 kVar, in steps of 10 kVar (in a balanced three-phases system). For each simulation, voltage variations relative to the base case are recorded. Based on these variations, sensitivity factors are extracted for each parameter, under every scenario included in the database. Finally, the sensitivity factors are determined through linear regression for voltage.

Figure 12 illustrates the behavior of the relationship between voltage and reactive power at bus 1, for phase 1 at hour 1.

3.4. Post-Optimization Voltage Control Process

The optimization model defines voltage control levels at buses with DERs. However, in certain cases, voltages levels may exceed regulatory limits, requiring a post-optimization control process using reactive power from DER inverters.

In Brazil, voltage limits for low-voltage circuits are established by Prodist Module 8 (ANEEL, 2016). For circuits with a nominal voltage of 220 V, the acceptable voltage range is between 202 V (0.92 pu) and 231 V (1.05 pu).

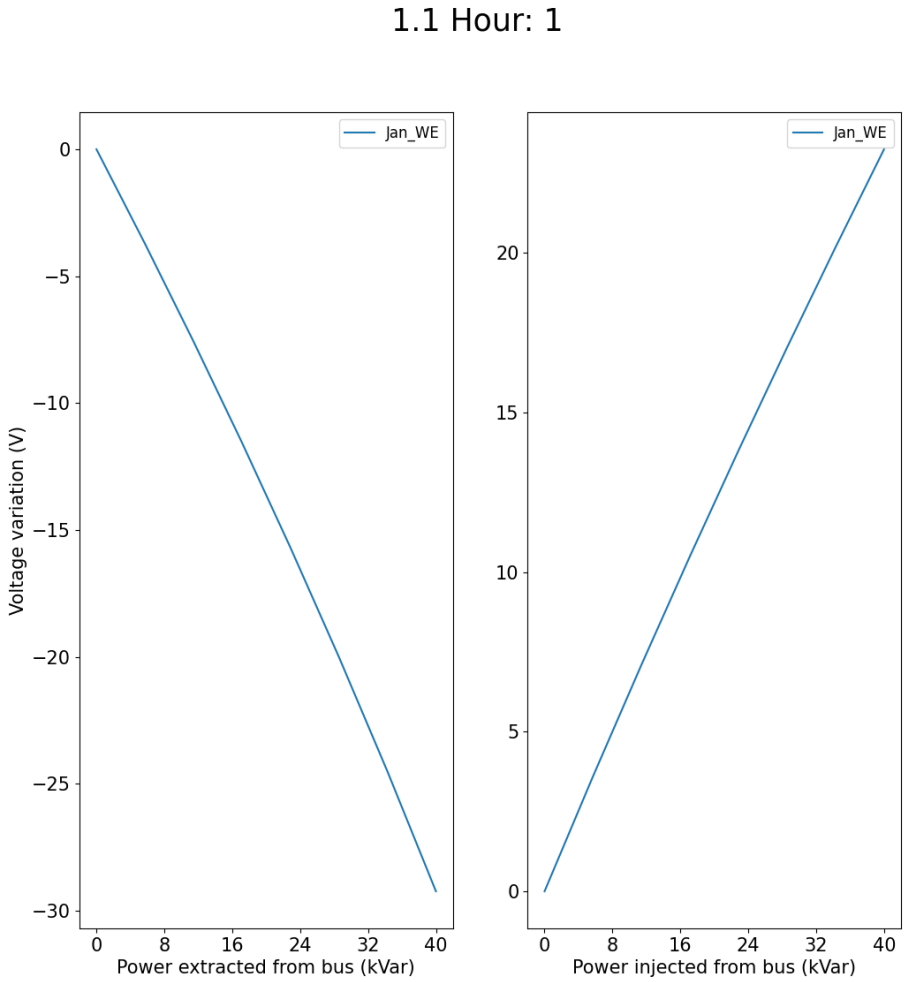

Figure 12 - Voltage variation on bus 1 for phase 1 at hour one.

After obtaining the results from battery operation optimization process, all scenarios are reviewed to identify potential voltage violations. If any violations are detected, they are mitigated through reactive power control.

Thus, in the post-optimization process, the voltage control considers the potential use of inverters to inject or extract reactive power, ensuring that voltage levels remain within the legal limits of 0.92 pu to 1.05 pu.

Two distinct scenarios are considered for reactive power control, when reactive power can be injected or extracted without affecting active power or when reactive power injection or extraction requires reducing active power to accommodate the inverter capacity.

In first case, the valuation of ancillary services related to reactive power can be based on the avoided penalties for maintaining the voltage within legal limits. In second case, the economic impact of reactive power injection stem from the reduction of active power, which affects the generation of energy credits.

The required reactive power (ΔQ) to decrease or increase voltage is calculated using Equations (60) and (61). Here, $\alpha_{kvar}^{inj/ext}$ represents the reactive voltage sensitivity factor (Section 3.3.2).

$$\Delta Q = 0 \qquad if\ 0.92 \leq V_{DER} \leq 1.05 \tag{60}$$

$$\Delta Q = \frac{\Delta V_{exc}}{\alpha_{kvar,b,h}^{inj,ext}} \qquad if\ V_{DER} < 0.92\ or\ V_{DER} > 1.05 \tag{61}$$

If the inverter capacity requires a reduction in active power injection/extraction to accommodate reactive power control, the apparent power (S) is now limited by the inverter rated capacity. The new active power injection or extraction is calculated by equation (62).

$$P_{new}^{inj/ext} = \sqrt{S^2 - \Delta Q^2} \tag{62}$$

3.5. Framework Analysis

This section provides a detailed analysis of the essential framework for formulating the VPP operational plan. Figure 13 presents the proposed methodology in a flowchart. The process begins with the reading of grid parameters,

load profiles over the analyzed, and the connections of DERs to the buses. This dataset is used to compute the power flow solution using OpenDSS, establishing the base line power flow (step 1). At this stage, the maximum power flow at substation is determined throughout the analysis period, along with the computation of model sensitivities.

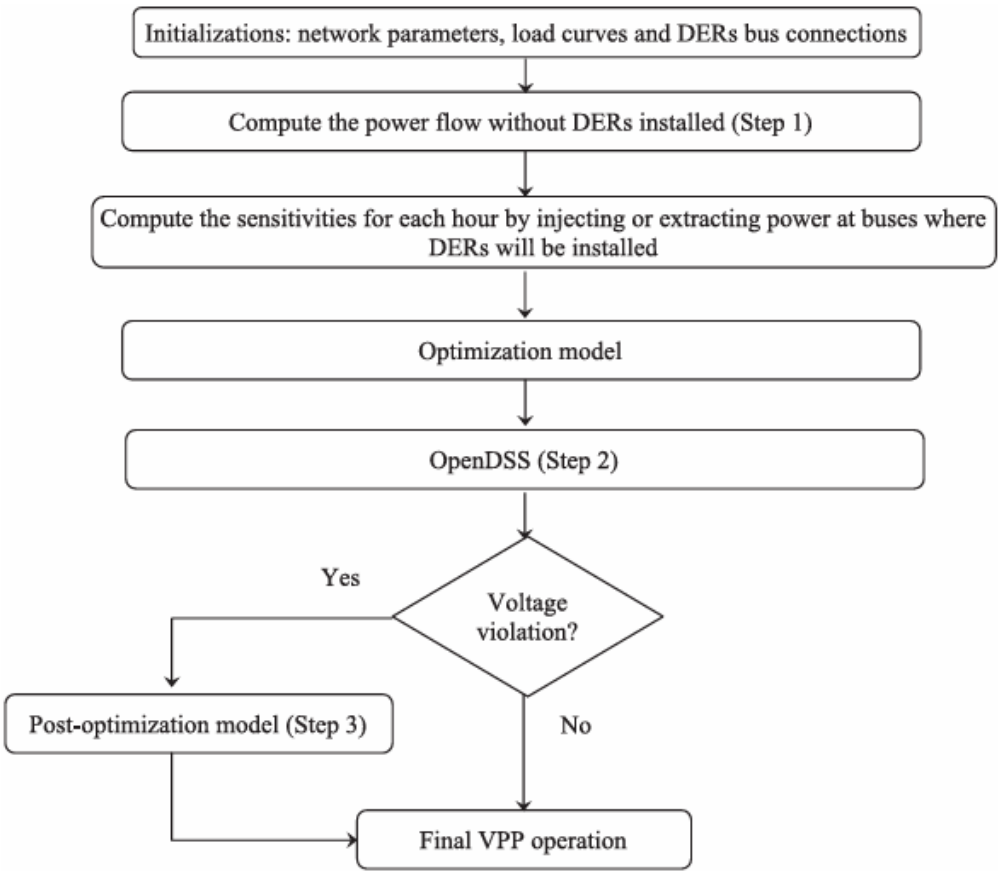

Figure 13 - Information flow of the VPP operational plan

The sensitivities related to voltage and losses are computed for each hour and day by increasing the active power injection or extraction in steps of 5 kW per phase. Additionally, the reactive voltage sensitivity is determined by injecting or extracting reactive power in 3.3 kVar steps per phase.

The optimization model is applied to formulate the VPP operational plan, scheduling the BESS charging and discharging periods to maximize the economic benefits, mitigate losses, and manage peak demand at substation throughout the analyzed period. Additionally, the optimization model aims to minimize voltage

violations. The VPP operation is simulated in OpenDSS to compute voltage levels and assess potential violations.

In cases of voltage violations, after the optimization process and power flow solution, a post-optimization step is performed. This step involves the injection or extraction of reactive power at each time interval, aligning with inverter operation to ensure that voltage levels comply with the legal limits. Finally, the VPP operational plan is scheduled.

4
Results

4.1.
ETO-2023 System Data

Simulations were performed on the ETO-2023 system to illustrate the practical implementation of the proposed model. Figure 14 shows the single-line diagram of the ETO-2023 system, where the colored circles represent the installed DERs on grid and the large blue circle at the bottom of the diagram represents the substation location of this grid. Table 3 presents the bus, type, and associated power of each DER. The DERs were chosen to evaluate the business model with different types of DERs, and the number of DERs reached was eight. The PVs systems make a higher contribution to commercial part, since these are projects that are easily viable. The BESS are oriented to ancillary services, since tariff arbitrage has a relatively lower value in energy credit. Otherwise, hybrid systems are a combination of both gains, arbitrage tariff and ancillary services.

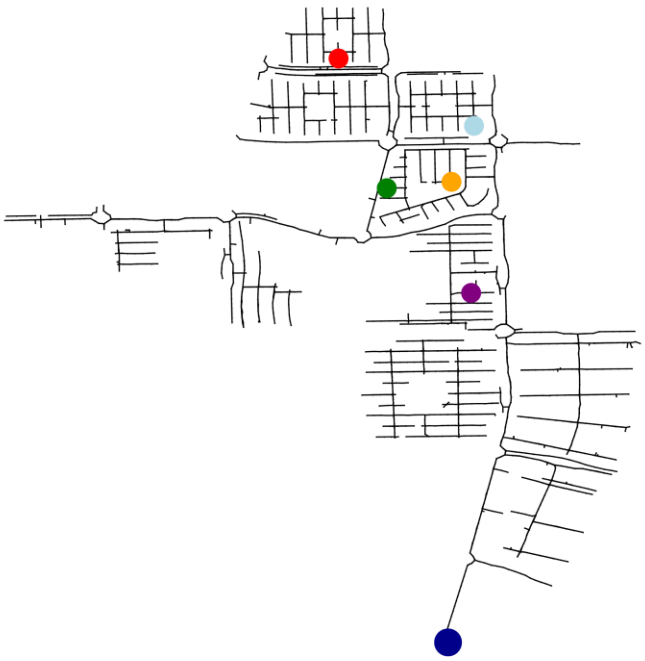

Figure 14 - Single line diagram for ETO-2023 system with DER and Substation localization

Table 3 - Information about DERs

Bus	DER	Transformer (Feeder)	Capacity (kVA)	Color at Diagram	Nominal Power	Energy
bt3136	Hybrid (PV and BESS)	bt1281	45	Red	(75 kW, 150 kW)	(-, 472 kWh)
bt3399		bt1287	75	Green		
bt4088	BESS	bt1306	45	Light blue	75 kW	236 kWh
bt3876		bt1355	150	Yellow		
bt6394	PV	bt1294	150	Purple	75 kW	-
PV1	PV	-	-	-	75 kW	-
PV2	PV	-	-	-	75 kW	-
PV3	PV	-	-	-	75 kW	-

This feeder has 6,555 buses, 20,772 nodes, three voltage levels (13.8 kV, 0.44 kV, 0.38 kV), and 545 photovoltaic systems (placed at low voltage). Furthermore, this grid has residential, rural, industrial, commercial, among others load types.

For each load type, there are nine distinct load shapes, each containing twenty-four points. The data for this corresponds to the first three months of 2023, which were the data provided by ENERGISA for validating the business model. For each month, three distinct types of data are: Weekday, Saturday and Sunday.

The simulated scenarios represent a 24-hours period for both weekdays and weekends over three months (from January to March) of 2023. These data correspond to typical weekday and weekend load profiles for the feeder used in this thesis. The reference (Massari, 2023) presents the OpenDSS simulation result used to obtain the sensitivity factors shown. It is important to note that the data used in the system were not obtained through direct measurement but rather assigned based on available information.

The tariffs considered are those applied by Energisa Tocantins in Palmas as of May 2023, as presented in Table 4. The green tariff has two time-of-use periods: peak and off-peak. The white tariff is the only one that includes three distinct periods: peak, off-peak and mid-peak. The conventional tariff is a flat rate, with no variation throughout the day. The specifications of the equipment used for DERs installation are listed in Table 5. The hours referent to each period (peak, off-peak and mid-peak) are presented in Table 6.

Table 4 - Tariffs used for contract formation

Green Tariff	
Peak	R$ 2,32 /kWh
Off-Peak	R$ 0,34 /kWh
White Tariff	
Peak	R$ 1,82 /kWh
Off-Peak	R$ 0,63 /kWh
Mid-Peak	R$ 1,14 /kWh
Conventional Tariff	
-	R$ 0,76 /kWh

Table 5 - Specification of the equipment used for DERs installation

PVs	
Capacity/panel	545 Wp
Number of panels per DER	180
Maximum injected power	75 kW
BESS	
Capacity	75 kW
Efficiency	95 %

Table 6 - Periods

Period	Hour
Peak	19, 20, 21
Off-Peak	1, 2, 3, …, 16, 17, 23, 24
Mid-Peak	18, 22

It is assumed that 100% of contracts signed for peak periods are under green tariff, meaning that contracts under the white tariff are not considered. During off-peak periods, all contracts are signed under conventional tariffs, with no contracts in the white tariff. For mid-peak periods, only white tariff is considered. For this reason, the parameters α and β are set to 1 and 0, respectively. This configuration occurs to seek the greatest possible financial gain.

To simulate the electrical system and obtain the sensitivity factors required to the proposed model, the OpenDSS platform was used with a Python interface. The optimization model was constructed in Pyomo, version 6.4.4. The total number of variables for this optimization model was 63,907 and the total of constraints was 37,379, and the simulations were divided into two groups: (i) computation of sensitivity parameter, which lasts about four hours for five DERs in grid; (ii) the optimization model, which lasts about fifteen minutes.

The technical data related to inverters, for both panel and battery, are present in Appendix C.

4.2. Sensitivity Factors Analyze

The proposed model integrates power system sensitivities related to voltage, losses, peak demand, and transformers usage. These sensitivities were computed using the OpenDSS software, where calculations are performed for all hours of the day, considering power injections or extractions at buses with installed DERs. This section provides the results for the sensitivities factors at ETO-2023 system, used in the VPP business model.

4.2.1. Voltage Sensitivity Factor

For voltage, since the DERs are installed on low voltage feeders, there is a linear relationship between active/reactive power and voltage. Consequently, constraints involving active/reactive power can be modeled as a linear function.

Figure 15 represents the voltage variation for active power extraction or injection for phase 1, and hour 1 through all days in dataset, which are weekday, Saturday, or Sunday for January, February, and March, indicated in each graphic by the legend. This linear behavior remains throughout the buses, phases, days and hours. Figure 16 to Figure 20, the voltage sensitivity factors associated with active power for each bus with a DER in ET0-2023 system are presented.

It is important to notice that the active power injection/extraction from a DER does not affect the voltage at bus with another DER, since they are not in the same low-voltage circuit, as shown in Appendix B, in ETO2023.

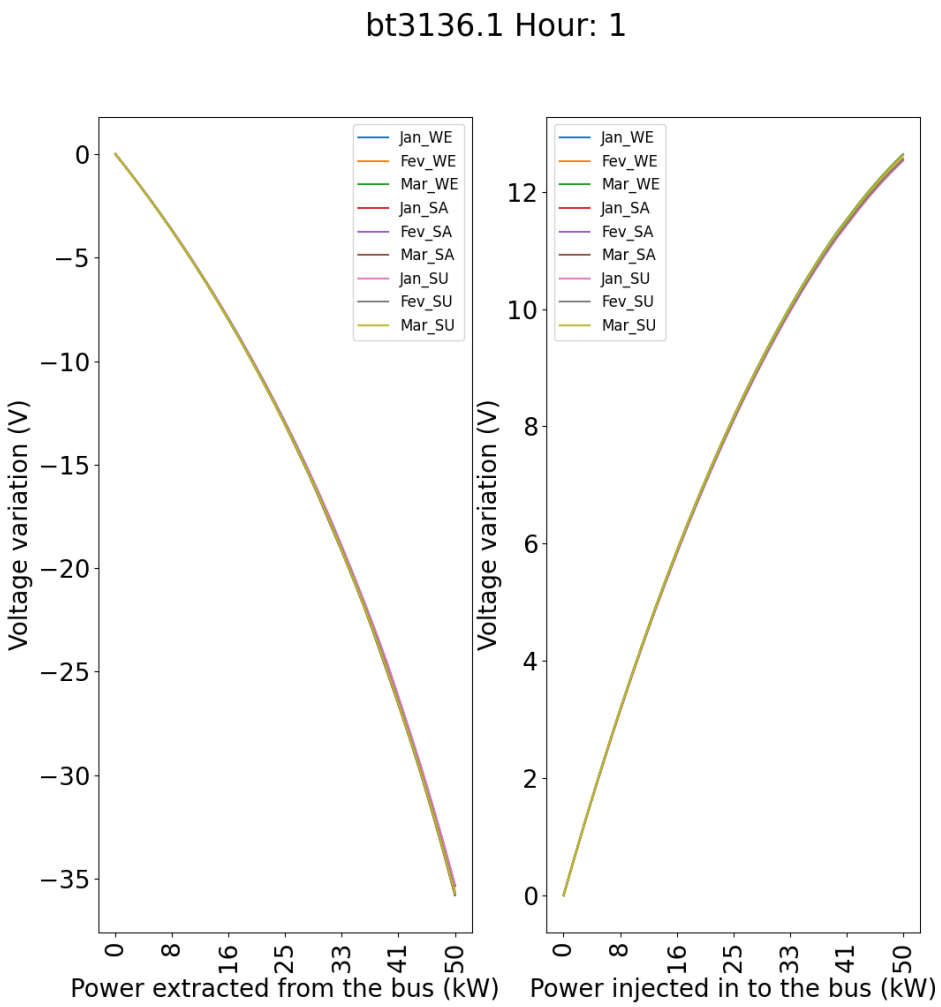

Figure 15 - Voltage variation for active power extraction (left) or injection (right) at bus 'bt3136', phase 1 and for hour 1 through all days analyzed

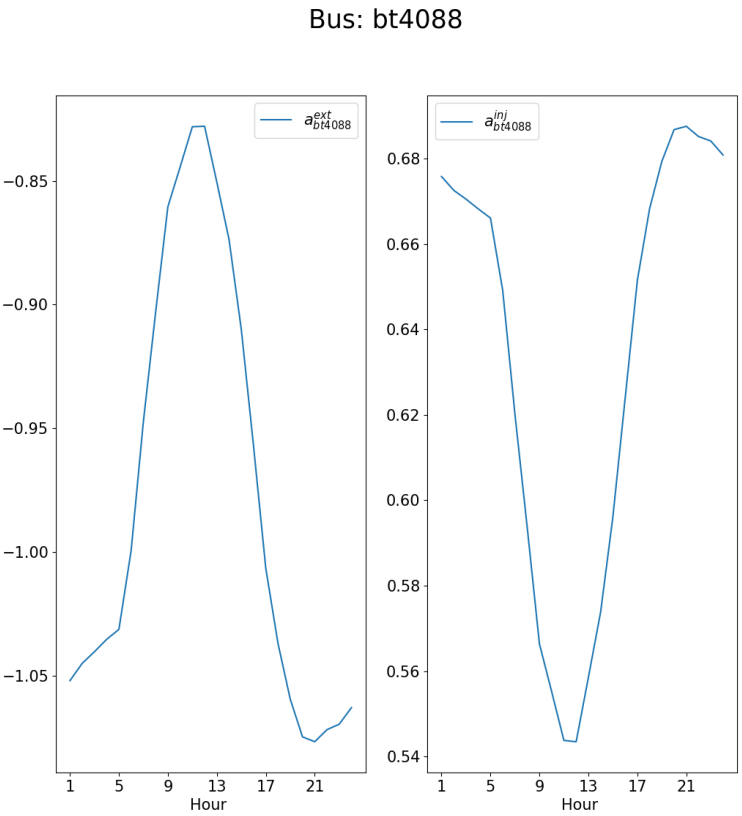

Figure 16 - Voltage sensitivity factor for active power at bus “bt4088”

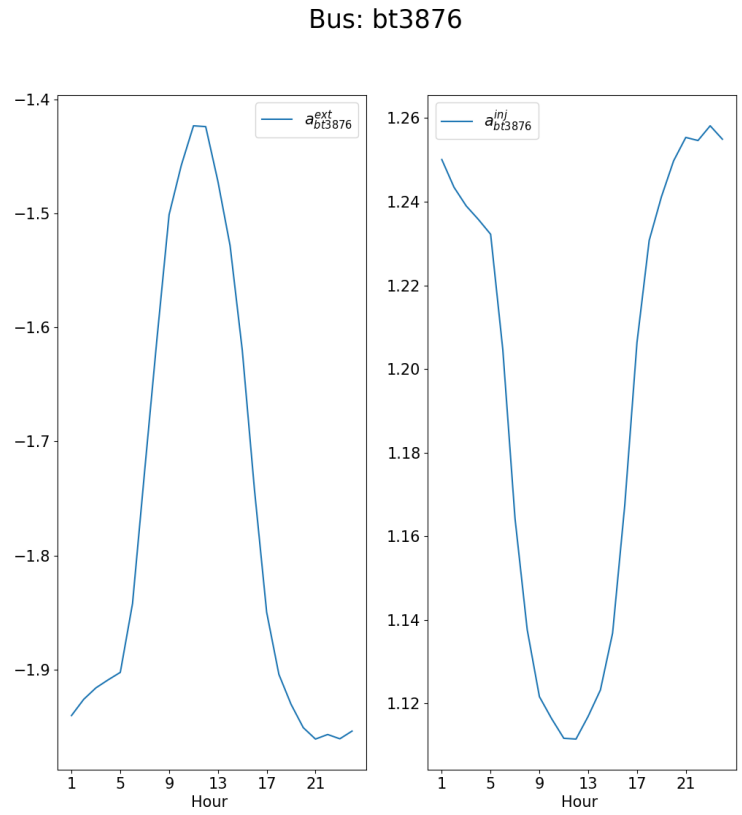

Figure 17 - Voltage sensitivity factor for active power at bus “bt3876"

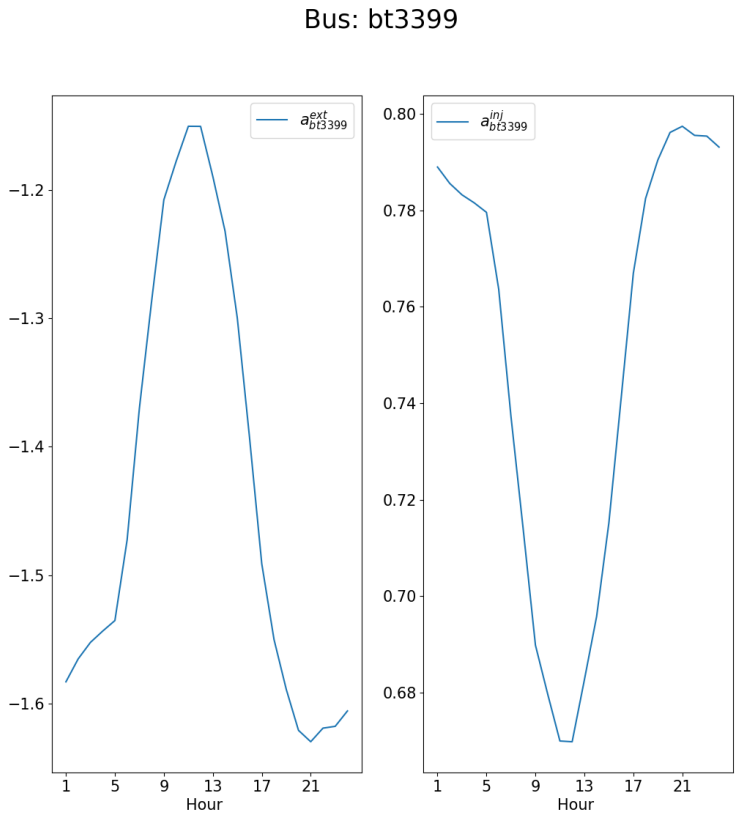

Figure 18 - Voltage sensitivity factor for active power at bus “bt3399”

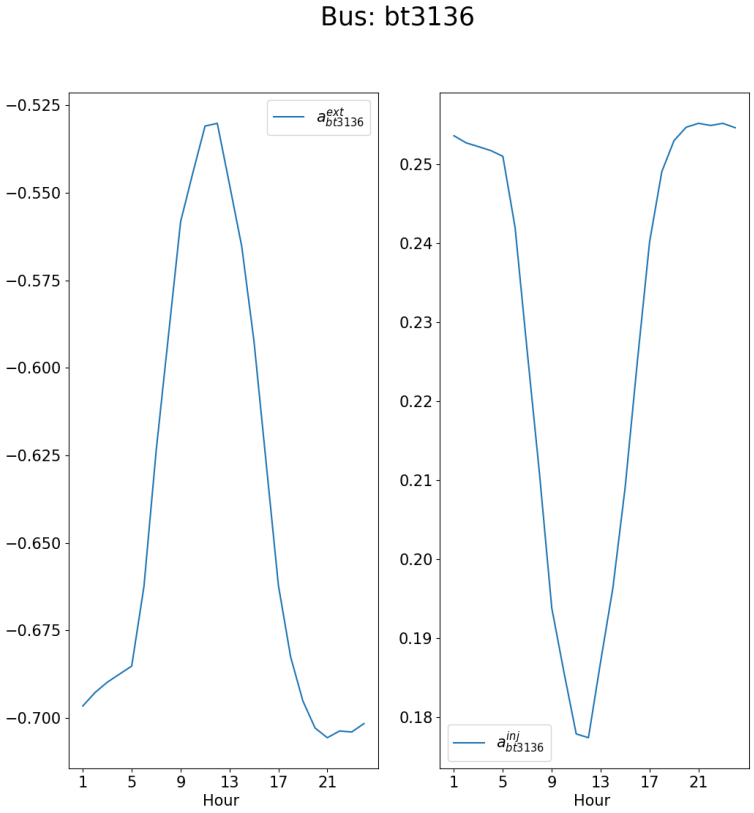

Figure 19 - Voltage sensitivity factor for active power at bus “bt3136”

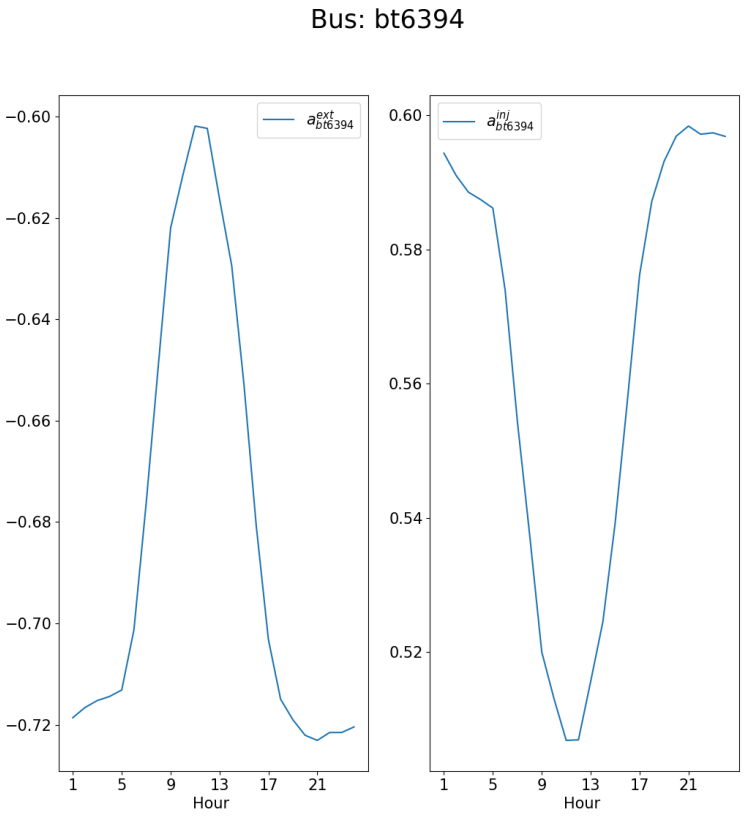

Figure 20 - Voltage sensitivity factor for active power at bus “bt6394”

4.2.2. Loss Sensitivity Factor

On the other hand, electrical losses exhibit a nonlinear pattern. To accurately characterize this behavior, the model employs three parameters, capturing electrical loss reductions, and scaling effects.

Figure 21 shows the losses variation into ETO-2023 system, due to extraction or injection of active power in the bus “bt3136” at hour 1. For the presented hour, losses are increased for active power extraction and initially reduced until reaching a minimum value then increasing again, for active power injection. This behavior continues for the rest of the day, except for the maximum injection of the PVs, where the network will already be more loaded with reverse power flow, causing only an increase in losses (as shown in Figure 22). Losses variation has the same behavior for other buses in the system.

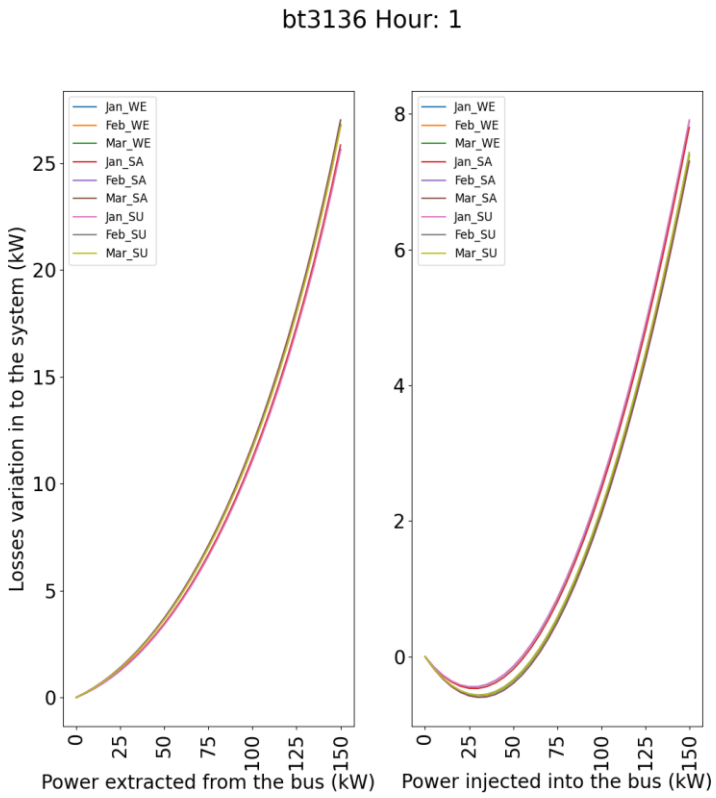

Figure 21 – Losses Variation for bus “bt3136” in ETO-2023 at hour 1

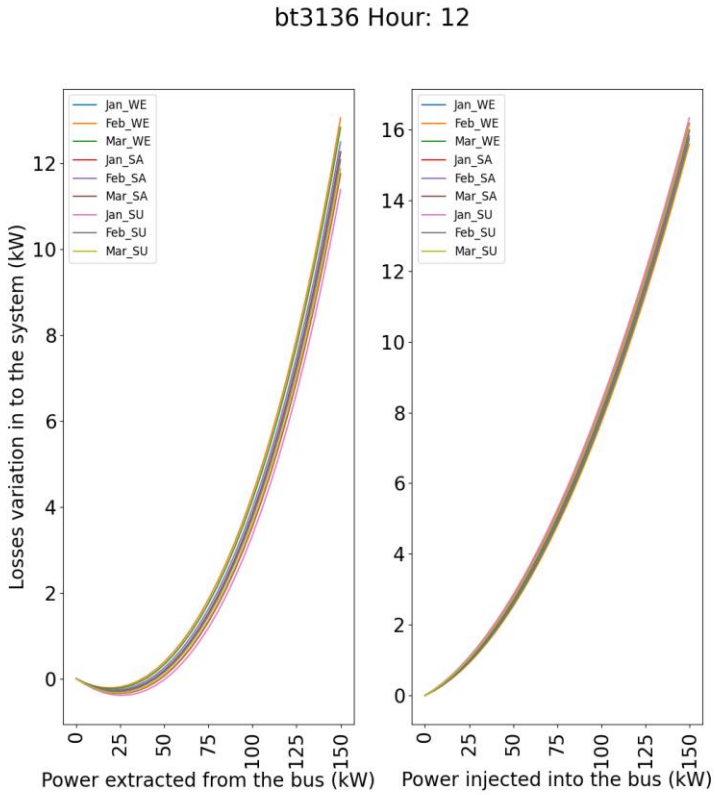

Figure 22 – Losses Variation for bus “bt3136” in ETO-2023 at hour 12

4.2.3.
Substation Power Flow Sensitivity Factor

Notably, the peak demand at the substation is directly correlated with the active power injected or extracted by the DERs, implying a direct relationship.

Figure 23 presents the substation power flow variation when active power is extracted or injected at bus “bt3136” for hour 1. It is noted that when extracted 150 kW from bus, the substation power flow variation is 170 kW, approximately, while when injected 150 kW, the substation power flow variation is -140 kW, approximately. This indicates that the relationship between active power injection or extraction and substation power flow is almost the same. Other buses with DERs have the same behavior presented here, which also extends to other days and hours.

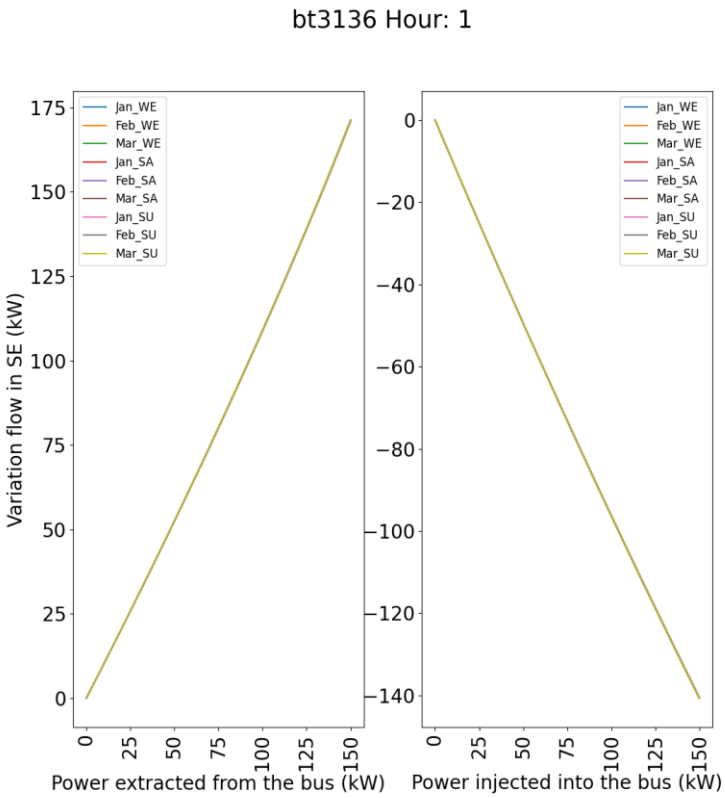

Figure 23 – Substation power flow variation for active power extraction/injection at bus “bt3136”, for hour 1

4.2.4. Transformers Power Flow Sensitivity

The relationship between transformer power flow and active power injection or extraction is the same as relationship between substation power flow and active power injection or extraction. Then, this relationship is presented in Figure 24, and it is shown that the variation is linear, with the variation of power flow at transformer is equal to the variation of active power injection at bus with DER.

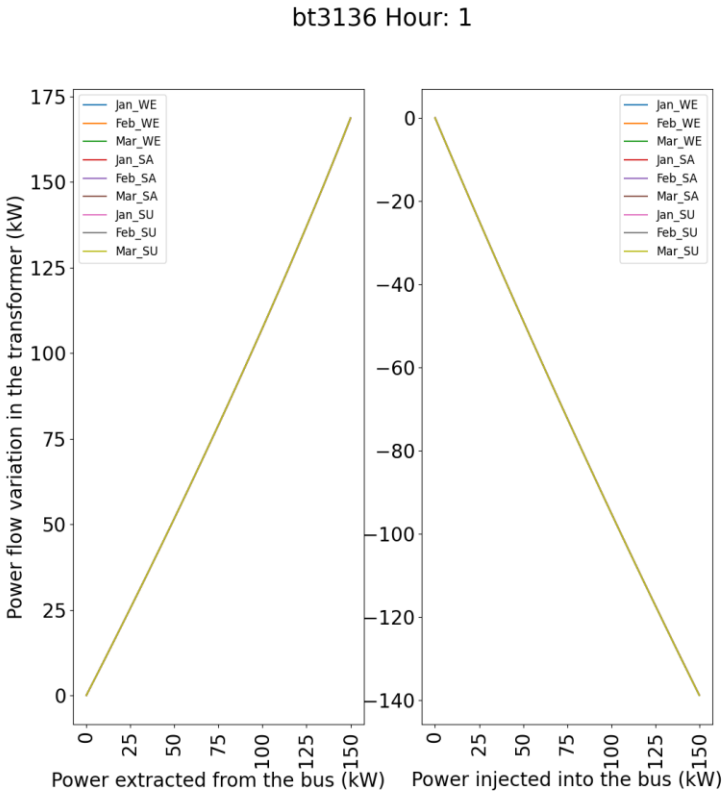

Figure 24 – Transformer power flow variation for extraction and injection of active power at bus "bt3136" in hour 1.

4.2.5. Transformers Lifespan

The associated transformers lifespan for each transformer with a DER in their circuit is presented in Figures 25, 26, and 27.

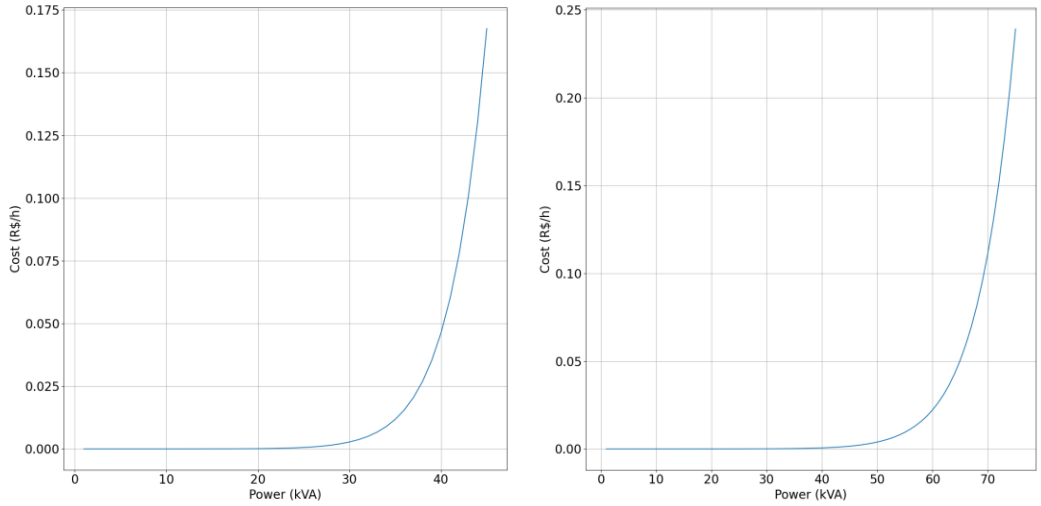

Figure 25 - Transformer lifespan cost in circuit with buses: bt3136 (left) and bt1297 (right)

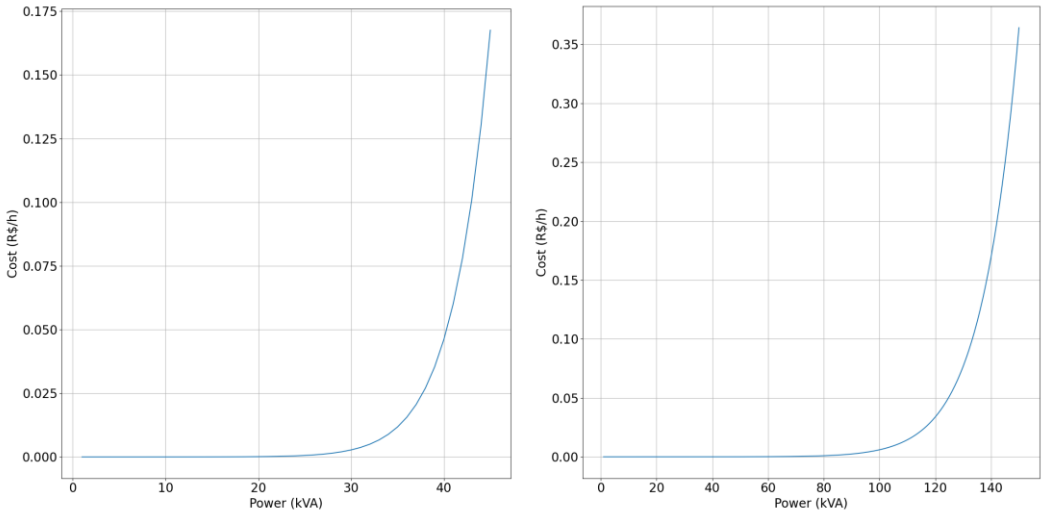

Figure 26 - Transformer lifespan cost in circuit with buses: bt4088 (left) and bt3876 (right)

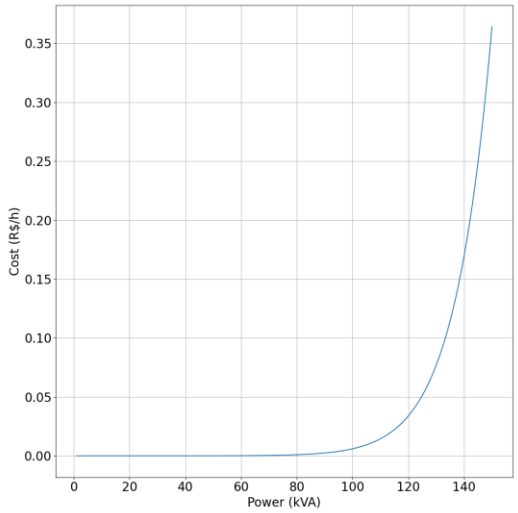

Figure 27 - Transformer lifespan cost in circuit with bus: bt6394

The transformer lifespan cost per hour is zero, in all transformers, when charging is less than 66% of their nominal rate. When charging is greater than 66%, the costs per hour start to increase, reaching the maximum value at nominal load. If the transformer operates with overload, then their lifespan cost per hour is highly increased.

4.3. Commercial Results

This section provides the commercial results from the business model for the VPP via MINLP. It is considered as VPP operation the sum of the net power (from the PV generation and BESS charge or discharge) for all DERs, for each day and hour. The revenue associated with each contractual modality is the product between the net energy and the tariff associated with that modality and the period for each modality.

Figure 28 presents the VPP operation over nine analyzed days, considering all eight DERs: five of them connected to the ETO-2023 grid, and the remaining three not physically installed in the system (not associated with grid sensitivities), to compose VPP, increasing commercial gains. Throughout these nine days, the PV generations are bigger than the BESS charging, resulting in creation of energy credits. All energy stored during off-peak times is partially discharged during peak hours, since the model is designed to maximize the revenue from energy injection,

when tariffs are higher. Other parts of the energy charged are discharged during off-peak and mid-peak periods, become energy credit in these periods and used for ancillary services.

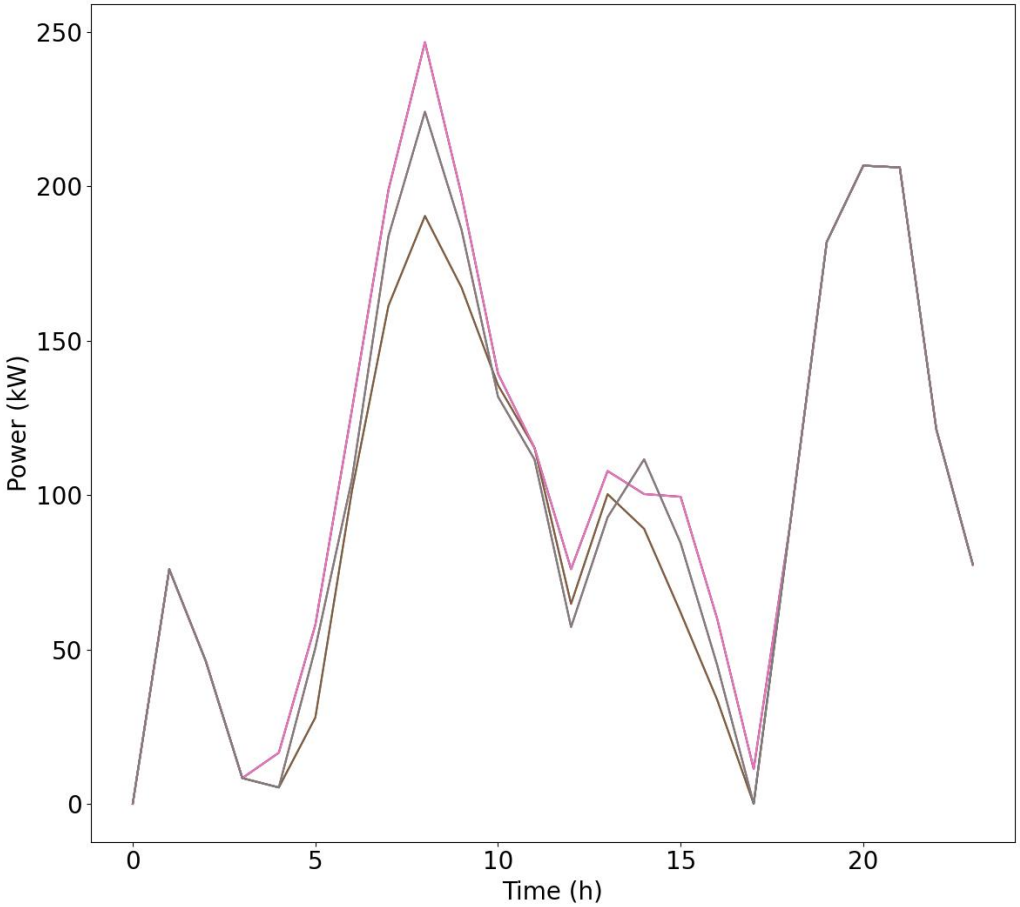

Figure 28 - Virtual Power Plant operation through all days and with 8 DERs

Table 7 presents the revenue associated with each contractual modality and tariff post over nine-days analysis, as well as the annualized revenue[1]. As expected, the highest revenue is generated by BESS discharging during peak periods, due to the arbitrage obtained when charging the battery with energy credits from PV generation. On the other hand, the revenue linked to mid-peak contracts is more associated with ancillary services. This occurs because the battery reduces its discharge during peak periods to partially discharge in mid-peak periods, thereby helping to avoid having overvoltage during peak periods.

[1] Annualized revenue was calculated as follows: $Revenue \cdot \frac{365}{9}$

Table 7 - Revenue for each contract modality and tariff post over nine days of analysis

Contract	Period	Energy (kWh)	Tariff (R$/kWh)	Revenue (R$)	Annualized Revenue (R$)
Green (A4)	Peak	5,031.08	2.32	11,695.01	474,297.50
Conventional	Off-Peak	16,503.07	0.76	9,908.09	458,119.11
White Tariff	Mid-Peak	2,382.81	1.14	2,721.55	84,848.16
Total	-	25,103.44	-	27,082.67	1,017,264.77

When considering ancillary services, it is important to observe the variations in electrical losses, maximum power demand at the substation, accumulated energy in mid-peak periods, transformers lifespan and replacements, and the reactive energy needed to compensate for active power.

4.4. Technical Results

To evaluate the technical results of the proposed business model, the results were separated in three distinct scenarios: the first scenario is the simulations of the circuit without DERs, denominated step 1, second scenario is simulations of the circuit with DERs operation originating from the VPP business model (optimization model), denominated as step 2, and third scenario is the simulations of the circuit with inverters operation, if needed to regulate voltage and ensure compliance with statutory limits, also denominated as step 3.

Figure 29 presents the voltage for each node with installed DERs, in each scenario. PVs, that are not installed in ETO-System, were not analyzed in this stage, since there are no simulated sensitivities. Step 1 revealed voltage limits violated at specific buses, days, and hours. Instances of undervoltage were observed during the early morning period and near peak periods, while overvoltage occurred around 12:00 PM, when PV systems inject their maximum power into the grid. It can also be observed that the DERs operations computed in step 2 were not sufficient to maintain voltage within acceptable limits, controlling some buses, however, in other buses, presents overvoltage at peak-times, due to BESS injection, and in off-peak times due to the injection of PV or hybrid system. These results reinforce the necessity of inverters operation (step 3), which consumes reactive power from grid

to reduce the voltage, or inject reactive power on grid to raise voltage, if needed, regardless of the type of the DER, controlling the voltage within statutory limits.

Table 8 - Ancillary services associated with active energy or power reduction.

Ancillary Services	Step 1 (Without DERs)	Step 2 (With DERs)	Difference (Step1 - Step2)
Losses in peak periods (kWh)	4,009.72	4,037.03	-27.31
Losses in off-peak periods (kWh)	14,743.89	14,966.47	-222.58
Losses in intermediate periods (kWh)	2,366.77	2,365.07	1.70
Maximum power demand (kW)	4,692.05	4,492.47	199.58
Active Energy Credit in peak to the intermediate (kWh)	0.00	1,793.68	1,793.68
Active Energy Credit in peak to off-peak (kWh)	0.00	2,412.70	2,412.70
Ancillary Services	Step 1 (Without DERs)	Step 3 (Inverters)	Difference (Step1 - Step3)
Active Energy credit (kWh) to the reactive energy (kVArh)	0.00	686.14	686.14

Table 9 - Reactive energy associated with ancillary services without compromising optimal commercial operation.

Ancillary Services	Step 3 (Inverters operations)
Inductive energy in peak periods (kVArh)	125,55
Inductive energy in off-peak periods (kVArh)	1,711.30
Inductive energy in mid-peak periods (kVArh)	46,25
Capacitive energy in peak periods (kVArh)	1,056.04
Capacitive energy in off-peak periods (kVArh)	1,539.36
Capacitive energy in mid-peak periods (kVArh)	511.18

Figures 30 to 37 illustrate DERs operations from step 2. Positive values indicate energy injection into the grid, while negative values represent energy extraction from grid. It is important to highlight that, although voltage control is a

crucial aspect of the optimization model, commercial results also play a crucial key. The BESS operation prioritizes charging during off-peak hours (around noon), not only extracting power from the grid, but also charging from PV systems, maximizing the tariff arbitrage, also contributes to voltage control, in addition to reducing impacts of electrical losses. The discharge occurs during peak hours to maximize commercial benefits, and for peak shaving.

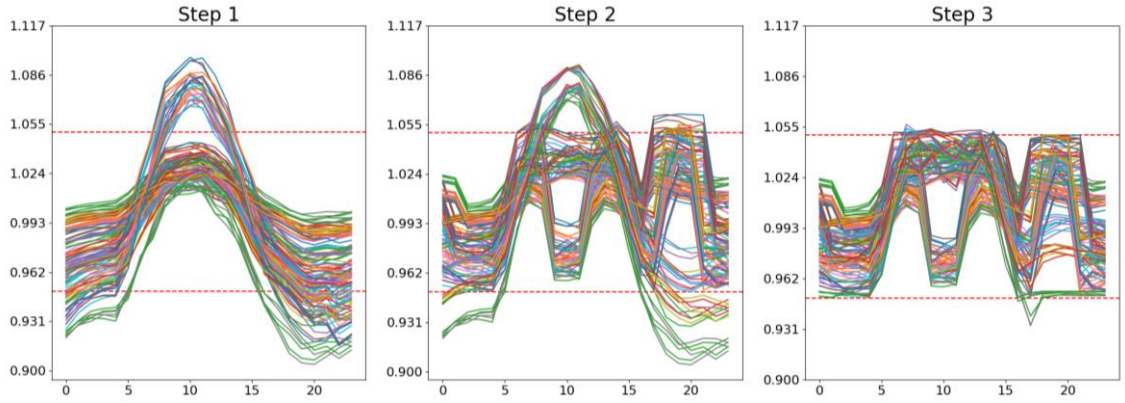

Figure 29 – Voltage in each node with installed DER, in steps 1, 2, and 3

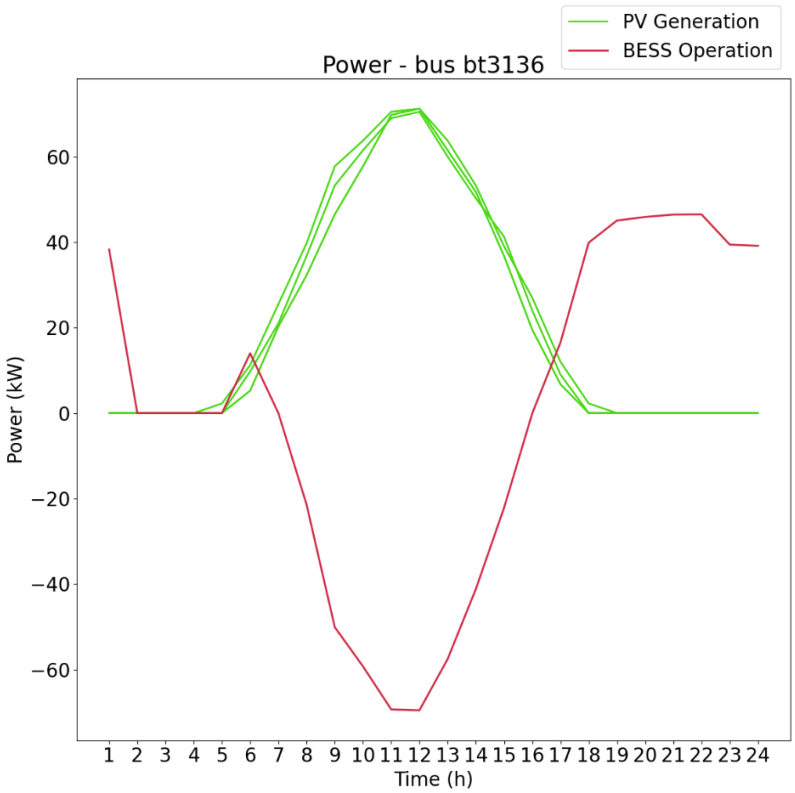

Figure 30 – DER (Hybrid) operation connected at bus bt3136

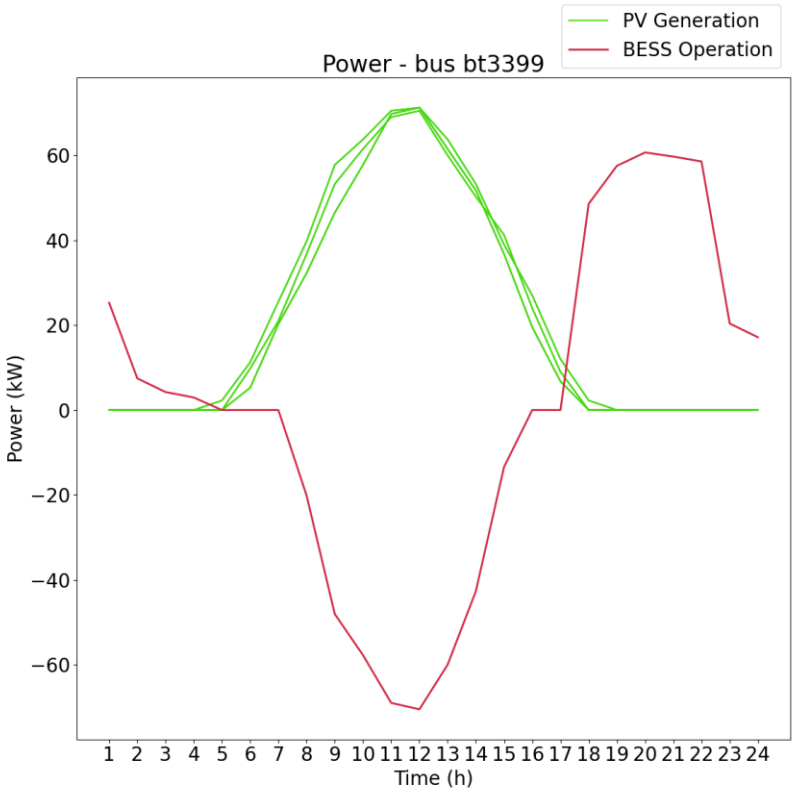

Figure 31 – DER (Hybrid) operation connected at bus bt3399

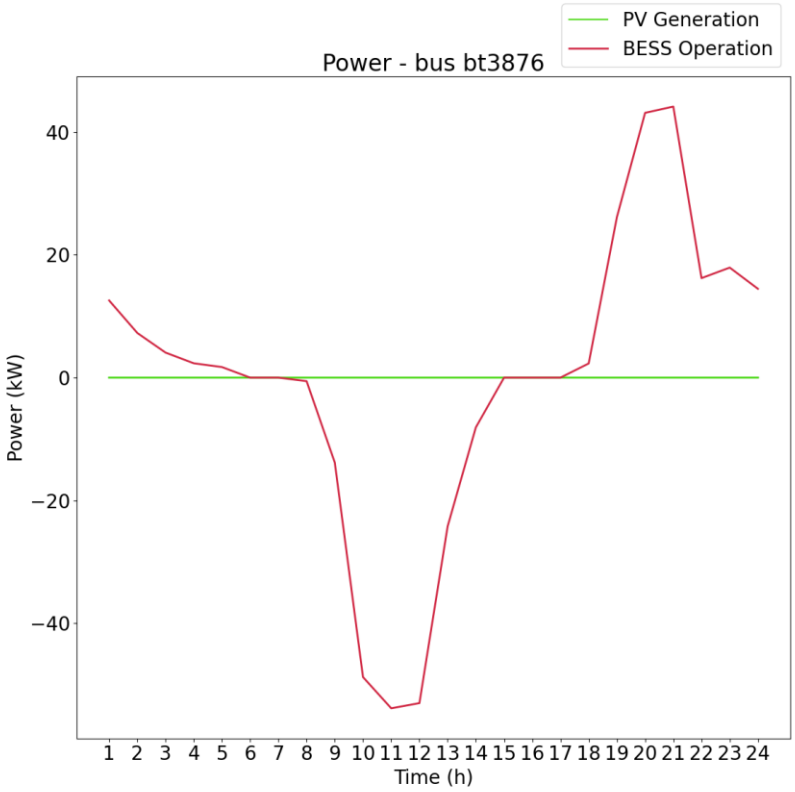

Figure 32 - DER (BESS) operation connected at bus bt3399

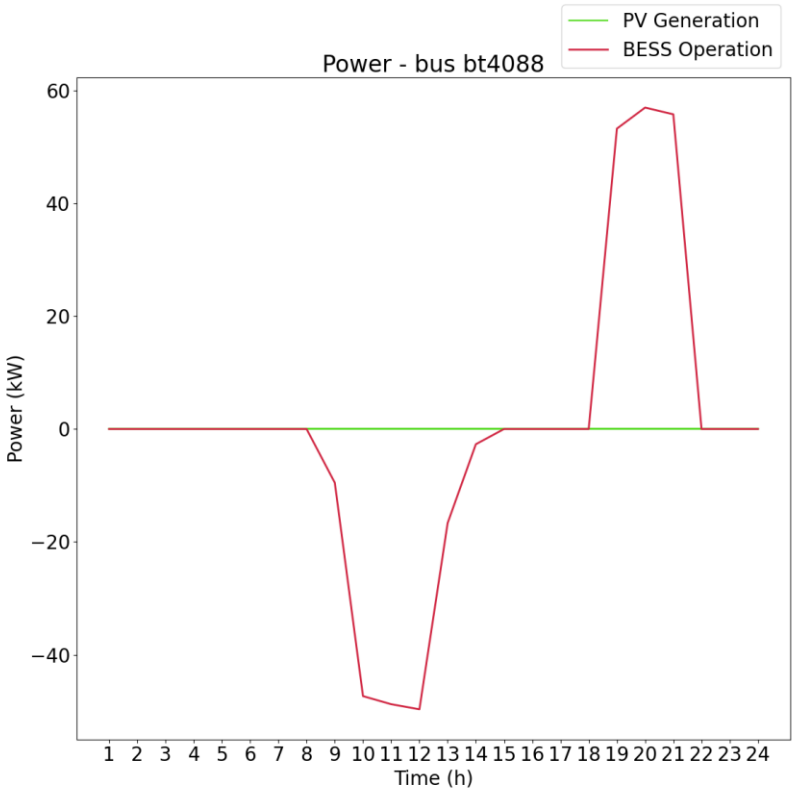

Figure 33 - DER (BESS) operation connected at bus bt4088

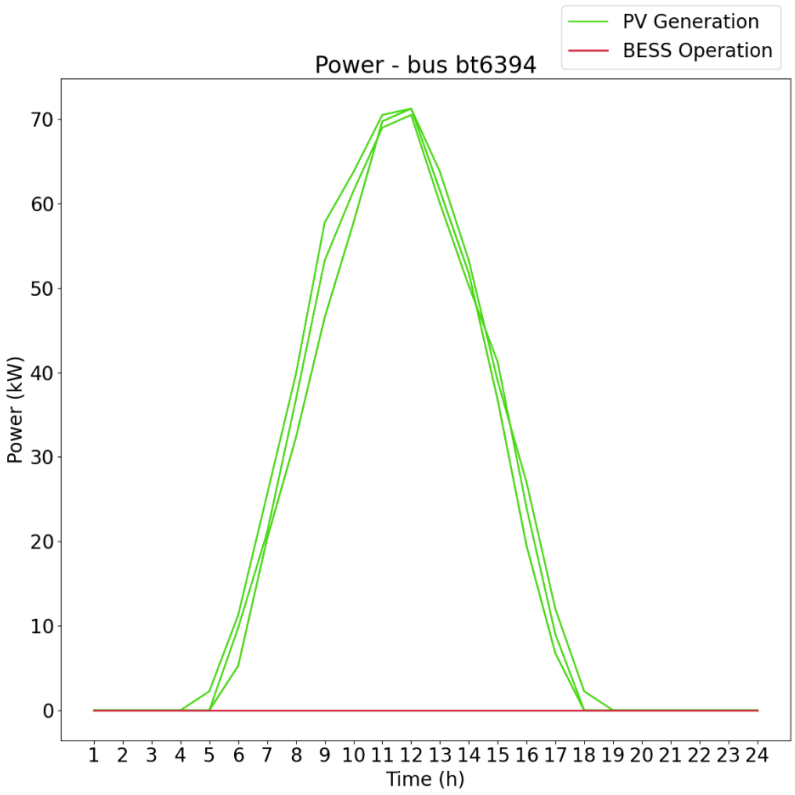

Figure 34 - DER (BESS) operation connected at bus bt6394

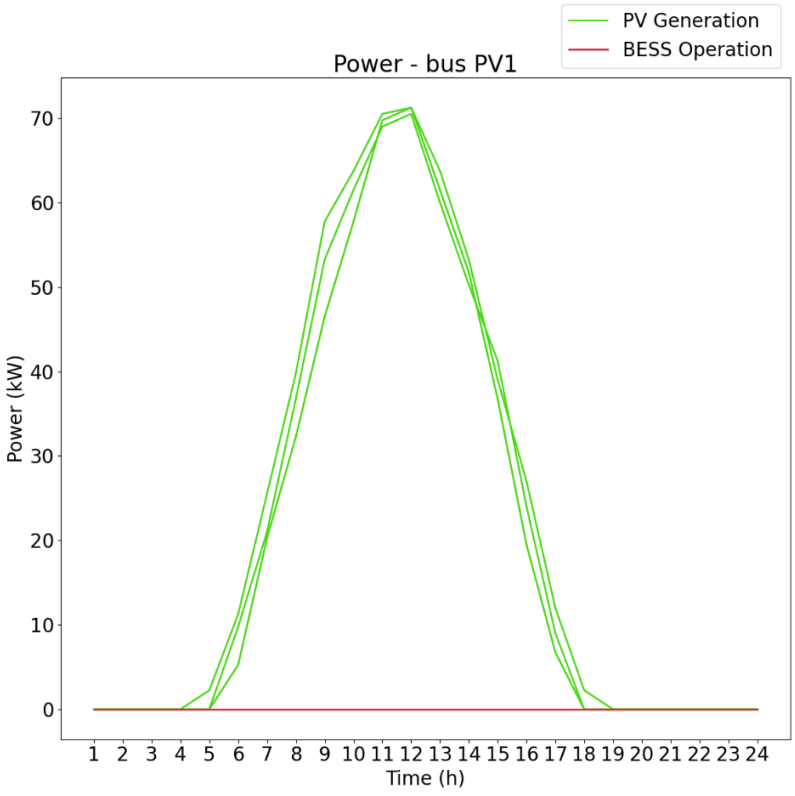

Figure 35 – PV 1 operation: connected outside the ETO-2023 grid

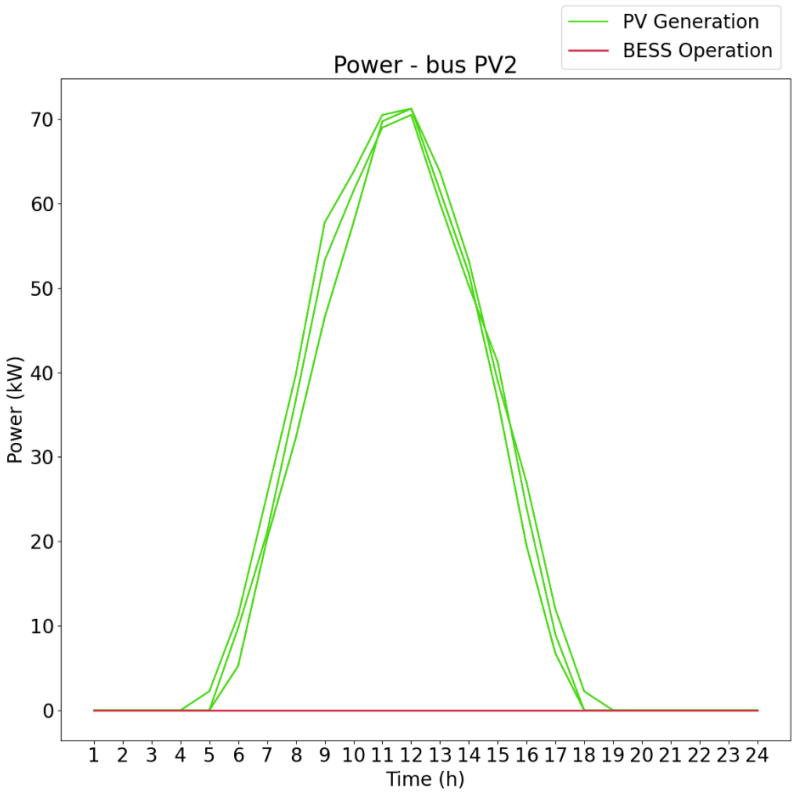

Figure 36 - PV 2 operation: connected outside the ETO-2023 grid

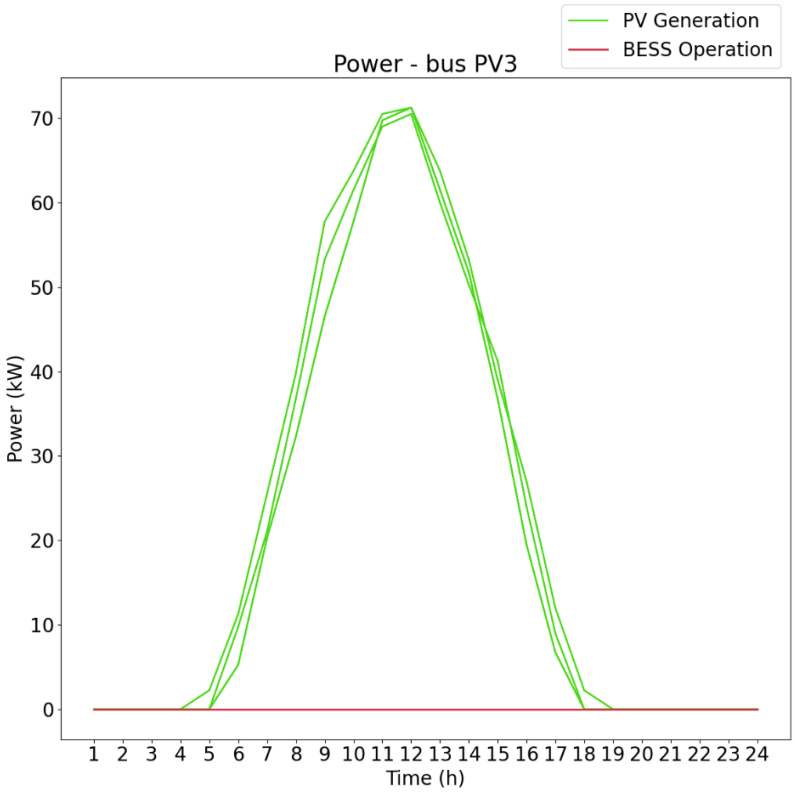

Figure 37 - PV 3 operation: connected outside the ETO-2023 grid

Figures 38 to 47 present voltage profile before and after the implementation of BESS operation, in all three phases for all buses with DER. After BESS operation, some buses still present overvoltage. These buses are “bt3399” (all three phases), and “bt3876” (phase 2 and 3). Most of the overvoltage occurrences are due to linear approximation adopted in the model, which tends to leave a small slack in the voltage constraints. Additionally, in certain situations, overvoltage is a result of commercial optimization becoming more advantageous to dispatch slightly more energy during peak hours rather than reduce dispatch and inject energy at off-peak hours. Furthermore, there is overvoltage on bus “bt6394”, however there is no BESS installed on this bus, then voltage control must be done only by reactive control of the inverter. In this same bus, it still has undervoltage, caused by own grid behavior. Figures 41, 43, and 47 illustrate the voltage profile for these specific buses and phases. For all other buses, voltage level remained within the regulatory limits, and no violations were observed.

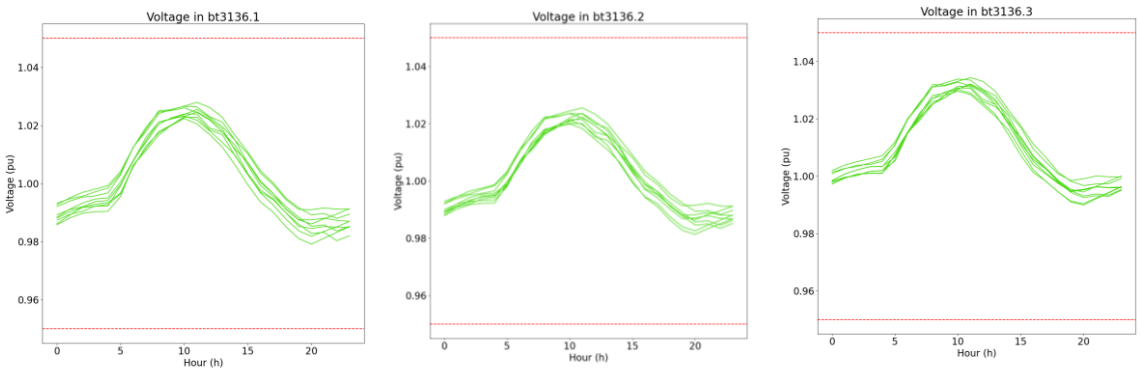

Figure 38 - Voltage at bus bt3136, for three phases in step 1

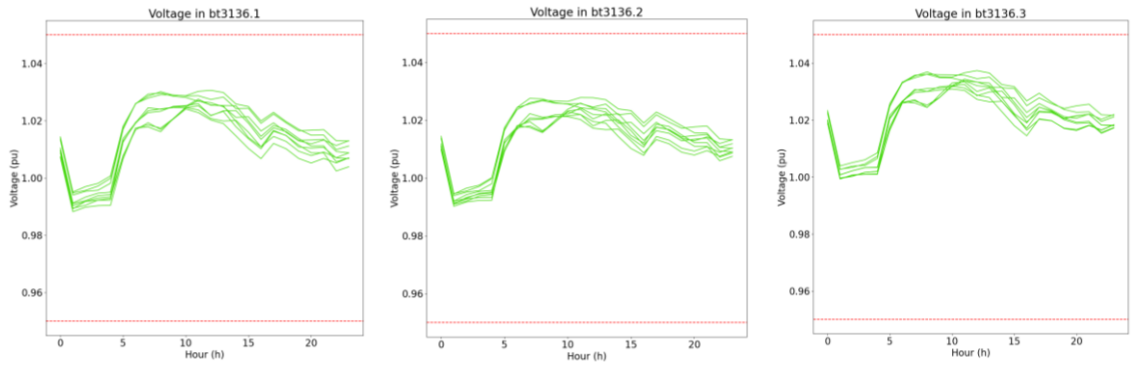

Figure 39 - Voltage at bus bt3136, for three phases in step 2

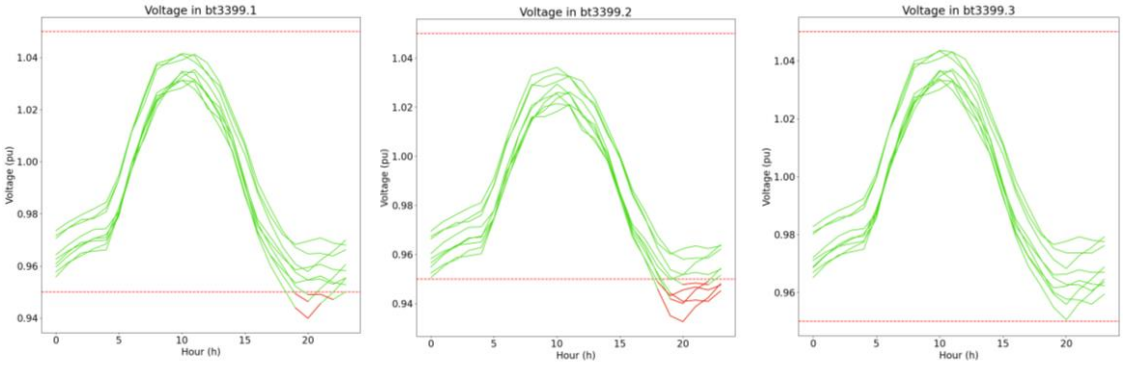

Figure 40 - Voltage at bus bt3399, for three phases in step 1

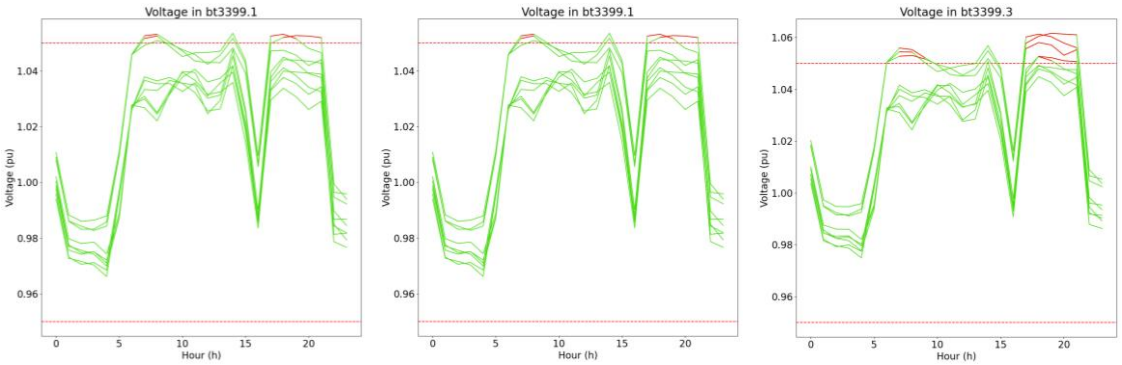

Figure 41 - Voltage at bus bt3399, for three phases in step 2

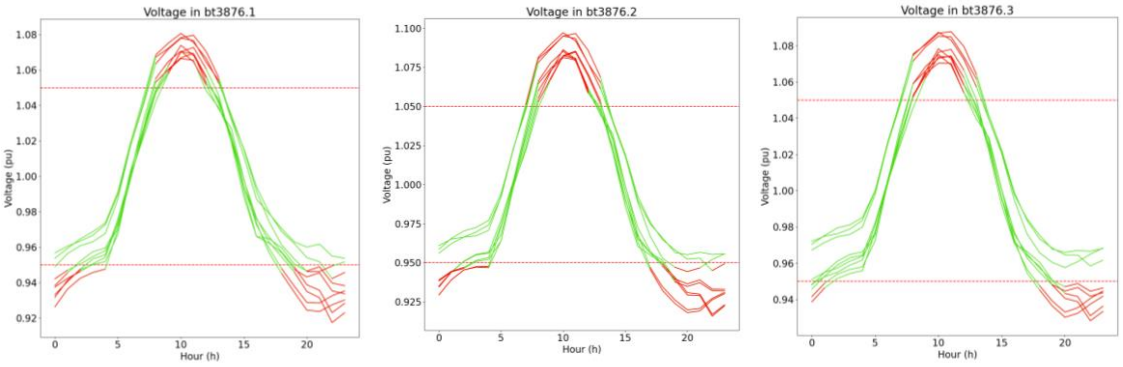

Figure 42 - Voltage at bus bt3876, for three phases in step 1

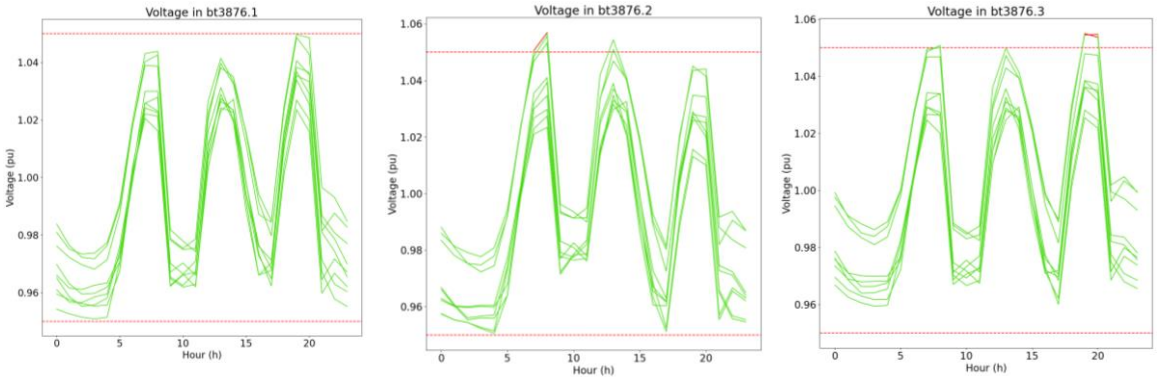

Figure 43 - Voltage at bus bt3876, for three phases in step 2

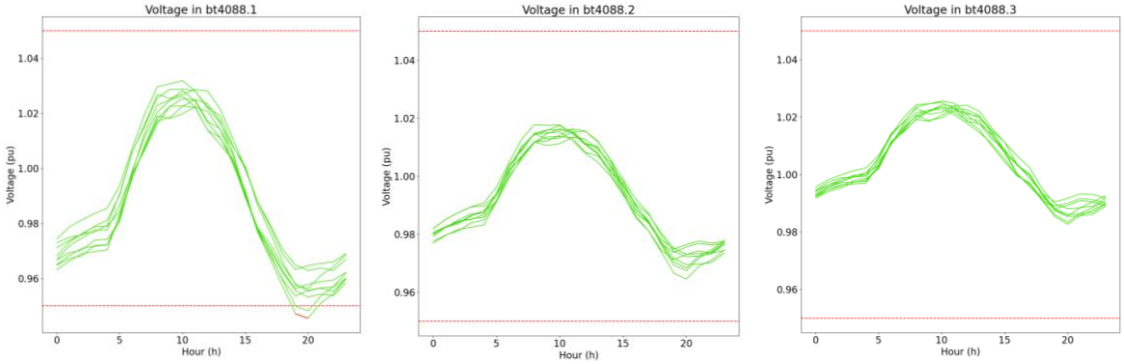

Figure 44 -Voltage at bus bt4088, for three phases in step 1

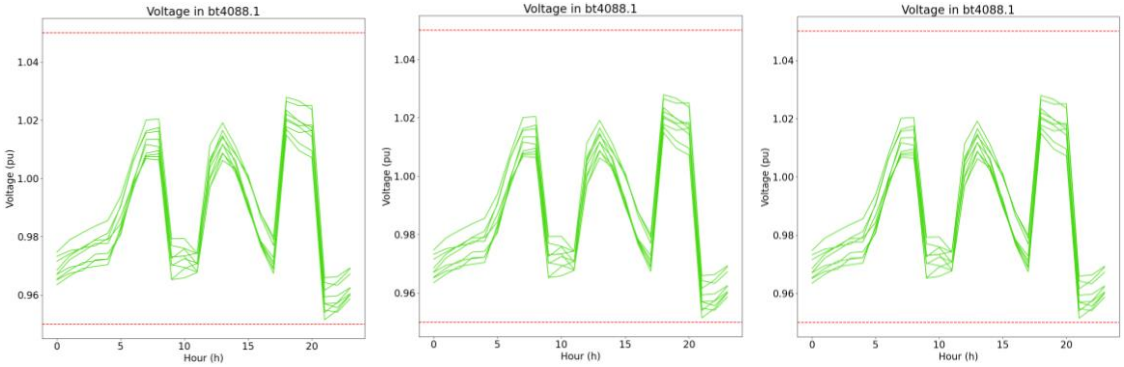

Figure 45 -Voltage at bus bt4088, for three phases in step 2

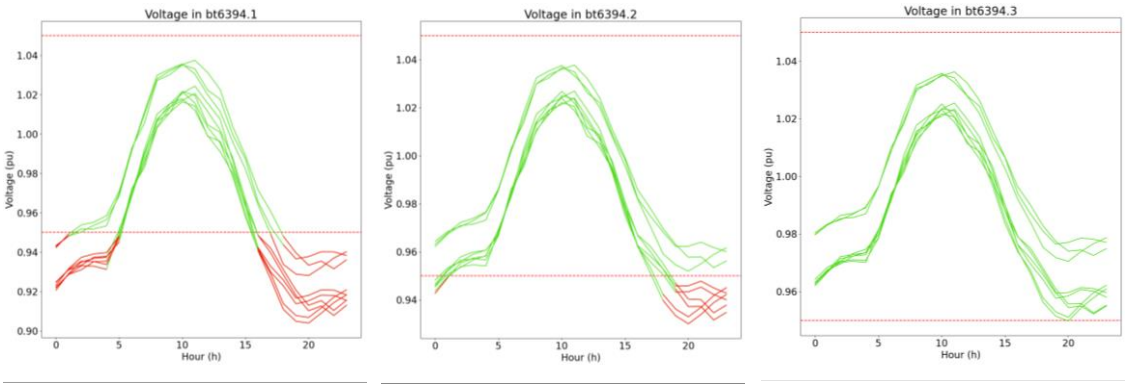

Figure 46 - Voltage at bus bt6394, for three phases in step 1

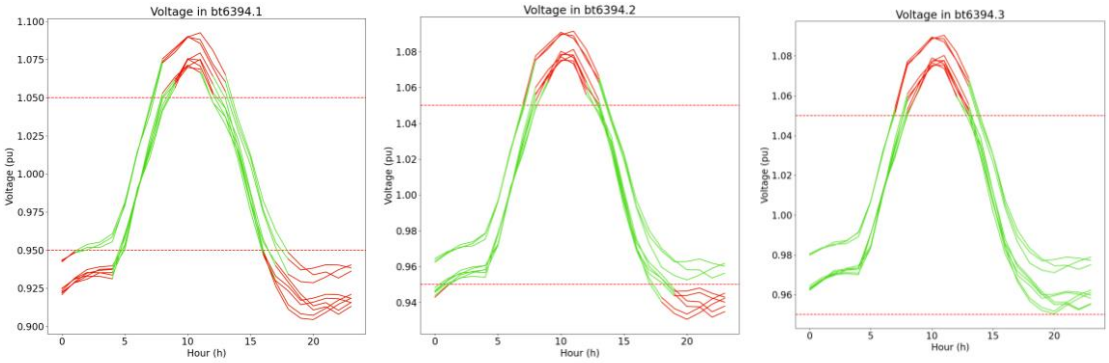

Figure 47 - Voltage on bus bt6394, for three phases in step 2

To keep voltages within regulatory limits, it is necessary to consider the inverters operation. Figures 48 to 52 show this operation for reactive power injection or extraction. Positive values indicate power extraction while negative values indicate power injection. It is observed that inverter activation occurs only during periods of voltage violation, identified in step 2. Additionally, in some periods, curtailment can occur due to the inverter capacity limits.

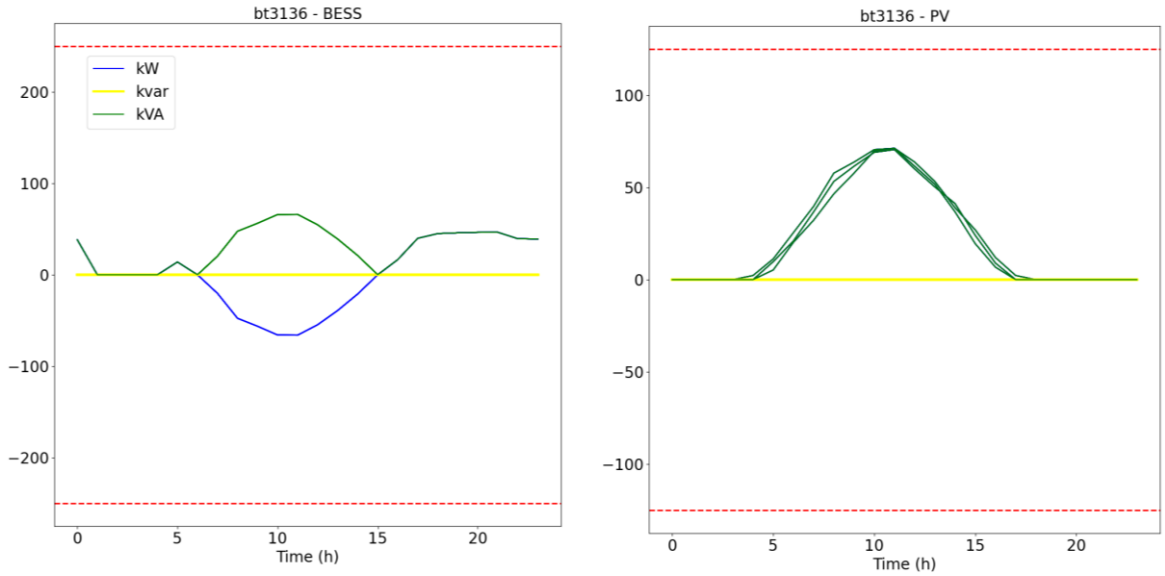

Figure 48 - Inverter operations for BESS and PV on bus bt3136

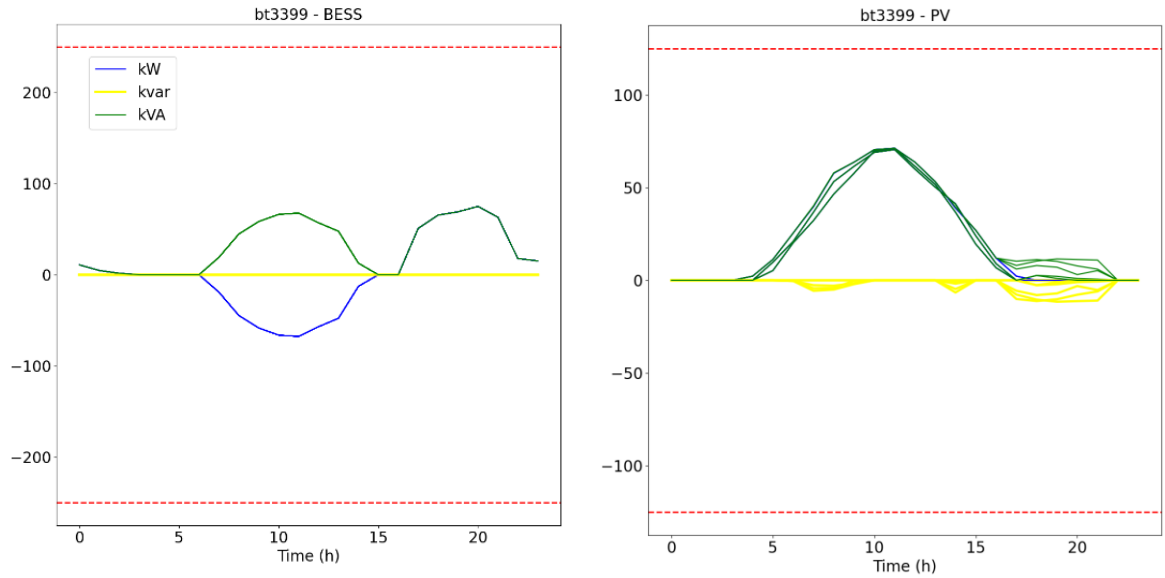

Figure 49 - Inverter operations for BESS and PV on bus bt3399

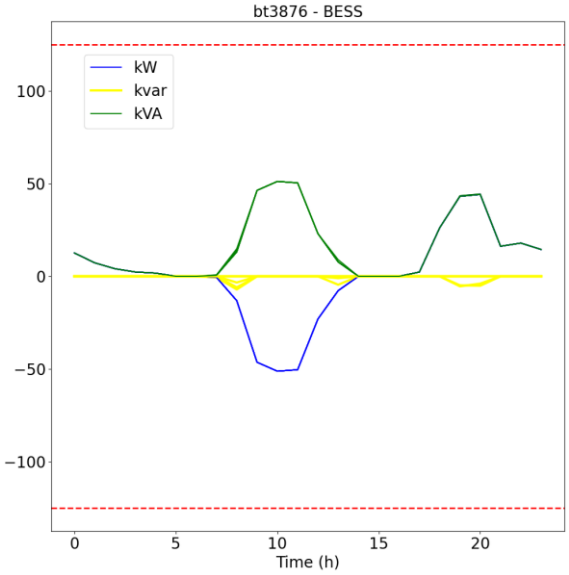

Figure 50 - Inverter operations for BESS on bus bt3876

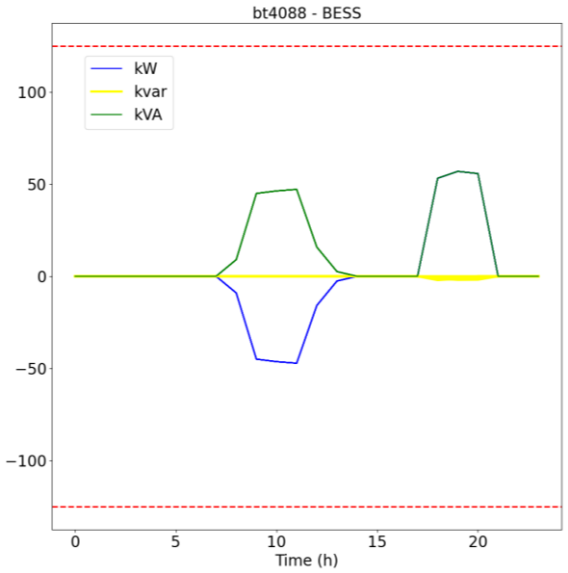

Figure 51 - Inverter operations for BESS on bus bt4088

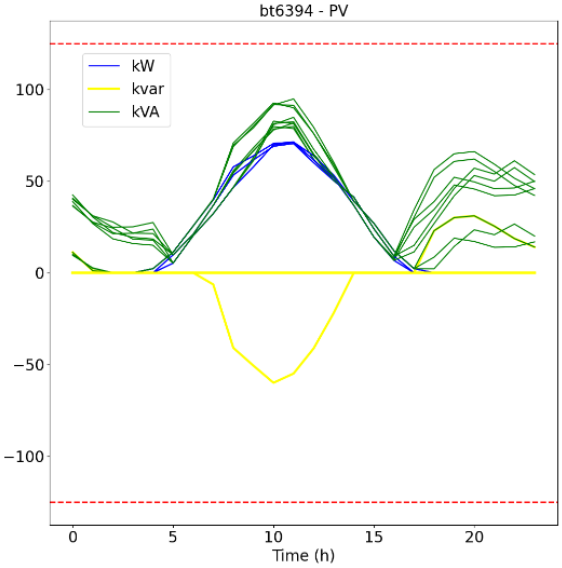

Figure 52 - Inverter operations for PV on bus bt6394

After the inverter operation, as shown in Figures 48 to 52, it can be observed that the amount of inductive reactive energy required to mitigate overvoltage's during peak hours is the highest, due to conditions occurring at buses "bt3399", and "bt3876" during these periods. Figures 49 and 50 demonstrate this behavior. Also, PV inverters use capacitive reactive power on bus "bt6394", which demands a significant amount. Figure 52 illustrates this amount, and PV generation is higher during off-peak periods, which would suggest a large voltage increase. However, the BESS can accommodate this energy, avoiding the need for large voltage reductions. Therefore, inverters consume only a small amount of reactive power to maintain voltages within permitted limits, except at bus "bt6394", which has only PV installed. In this case, the inverter must use a greater amount of reactive power.

Figures 53, 54, 55, 56, and 57 present the voltage profile after the inverter operation. It is presented that the voltage remains within regulatory limits. Buses "bt3399" and "bt3876" and "bt6394", which presented overvoltage previously, with the inverter operation, this overvoltage has been eliminated. The undervoltage on bus "bt6394", as also controlled.

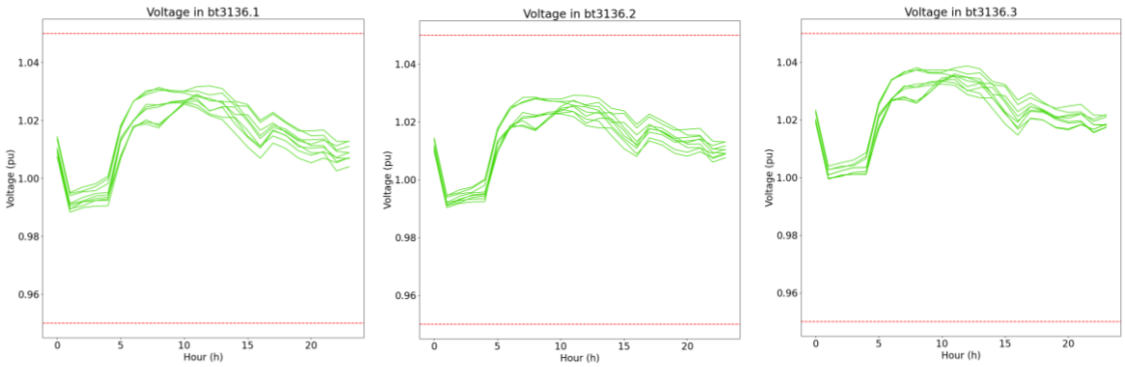

Figure 53 - Voltage on bus bt3136, for three phases in step 3

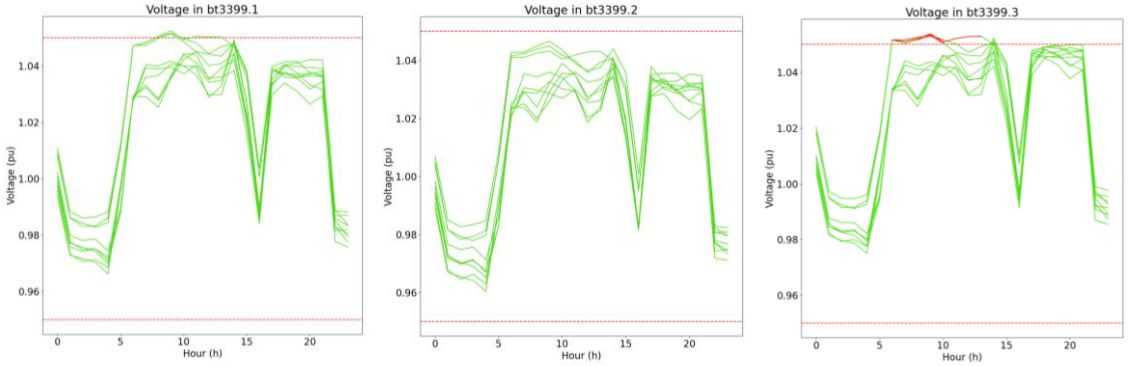

Figure 54 - Voltage at bus bt3399, for three phases in step 3

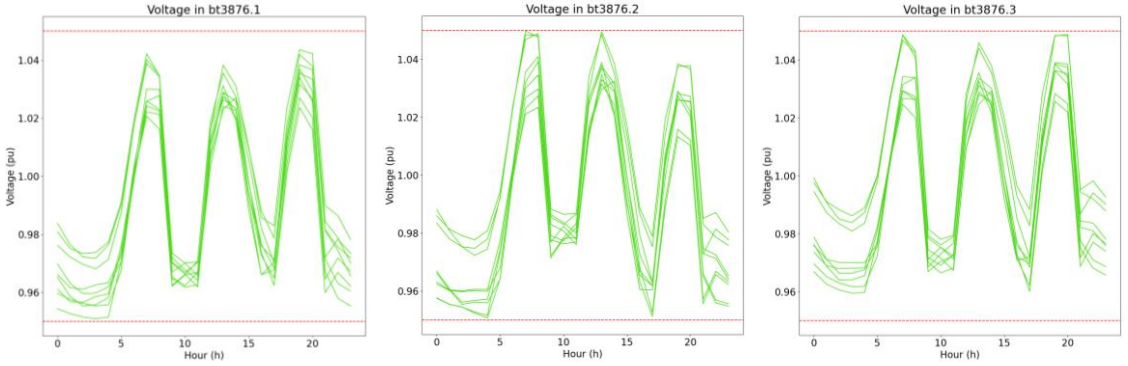

Figure 55 - Voltage at bus bt3876, for three phases in step 3

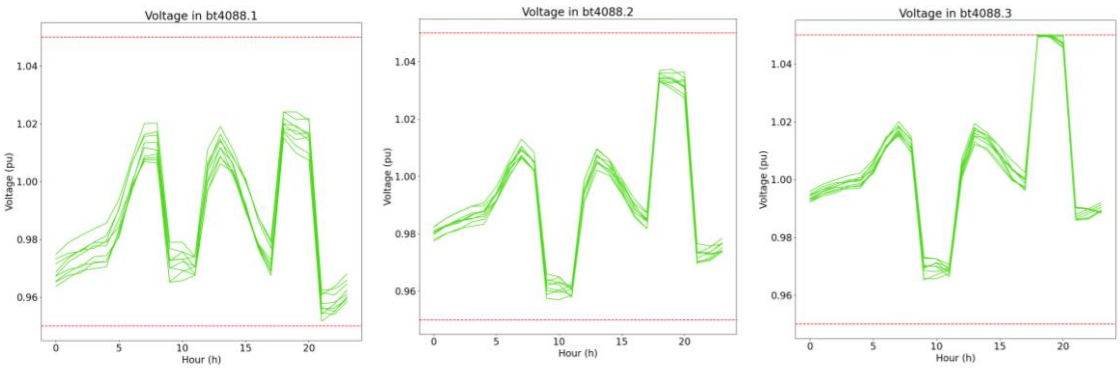

Figure 56 - Voltage at bus bt4088, for three phases in step 3

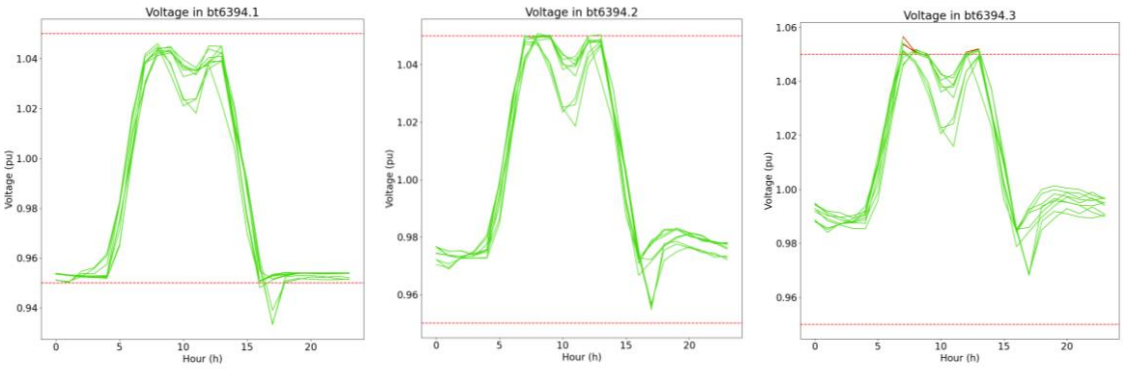

Figure 57 - Voltage at bus bt6394, for three phases in step 3

If the voltage is under 0.92 or above 1.05 (with a slack of 0.005), it is counted as a violation. Table 10 presents count for the number of violations for each bus and in each scenario. It is noticeable that for bus bt3876, the number of violations decreases, because on this bus, only one BESS is placed, while for buses bt3399 and bt6394 there is placed a PV system, which makes it more difficult to control voltage. On the other buses, the number of violations is zero (or very small). Furthermore, the total of violations decreases when the optimization model is applied.

It also can be noted that with the inverter operation, the violations decrease significantly, having a total of 4 violations, which is associated with the approximation made by linear regression.

Table 10 - Number of voltage violations for each bus with a DER and total violations in each scenario

Bus	Step 1	Step 2	Step 3
bt3136	0	0	0
bt3399	14	17	0
bt4088	0	0	0
bt3876	232	2	0
bt6394	126	249	4
Total	372	319	4

When analyzing the substation power flow (Figure 58), both with and without VPP operation, it is observed that the VPP operation leads to a reduction in the maximum demand at the substation. Before the implementation of VPP business model, the maximum demand was 4.69 MW, while after VPP operation, this value decreased to 4.49 MW, representing a reduction of 0.199 MW, which corresponds to a reduction of 4% of the total demand.

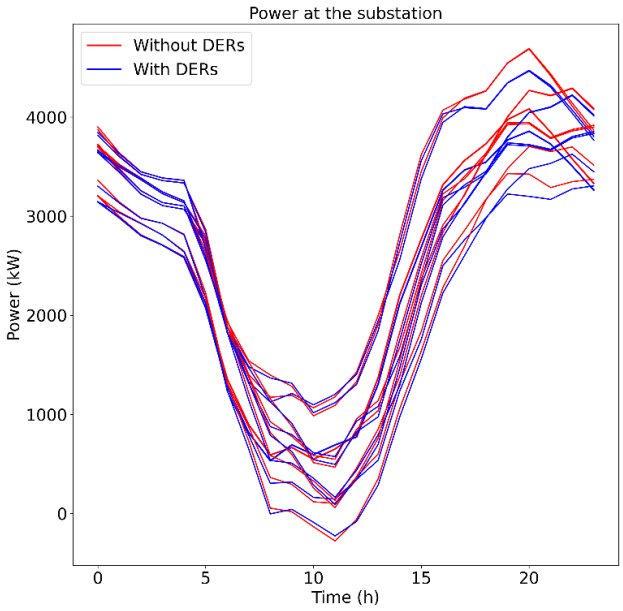

Figure 58 - Power demand at substation with and without VPP operation

This circuit has high penetration of photovoltaic system, which leads to power flow inversion in transformers, and this power inversion leads to an overload in them. According to Energisa, the replacement of transformers is made when their loads reach 80% of its capacity. Then, the result of step 1 and step for transformers loading is presented in Figures 59, 60, 61, 62 and 63, for circuit containing all buses with DER.

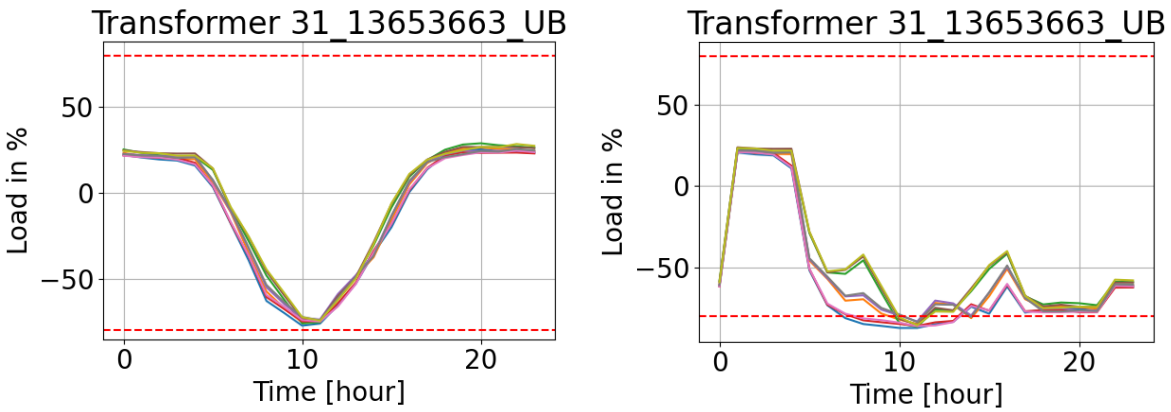

Figure 59 – Transformer loading for circuit containing bus bt3136 in step 1 (left) and step 2 (right)

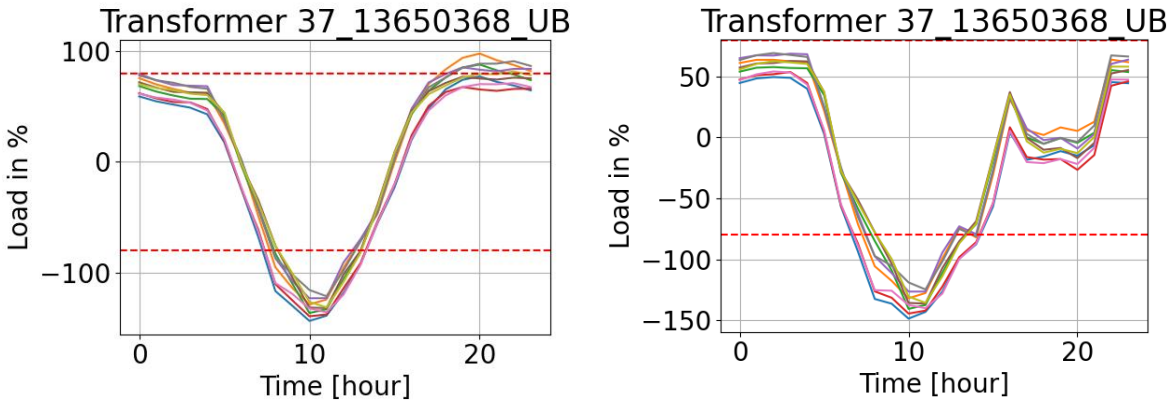

Figure 60 – Transformer loading for circuit containing bus bt3399 in step 1 (left) and step 2 (right)

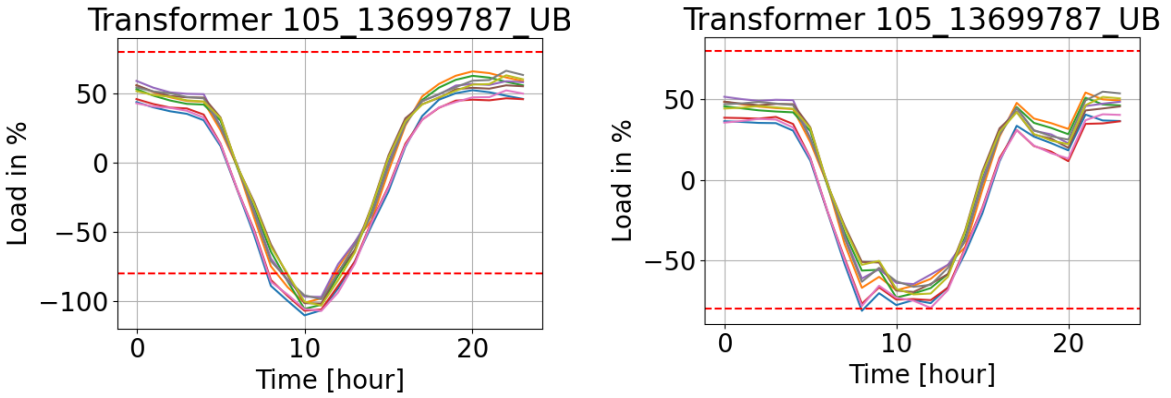

Figure 61– Transformer loading for circuit containing bus bt3876 in step 1 (left) and step 2 (right)

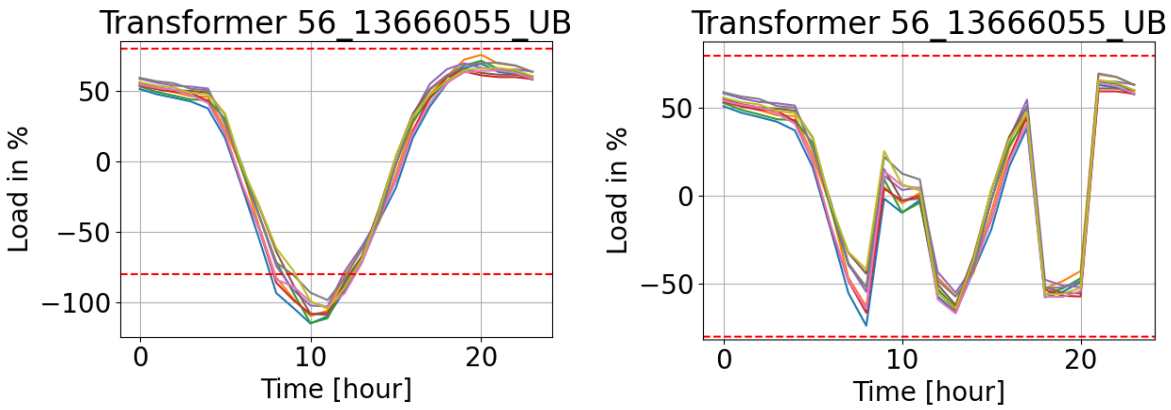

Figure 62 – Transformer loading for circuit containing bus bt4088 in step 1 (left) and step 2 (right)

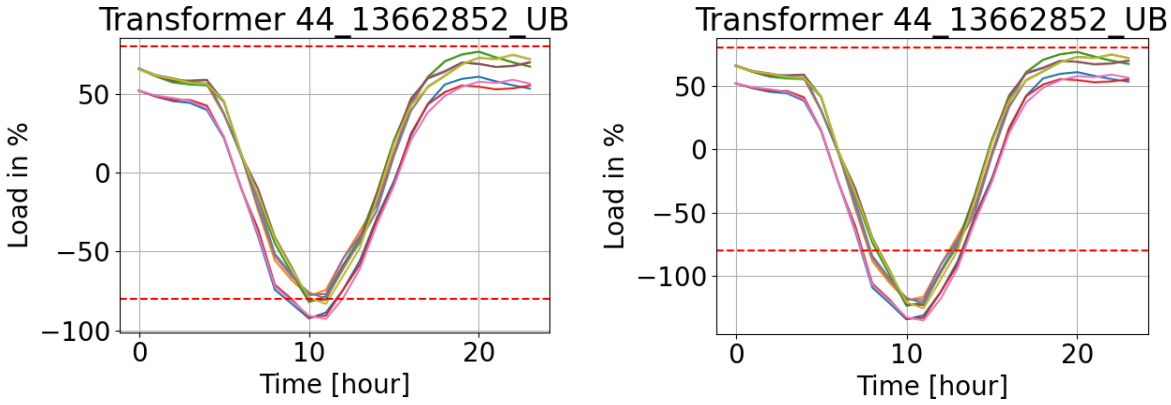

Figure 63 – Transformer loading for circuit containing bus bt6394 in step 1 (left) and step 2 (right)

It is observed that all transformers are overloaded in step 1, except for transformer which contain the bus bt3136. In step 2, it is observed that BESS can control the overload within limits proposed by ENERGISA, except in two transformers: bt3399 and bt6394. For circuit with bus bt3399, the BESS cannot control the overload due to higher penetration of the PV, indicating the necessity to replace the transformer. For circuit with bus bt6394, there is no BESS, then the overload cannot be controlled.

4.5. Ancillary Services Evaluation

To enable a more comprehensive assessment of the proposed model, seven distinct simulations were conducted, referred to as cases. These cases explore the range of ancillary services that can be provided by DERs, as well as their respective valuations.

In the first simulated case (Case 1), only the commercial part was considered in objective function, serving as a baseline for comparison. For didactic purposes, the power injection at this case is not limited to 75kW, which is the injection limit for distributing micro generation in Brazil. In the second case (Case 2), the commercial part was considered, and a voltage constraint was added to limit violation at the buses where DERs are installed. Case 3 modified the objective function to maximize the commercial value while minimizing electrical losses costs. In Case 4, in addition to commercial components, the objective function included the minimization of the maximum power demand cost at the substation. Case 5 combined the commercial analysis with the cost minimization related to transformer lifespan cost at locations in the circuit where DERs are connected. Case 6 integrated the commercial component with minimizing the cost of transformer replacement was considered. Lastly, in Case 7, all ancillary services and commercial aspect were simultaneously considered, fully leveraging the proposed optimization model. This structure allows for both an individual evaluation of each service's impact and an analysis of their combined effects.

To complete the evaluation of studied cases, each DER installed in the low voltage is associated with a distribution transformer, which is analyzed in terms of both lifespan and the need for replacement. Table 11 indicates the DERs along with their respective associated distribution transformers.

Table 11 - Association of DERs with Distribution Transformers

DER	DER Power (kW)	DER Bus	Transformer Bus	Transformer Power (kVA)
HIB	75/150	bt3136	bt1281	45
HIB	75/150	bt3399	bt1287	75
BESS	75	bt4088	bt1306	45
BESS	75	bt3876	bt1355	150
PV	75	bt6394	bt1294	150
PV	75	PV1	PV1	45
PV	75	PV2	PV2	45
PV	75	PV3	PV3	45

Table 12 and Table 13 present the simulation results. In the context of this thesis, a net gain was observed when ancillary services were considered, in comparison with the baseline case (Case 1), where only the commercial component was included in the objective function. According to Table 13, the percentage of gain is higher when all ancillary services are included, except for case 6, where the gain is bigger than case 7, due to voltage control, which decreases the gain in counterpart for improving voltage levels.

Table 12 - Commercial Results and the ancillary services associated for each case

Strategy	Cases	Revenue (R$)	Voltage Violation	Ancillary Services Costs (R$)			
				Losses	Substation Demand	Lifespan Transformer	Replacement Transformer
Commercial (Com.)	Case one	R$ 31,592.58	Yes	R$ 16,854.17	R$ 167,825.73	R$ 3,524.28	R$ 209,022.47
Com. + V	Case two	R$ 26,436.30	Yes	R$ 15,382.97	R$ 169,010.84	R$ 503.09	R$ 191,962.89
Com. + L	Case three	R$ 28,327.51	Yes	R$ 15,748.45	R$ 167,573.65	R$ 352.67	R$ 191,962.89
Com. + P_SE	Case four	R$ 28,327.51	Yes	R$ 15,934.75	R$ 167,573.65	R$ 1,286.27	R$ 202,878.28
Com. + LS Transformer	Case five	R$ 28,327.51	Yes	R$ 15,711.50	R$ 167,573.65	R$ 348.09	R$ 119,465.11
Com + Replac. Transformer	Case six	R$ 26,937.45	Yes	R$ 15,630.52	R$ 168,630.42	R$ 205.87	R$ 89,540.40
Com. + Tecn. Constraints	Case seven	R$ 25,083.25	Yes	R$ 15,276.99	R$ 170,040.10	R$ 204.83	R$ 89,540.40

Table 13 - Associated Gain for each case

Case	Balance(R$)	Gain (R$)	Gain (%)
Case 1	-R$ 365,634.07	-	-
Case 2	-R$ 350,423.49	R$ 15,210.58	4.16%
Case 3	-R$ 347,310.15	R$ 18,323.92	5.01%
Case 4	-R$ 359,345.43	R$ 6,288.64	1.72%
Case 5	-R$ 274,770.84	R$ 90,863.24	24.85%
Case 6	-R$ 247,069.76	R$ 118,564.31	32.43%
Case 7	-R$ 249,979.07	R$ 115,655.00	31.63%

Table 14 details the voltage violations corresponding to each case, for all buses with BESS. It is shown that count of voltage violations decreases for cases 2 and 7, which have voltage control activated, in comparison with case 1.

When only commercial performance is optimized (as in case 1), it can be observed that the VPP operation, while maximizing revenue, leads to overload in all five transformers associated with the circuits where DERs are installed (Figures 64, 65, and 66) . These overloads contribute to the reduction of transformer lifespan and generate the need for replacement, resulting in higher operational costs.

Case 2 enables control over the number of voltage violations at buses with BESS (including buses with hybrid DERs). Buses bt3399 and bt3876 presented 0.3% and 0.4% of voltage violations, respectively. These occurrences can be attributed to the linear approximation. According to (Brazilian Chamber of Deputies, 2022), voltage violations within the precarious range are tolerated up to 3%, and up to 0.5% within the critical range, without incurring penalties. Other buses with BESS presented no voltage violations. The VPP operation, designed to perform this voltage control, also contributed to a reduction of electrical losses and mitigated transformer overloading. Although the revenue decreased compared to Case 1, benefits were observed due to the reduction in transformers' replacement needs. Overall, this case presented a total gain of 4% when compared to Case 1.

Table 14 - Voltage violations for each case

Case	bt3136	bt3399	bt4088	bt3876	Total
1	0	132	106	334	572
2	0	22	0	2	24
3	0	123	77	251	451
4	1	146	106	360	613
5	0	114	41	159	314
6	0	129	22	183	334
7	0	17	0	2	19

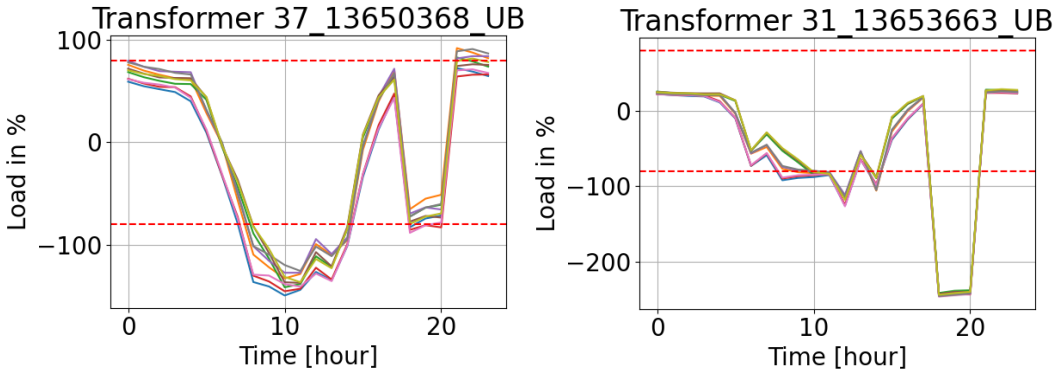

Figure 64 - Power transformer for Case 1: buses bt1287 and bt1281

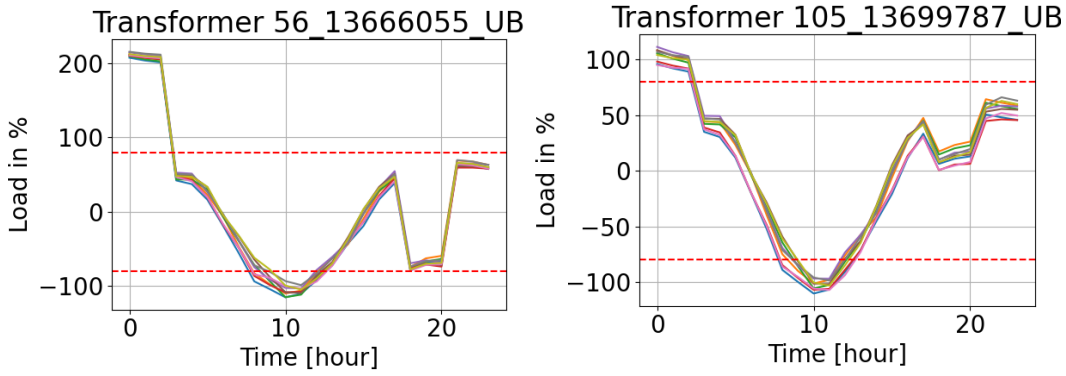

Figure 65 - Power transformer for Case 1: buses bt1306 and bt1355

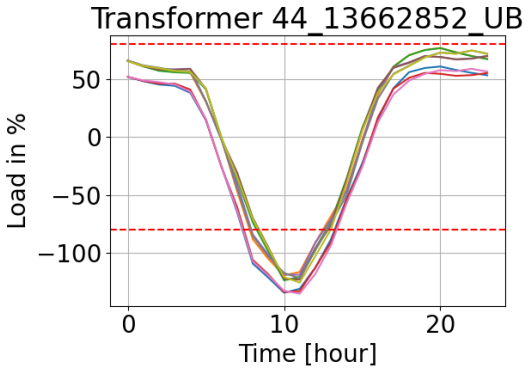

Figure 66 - Power transformer for Case 1: bus bt1294

Case 3, the objective function was defined to minimize electrical losses while maximizing the commercial revenue of the optimization model. Although the reduction loss-related costs were relatively small, the VPP operation reduced the transformer overload, avoiding the need to replace them with higher capacity units. This resulted in a 5% gain compared to Case 1.

Case 4, a 0.15% reduction was observed in the cost associated with the maximum power at substation. Due to VPP operation, a lower load on transformers was achieved, resulting in reduced costs related to their lifespan and replacement. The total gain compared to case one was 1%.

Case 5, by minimizing the impact on transformer lifespan, the VPP operation avoided replacing the transformer at bus “bt1287”, leading to a 25% gain over the baseline.

Case 6, minimizing transformer replacements resulted in a 43% gain compared to the base case. Through the VPP operation, it was possible to avoid transformers substitution at buses “bt1294”, “bt1287” and “bt1306”, in addition to reducing loss-related costs.

Case 7 presented the best overall result. The gain compared to the baseline was 47%, while keeping the voltage within allowed limits. Although economic revenue was lower compared to the case base, the ancillary services, especially avoiding transformer replacements, compensated for commercial loss. As demonstrated, the VPP operation allows for loss cost reductions, voltage control, extension of transformer lifespan, and prevention of transformer overload, avoiding the need to replace them.

Case 7, there is effective control over transformer loading in bt1281, bt1306 and bt1355 (Figures 67, and 68), avoiding the need for replacement with higher-capacity and, consequently, extending their expected useful life. However, transformers at buses bt1287 and bt1294 present overloading, due to hybrid or PV system, needing the replacement of them (Figures 67 and 69).

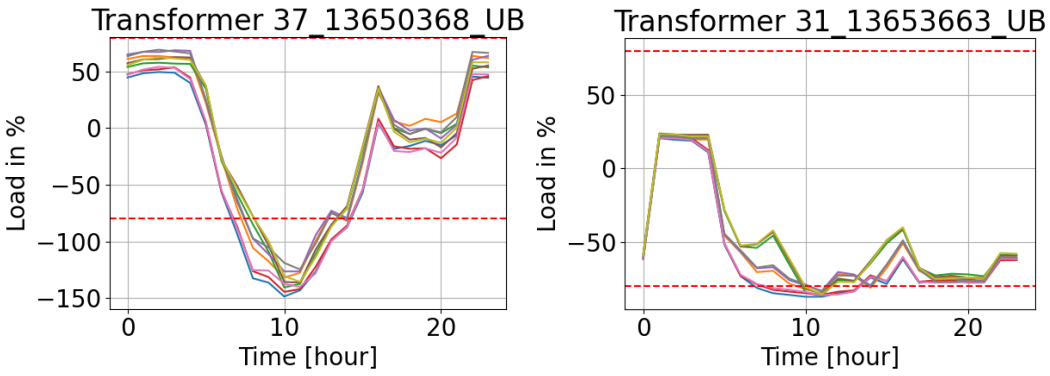

Figure 67 – Power flow transformer for Case 7: buses bt1287 and bt1281

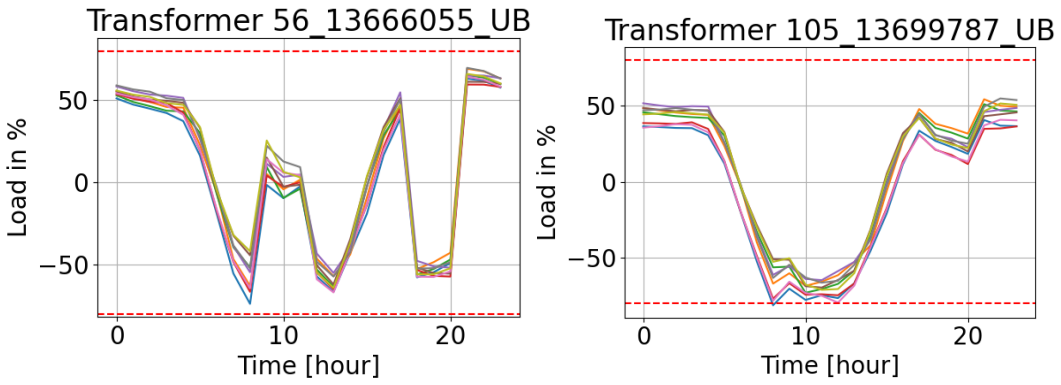

Figure 68 - Power flow transformer for Case 7: buses bt1306 and bt1355

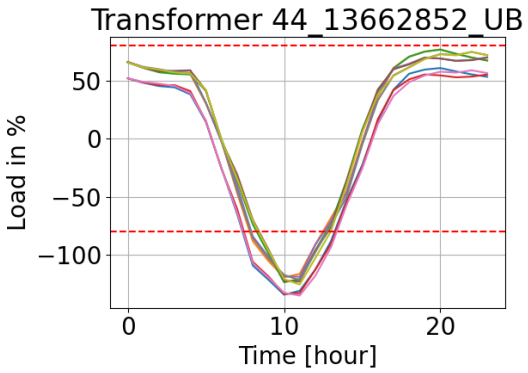

Figure 69 – Power flow transformer for Case 7: bus bt1294

These results highlight the role of ancillary services with the VPP commercial operation, particularly in mitigations of voltage violations and balancing costs related to losses, peak demand reduction, transformer lifespan and replacement needs.

5
Conclusions and Future Works

5.1.
Conclusions

The introduction of VPP systems into the energy credit transaction market, particularly when considerate ancillary services, appears to be a promising solution following the enactment of law 14,300/22 in Brazil.

The energy credit transaction model involves photovoltaic generation during off-peak periods and BESS discharge during peak periods. Thus, the optimization model extracts value from highest tariff periods to maximize energy credit generation. When it is not possible to inject energy into the grid during peak hours, it is due to the necessity of providing ancillary services, such as voltage control and transformers power flow control.

It is important to note that, regarding ancillary services, there was no significant reduction in electrical losses, due to high power injection (75 kW) from DERs at low voltage systems, aiming to minimize their impact on grid. On the other hand, the coordination of the DERs enabled a reduction in the maximum energy demand at the substation, thus lowering the cost associated with the distributor's DUT.

The VPP operation also targeted voltage control at the buses where DERs were installed. Voltage control was more effective at buses equipped with BESS without considering the inverter operation. Voltage control was targeted only in one bus (with DER), although, it is expected that this will control in neighborhood buses. On buses with hybrid systems (PV and BESS), voltage control proved more challenging due to the influence PV generation. In buses with only PV system, there was no voltage control related to active power injection, unless the inverter operation

Another point evaluated was the impact of DERs impact on transformers, both regarding to lifespan extension and avoidance of replacement due to overloading. In circuits with BESS installed, overloading was successfully managed, contributing to increased transformer lifespan. In circuits with hybrid systems, overload control was most difficult due to PV insertion, depending on the circuit's operating. In circuits with only PV systems, it was not possible to control transformer overloading or extend their lifespan.

Furthermore, the assignment of contracts for BESS operation during off-peak and mid-peak periods can be considered an ancillary service, as it deviates from purely commercial optimization. A promising opportunity of ancillary service is the injection of reactive power via inverters for voltage control if it does not compromise the active power injected by DERs, a result also observed in this thesis.

From a technical perspective the proposed model was able to achieve improvements in voltage levels, reduction of peak demand, lifespan transformers and reduce the need of transformers replacement.

The methodology and results presented aim to offer technical elements and economics to auxiliary in the criterion formulation of contracts and remuneration for distribution companies and aggregators, providing a technical basis which supports the evolution in the electrical sector towards a greater integration of DERs as active agents in electrical systems, and also enables a regulatory proposal for contracting ancillary services provided by DERs for distribution companies.

5.2. Future Works

From the implemented methodology and obtained results through the model, the main actions envisaged for the continuation of the study are presented in this section.

The dataset presented in this work is from BDGD ETO-2023, which can differ from real scenarios in that location. Therefore, to implement the proposed methodology in grid with real measurement in several points, such as transformers, loads and DERs, so that the simulated results are close to reality as possible. Measurements must be made for active power and voltage, which is important to apply associated benefits to voltage control, since simulations cannot accurately

reflect the actual operation. It is also important to note the randomness and uncertainties from the load and the PV generation, which can generate different operation for each scenario.

This work presented a method to voltage control through limitation of BESS charging or discharging, as a constraint in a MINLP, or using the DER inverter. However, some suggestions for future works related to voltage control are the implementation of the cost of overvoltage/undervoltage in the objective function, with the aim of minimizing this cost, to avoid voltages outside the regulatory limits for remuneration of this service in the proposed model, and the implementation of voltage control through reactive power in an optimization model.

A single BESS operation design was built through MINLP for ETO-2023, encompassing three months, which has three distinct days for each month (Weekday, Saturday, and Sunday). However, for future works, specify battery operation on three specific bases: for weekdays, Saturdays and Sundays. If the dataset is larger, to the point that it becomes difficult for the model convergence, carry out battery operation based on a load clustering process, respecting the seasonality of the different periods of the year. Also test on different electrical networks.

Various aspects presented in this work, such as losses and transformer lifespan, were linearized. Then, using polynomial regression to approximate more accurately the real losses and transformers lifespan at the system, this would lead to better results for costs allocation or ancillary services.

The DER localization in the system was previously defined by ENERGISA, then, as a future work, to compute the optimal location for DERs, considering economical and technical aspects.

It is also possible to evaluate the application of the model considering strong penetration of photovoltaic systems and distributed energy resources and evaluate hosting capacity on the system with and without VPP operation.

The methodology can be used as an operation planning to validate an economic viability (as shown in Appendix E) of a VPP project.

Other suggestions for future works related to this thesis are minimize the power flow in the most loaded line through the optimization model, evaluate impacts of DER installed in low-voltage circuits at medium voltage and use a Second Order Cone Programming to evaluate a VPP operation.

6
Bibliography

Affonso, C. d., & Kezunovic, M. (2019, July). Technical and Economic Impact of PV-BESS Charging Station on Transformer Life: A Case Study. (IEEE, Ed.) *IEEE Transactions on Smart Grid, vol. 10, no. 4*, pp. 4683-4692. doi:10.1109/TSG.2018.2866938

Akhil, A. A., Boyes, J. D., Butler, P. C., & Doughty, a. D. (2010). Batteries for Electrical Energy Storage Applications. In T. Reddy, & D. Linden, *Linden's Handbook of Batteries* (Fourth ed., pp. 30.1 - 30.45). Mc Graw Hill.

Almeida, D., Pasupuleti, J., & Ekanayake, J. (2021). Comparison of Reactive Power Control Techniques for Solar PV. *Electronics, vol.10(13)*, p. 1569. doi:https://doi.org/10.3390/electronics10131569

Almeida, D., Pasupuleti, J., Ekanayake, J., & Karunarathne, E. (2020). Mitigation of overvoltage due to high penetration of solar photovoltaics using smart inverters volt / var control. *Indones. J. Electr. Eng. Comput. Sci, vol. 19, no. 3*, pp. 1259-1266.

Alpízar-Castillo, J., Linders, K., Slaifstein, D., Ramírez-Elizondo, L., & Bauer, P. (2024). Economic Opportunities of Power Curtailment and Peak Shaving on Residential PV-BESS Systems. *International Conference on the European Energy Market (EEM)*. doi:10.1109/EEM60825.2024.10608921

Alyami, S., Wang, Y., Wang, C., Zhao, J., & Zhao, B. (2014, November 6). Adaptive real power capping method for fair overvoltage regulation of distribution networks with high penetration of PV systems. (IEEE, Ed.) *IEEE Transcions on Smart Grid, vol. 5, no. 6*, pp. 2729-2738.

ANEEL. (2012). *Normative Resolution No. 482*. Retrieved November 30, 2023, from www.aneel.gov.br/cedoc/ren2012482.pdf

ANEEL. (2016). *Module 8 – Quality of Electrical Energy.* Brasília. Retrieved from https://antigo.aneel.gov.br/documents/656827/14866914/M%C3%B3dulo8_Revisao_8/9c78cfab-a7d7-4066-b6ba-cfbda3058d19

ANEEL. (2016). *Normative Resolution No. 687*. Retrieved November 30, 2023, from www.aneel.gov.br/cedoc/ren2015687.pdf

ANEEL. (2021). *Normative Resolution No. 1,000*. Retrieved from https://www2.aneel.gov.br/cedoc/ren20211000.html

Antoniadou-Plytaria, K. E., Kouveliotis-Lysikatos, I. N., Georgilakis, P. S., & Hatziargyriou, N. D. (2017, November). Distributed and Decentralized Voltage Control of Smart Distribution Networks: Models, Methods, and Future Research. *IEEE Transactions on Smart Grid, vol. 8, no. 6*, pp. 2999-3008.

Apostolopoulou, D., Bahramirad, S., & Khodaei, A. (2016, May-June). The Interface of Power: Moving Toward Distribution System Operators. *IEEE Power Energy Magazine, vol. 14, no. 3*, pp. 46-51.

Badesa, L., Matamala, C., & Strbac, Y. Z. (2023, January). Assigning Shadow Prices to Synthetic Inertia and Frequency Response Reserves From Renewable Energy Sources. *IEEE Transactions on Sustainable Energy, vol. 14, no.1*, pp. 12-26.

Brazilian Chamber of Deputies. (2022). *Legal Framework for Distributed Microgeneration and Minigeneration, Law No. 14,300/22*. Retrieved from https://in.gov.br/en/web/dou/-/lei-n-14.300-de-6-de-janeiro-de-2022-372467821

Burger, S. P., & Luke, M. (2017, October). Business models for distributed energy resources: A review and empirical analysis. *Energy Policy, vol. 109*, pp. 230-248. doi:https://doi.org/10.1016/j.enpol.2017.07.007

Chand, A. A., Prasad, A. K., Mamun, A. K., Islam, F., Manoj, N. K., & Rajput, P. e. (2020). Microgrid modeling and simulations. In S. Padmanaban, K. Nithiyananthan, S. P. Karthikeyan, & J. B. Holm-Nielsen, *Microgrid* (First ed., pp. 392-400). Boca Raton. doi:https://doi.org/10.1201/9780367815929

Chaudhary, P., & Rizwan, M. (2018). Voltage regulation mitigation techniques in distribution system with high pv penetration: A review. *Renewable and Sustainable*

Energy Reviews. vol. 82, pp. 3279-3287. doi:https://doi.org/10.1016/j.rser.2017.10.017

Chirapongsananurak, P., & Hoonchareon, N. (2017). Grid code for PV integration in distribution circuits considering overvoltage and voltage variation. *TENCON 2017 - 2017 IEEE Region 10 Conference, Penang, Malaysia*, pp. 1936-1941. doi:https://doi.org/10.1016/j.rser.2017.10.017

Chua, K. H., Lim, Y. S., & Morris, S. (2016, April 4). Energy storage system for peak shaving. *Internaional Journal of Energy Sector Management, vol. 10*, pp. 3-18. doi:doi.org/10.1108/IJESM-01-2015-0003

Energy Research Company - EPE. (2025). *1st QUARTERLY REVIEW OF THE 2025-2029 PLAN.*

Farivar, M., Zho, X., & Chen, L. (2015). Local voltage control in distribution systems: An incremental control algorithm. *IEEE international conference on smart grid communications (SmartGridComm), Miami, FL, USA*, pp. 732-737. doi:10.1109/SmartGridComm.2015.7436388

Gokmen, N., Hu, W., & Chen, Z. (2017, June). A simple PV inverter power factor control method based on solar irradiance variation. *IEEE Manchester PowerTech, Manchester, UK*, pp. 1-6. doi:doi: 10.1109/PTC.2017.7981227

Guerrero, J., Gebbran, D., Mhanna, S., Chapman, A. C., & Verbič, G. (2020, October). Towards a transactive energy system for integration of distributed energy resources: Home energy management, distributed optimal power flow, and peer-to-peer energy trading. *Renewable and Sustainable Energy Reviews, vol. 132*, p. 110000. doi:10.1016/j.rser.2020.110000

Hashemi, S., & Østergaard, J. (2018, May). Efficient Control of Energy Storage for Increasing the PV Hosting Capacity of LV Grids. *IEEE Transactions on Smart Grid, vol. 9, no. 3*, pp. 2295-2303. doi:10.1109/TSG.2016.2609892

Ishimaru, M.-A., Komami, S., & Tamach, H. (2014, September). Positive Effect of PV's Constant Leading Power-Factor Operation in Power System. *Journal of International Council on Electrical Engineering, vol 190(1)*, pp. 276-282. doi:10.1002/eej.22467

Islam, F., Prakash, K., Mamun, K., Lallu, A., & Mudliar, R. R. (2016, June). Design an optimum MPPT controller for solar energy system. *Indonesian Journal of Electrical Engineering Computer Science, vol. 2, no. 3*, pp. 545-553.

Kersting, W. H. (2001). Radial distribution test feeders. *IEEE Power Engineering Society Winter Meeting, Columbus, OH, USA, vol. 2*, pp. 908-912. doi:10.1109/PESW.2001.916993

Kumar, M., & Krishan, R. (2021). Non-Linear Auto-Regressive Modeling based Day-ahead BESS Dispatch Strategy for Distribution Transformer Overload Management. *International Conference on Electrical, Communication, and Computer Engineering (ICECCE), Kuala Lumpur, Malaysia*, pp. 1-4. doi:10.1109/ICECCE52056.2021

Lakshmi, S., & Ganguly, S. (2019). Multi-objective planning for the allocation of PV-BESS integrated open UPQC for peak load shaving of radial distribution networks. *Journal of Energy Storage, vol. 22*, pp. 208-218. doi:10.1016/j.est.2019.01.011

Liang, Z., Mieth, R., & Dvorkin, Y. (2023). Inertia Pricing in Stochastic Electricity Markets. *IEEE Transactions on Power Systems, vol. 38, no. 3*, pp. 2071-2084. doi:10.1109/TPWRS.2022.3189548

Lima, D. A., & Rodrigues, V. F. (2022). Stochastic approach for economic viability of photovoltaic systems with battery storage for big electricity consumers in the regulated market in Brazil. *Electric Power System Research, vol. 205*, p. 107744. doi:10.1016/j.epsr.2021.107744

Lima, D. A., Teixeira, R. S., Massari, A. F., Valente, K. M., Milhorance, A., & Teixeira, W. W. (2023, November 28). Toward a New Transactive Energy System with Distributed Energy Resources in Brazil: A Real Case Application. *2023 IEEE PES Innovative Smart Grid Technologies Latin America (ISGT-LA), San Juan, PR, USA*, pp. 235-239. doi:10.1109/ISGT-LA56058.2023.10328261

Majeed, I. B., & Nwulu, N. I. (2022). Impact of Reverse Power Flow on Distributed Transformers in a Solar-Photovoltaic-Integrated Low-Voltage Network. *Energies 2022, vol. 15 (23)*, p. 9238. doi:10.3390/en15239238

Mamede, A. C., Lima, R. N., Novais, I. F., Almeida, L. R., Tavares, E. S., Buiatti, V. M., . . . Teixeira, W. W. (2023, November). Analysis of Different BESS Dispatch Strategies to Improve Low-Voltage Distribution Grid Performance. *IEEE PES Innovative Smart Grid Technologies Latin America (ISGT-LA), San Juan, PR, USA*, pp. 500-504. doi:10.1109/ISGT-LA56058.2023.10328349

Mamede, J. F. (2013). *Manual of Electrical Equipment.* Rio de Janeiro: National Editorial Group.

Mamun, K. A., Islam, F., Haque, R., Chand, A. A., Prasad, K. A., Goundar, K. K., & e. a. (2022, February). Systematic Modeling and Analysis of On-Board Vehicle Integrated Novel Hybrid Renewable Energy System with Storage for Electric Vehicles. *Sustainability, vol.14(5)*, p. 2538.

Massari, A. F. (2023). *SENSITIVITY FACTORS FOR THE ETO-2023 SYSTEM*. Retrieved 11 2023, from https://doi.org/10.17771/PUCRio.ResearchData.65042

Matamala, C., Badesa, L., Moreno, R., & G. Strbac. (2024). Cost Allocation for Inertia and Frequency Response Ancillary Services. *IEEE Transaction on Energy Markets, Policy and Regulation, vol. 2, no. 3*, pp. 328-338. doi:10.1109/TEMPR.2024.3355291

Molzahn, D. K. (2017, November). A Survey of Distributed Optimization and Control Algorithms for Electric Power Systems. *IEEE Transactions on Smart Grid, vol. 8, no. 6*, pp. 2941–2962. doi:10.1109/TSG.2017.2720471

Naval, N., & Yusta, J. M. (2021, October). Virtual power plant models and electricity markets - A review. *Renewable and Sustainable Energy Reviews, vol. 149*, p. 111393. doi:10.1016/j.rser.2021.111393

Okubo, R., Yoshizawa, S., Hayashi, Y., Kawano, S., Matsuda, K., Itaya, N., & Takano, T. (2020). Decentralized BESS charging and discharging control method for avoiding pole transformer overcapacity. *IEEJ Transactions on Power and Energy, vo. 140 (8)*, pp. 638-649. doi:10.1541/ieejpes.140.638

Prakash, K., Ali, M., Siddique, M. N., Chand, A. A., Kumar, a. M., Dong, D., & Pota, H. R. (2022, September 16). A review of battery energy storage systems for ancillary services in distribution grids: Current status, challenges and future directions. *Frontiers Energy Resources, vol. 10*. doi:10.3389/fenrg.2022.971704

Qu, R., Tang, C., Ni, Y., Zhang, X., & Yan, G. (2024). User-side distributed optimal control method for virtual power plant with demand response. *8th International Conference on Electrical, Mechanical and Computer Engineering, Xi'an, China,*, pp. 757-760. doi:10.1109/ICEMCE64157.2024.10862829

Rahimi, K., Tbaileh, A., Broadwater, R., Woyak, J., & Dilek, M. (2017, September 17-19). Voltage regulation performance of smart inverters: Power factor versus volt-VAR control. *North American Power Symposium (NAPS), Morgantown, WV, USA*, pp. 1-6. doi:10.1109/NAPS.2017.8107407

Renani, Y. K., Ehsan, M., & Shahidehpour, M. (2018, November). Optimal Transactive Market Operations With Distribution System Operators. *IEEE Transactions on Smart Grid, vol. 9, no. 6*, pp. 6692--6701. doi:10.1109/TSG.2017.2718546

Scott, P., Gordon, D., Franklin, E., Jones, L., & S. Thiebaux. (2019, November). Network-Aware Coordination of Residential Distributed Energy Resources. *IEEE Transactions on Smart Grid, vol. 10, no. 6*, pp. 6528-6537. doi:10.1109/TSG.2019.2907128

Smith, J. W., Sunderman, W., Dugan, R., & Seal, B. (2011, March 20-23). Smart inverter volt/var control functions for high penetration of PV on distribution systems. *2011 IEEE/PES Power Systems Conference and Exposition, Phoenix, AZ, USA,*, pp. 1-6. doi:10.1109/PSCE.2011.5772598

Wang, L., Bai, F., Yan, R., & Saha, T. K. (2018, May). Real-Time Coordinated Voltage Control of PV Inverters and Energy Storage for Weak Networks With High PV Penetration. *IEEE Transactions on Power Systems, vol. 33, no. 3*, pp. 3383-3395. doi:10.1109/TPWRS.2018.2789897

Zhang, L., Wang, Z., & Luo, W. G. (2024). Internal Aggregation Optimization Model of Virtual Power Plant Considering the Uncertainty of New Energy Output. *IEEE 8th Conference on Energy Internet and Energy System Integration (EI2), Shenyang, China*, pp. 3276-3766. doi:10.1109/EI264398.2024.10991434

Zhao, Z., Yi, Z., Xu, Y., Zhao, W., & Wang, T. M. (2024). Distributed Power Market Clearing Model based on ADMM for Virtual Power Plant composed of Energy

Storage. *3rd Asia Power and Electrical Technology Conference (APET), Fuzhou, China*, pp. 608-613. doi:10.1109/APET63768.2024.10882705

Appendix A

Relationship between X/R rate with voltage sensitivity

Figure 70 presents a simplified secondary model used to evaluate the impact of DER penetration.

The computation of voltage variation due to DER insertion:

$$\Delta V = V_1 - V_2 = I^* \cdot (R + jX) \tag{63}$$

Where:

$$I^* = \frac{(P_c - P_{DER}) + j(Q_c - Q_{DER})}{V_2} \tag{64}$$

Replacing (64) in equation (63):

$$\Delta V = \frac{(P_c - P_{DER}) + j(Q_c - Q_{DER})}{V_2} \cdot (R + jX) \tag{65}$$

$$\Delta V = \frac{(P_c - P_{DER})R + (Q_c - Q_{DER})X}{V_2} + j \cdot \frac{(P_c - P_{DER})X - (Q_c - Q_{DER})R}{V_2} \tag{66}$$

Considering the real and imaginary part:

$$\Delta V = V_d + j\Delta V_q \tag{67}$$

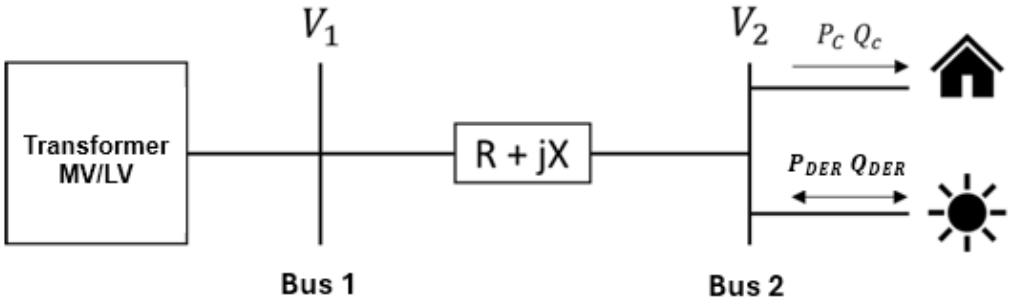

Figure 70 – Simplify secondary circuit

Source: (Almeida, Pasupuleti, & Ekanayake, 2021)

In distributions systems, it is common that the X/R rate is small, which means, $R \gg X$, so, $\Delta V_q \approx 0$, then:

$$\Delta V = \Delta V_d = \frac{(P_c - P_{DER})R + (Q_c - Q_{DER})X}{V_2} \quad (68)$$

Therefore, from equation (68), it is observed that:

- The relationship between active power with the voltage does not impact in relationship of reactive power with the voltage
- Voltage variation presents more impact from active power than for reactive power, when R is bigger than X, which means, if were injected 1 kW and 1 kVar, voltage variation will be bigger for active power injection

Table 15 exhibits relation X/R at distribution buses selected for DERs installation and the average coefficient of voltage sensitivity.

It is observed that "R" is bigger than "X" on buses: "bt3876" and "bt6394". On these buses, it is possible to notice that the active power injection influences more on the voltage variation than of reactive power ($|a_{inj,ext}| > |a_{neg,pos}^{kvar}|$).

Already the buses in which "X" is bigger than "R" are "bt3136", "bt4088". Then, it is noticed that on these buses, voltage variation is more sensible to reactive power than the active power ($|a_{inj,ext}| < |a_{neg,pos}^{kvar}|$).

For bus "bt3399", the rate X/R is approximately one, which means that voltage variation is almost the same for active and reactive power.

Table 15 - Rate X/R and voltage sensitivity for each bus with DER

DER	X/R	a_{ext}	a_{inj}	a_{neg}^{kvar}	a_{pos}^{kvar}
bt3136	2.9	-0.64	0.23	-1.64	0.86
bt3399	1.1	-1.43	0.75	-1.39	0.67
bt4088	2	-0.98	0.63	-1.64	1.01
bt3876	0.6	-1.77	1.19	-1.15	0.62
bt6394	0.8	-0.68	0.56	-0.6	0.45

Appendix B

Relationship Between Active Power and Voltage in buses with DER

Figures 71, 72, 73, 74, and 75 present voltage variation for each bus with DER, injecting or extracting 75 kW, in all possible hourly scenarios for all BDGD-2023 dataset. On this case, it is noticed that only the bus with DER, there are voltage variations. In other buses with DER, the variations are practically zero. Therefore injection/extraction of active power for each DER does not interfere in voltage of other bus with DER.

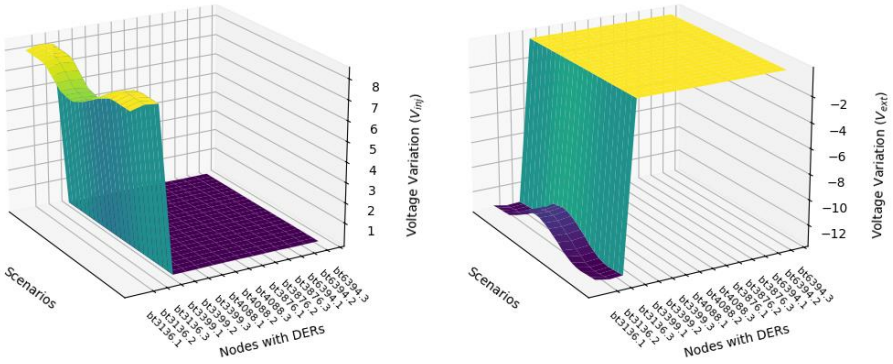

Figure 71 - Voltage variation in all buses with DERs, considering insertion only at bus bt3136

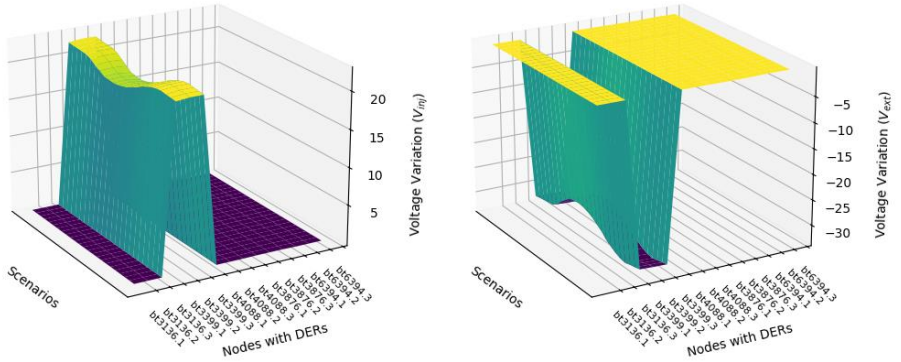

Figure 72 - Voltage variation in all buses with DERs, considering insertion only at bus bt3399

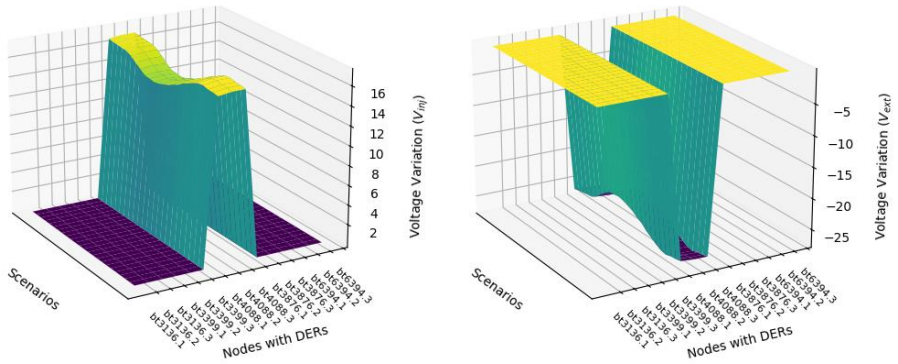

Figure 73 - Voltage variation in all buses with DERs, considering insertion only at bus bt3876

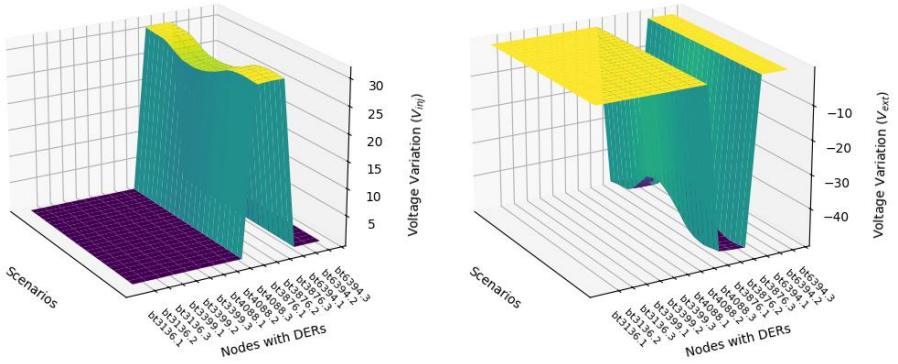

Figure 74 - Voltage variation in all buses with DERs, considering insertion only at bus bt4088

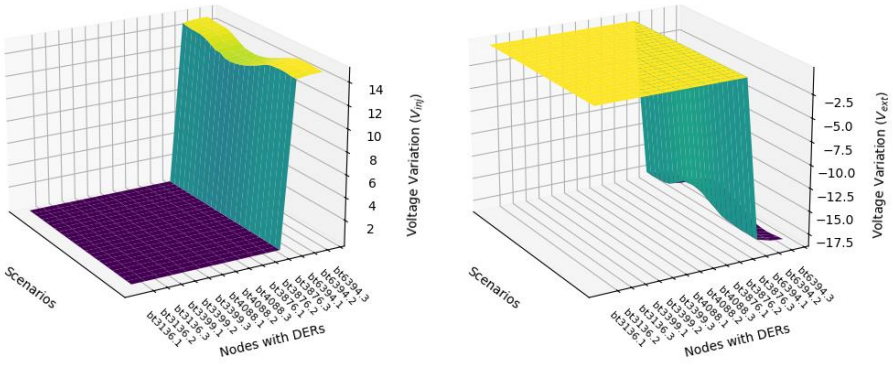

Figure 75 - Voltage variation in all buses with DERs, considering insertion only at bus bt6394

Appendix C
Inverter Data

Figure 76 shows the schematic connection of PV and BESS system.

The inverters used for connection of PVs and BESS with the grid were the Ingecon 100TL and Table 16 contains all need information about inverters.

Table 16 - Inverters data and information

Nominal Voltage	380 V
Maximum Power	75 kW
Maximum Temperature	50 °C
Maximum Current	145 A
Power Factor	1
Adjustable PF	Yes, 0 – 1 (capacitive/inductive)
Maximum efficiency	99,10%

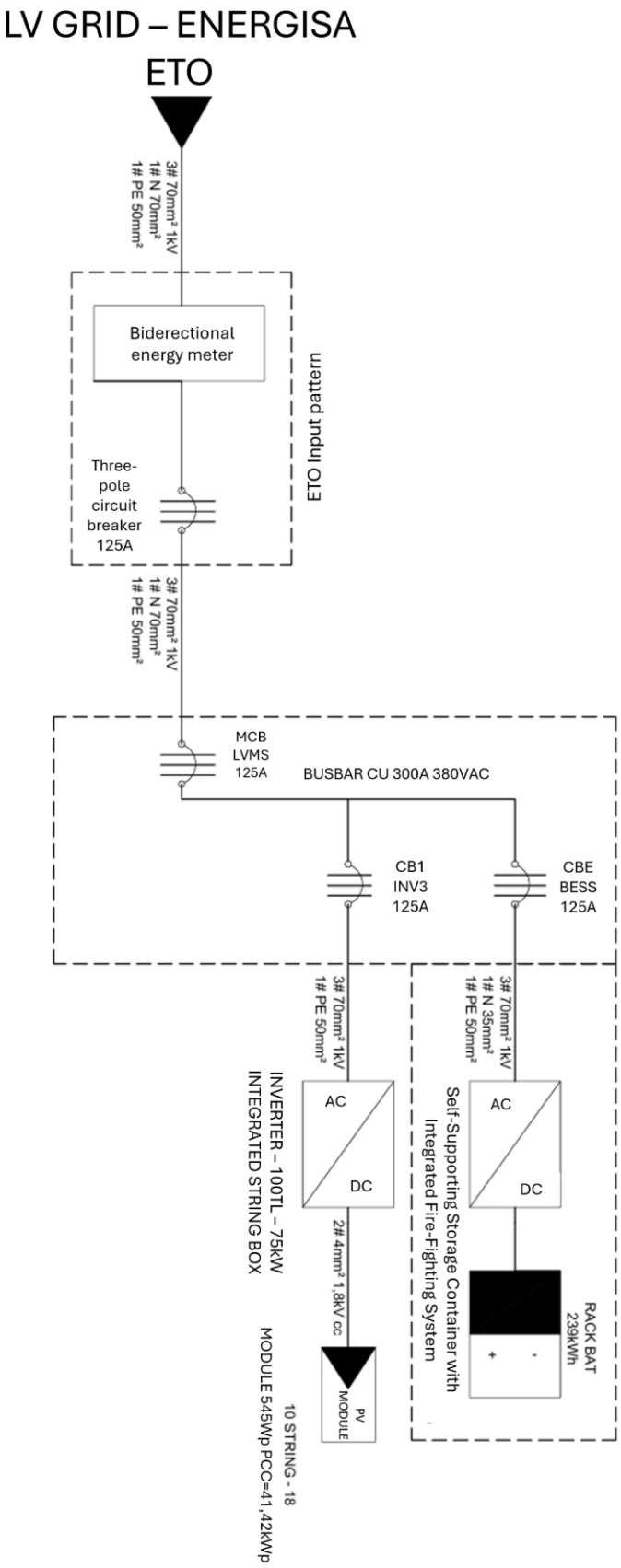

Figure 76 - Interconnection of photovoltaic generation and battery energy storage systems with the ETO distribution grid.

Appendix D
Voltage control for other points in low voltage system

The impact of DERs on voltage is not limited to the buses where they are installed but affects the entire surrounding area. This influence makes it possible to control the voltage at nearby buses that also have DERs, due to their proximity to the point of DER installation.

For this study, only the bus "bt3399" was considered, due to computational limitations. Three buses were selected to be controlled by the DER: "bt6301", "bt3447", and "bt4409". Bus "bt6301" is the closest to "bt3399", where the DER injection is connected, while "bt4409" is the farthest bus from DER.

Figure 77 and Figure 78 present voltage variation at buses located in the same regions as the DER installation, resulting from active power injection/extraction at bus "bt3399". Bus "bt6301" exhibits the largest voltage variation due to its proximity to DER. Bus "bt3447" presents the second-highest variation, while "bt4409" shows the smallest voltage variation caused by active power injection/extraction from the DER.

Based on these results, it is possible to relate the voltage variation with active power of the DER, through linear regression. After determining the regression parameters, three additional constraints were added to the optimization model, as described in (69), (70), and (71).

$$V_{cb,p,d,h} = V^{0}_{cb,p,d,h} + a^{+}_{cb,h} \cdot \frac{P^{+}_{b,d,h}}{N_f} - a^{-}_{cb,h} \cdot \frac{P^{-}_{b,d,h}}{N_f} \forall\, h \in H, b \in B,\ cb \in CB,\ d \in D \quad (69)$$

$$V_{cb,p,d,h} \geq V^{min}_{cb} - \gamma^{uv}_{cb,p,d,h} \forall\, h \in H,\ cb \in CB,\ d \in D \quad (70)$$

$$V_{cb,p,d,h} \leq V^{max}_{cb} + \gamma^{ov}_{cb,p,d,h} \forall\, h \in H,\ cb \in CB,\ d \in D \quad (71)$$

Constraint (69) simulates the voltage at controlled buses as a function of the net power at bus with DER. Constraints (70) and (71) represent the undervoltage and overvoltage limits, preventing the voltage from dropping below its lower limit

or exceeding its upper limit. Each constraint incorporates an auxiliary variable ($\gamma^{uv}_{cb,p,d,h}$ and $\gamma^{ov}_{cb,p,d,h}$), for undervoltage or overvoltage scenarios, respectively. These variables are subject to a penalty in the objective function.

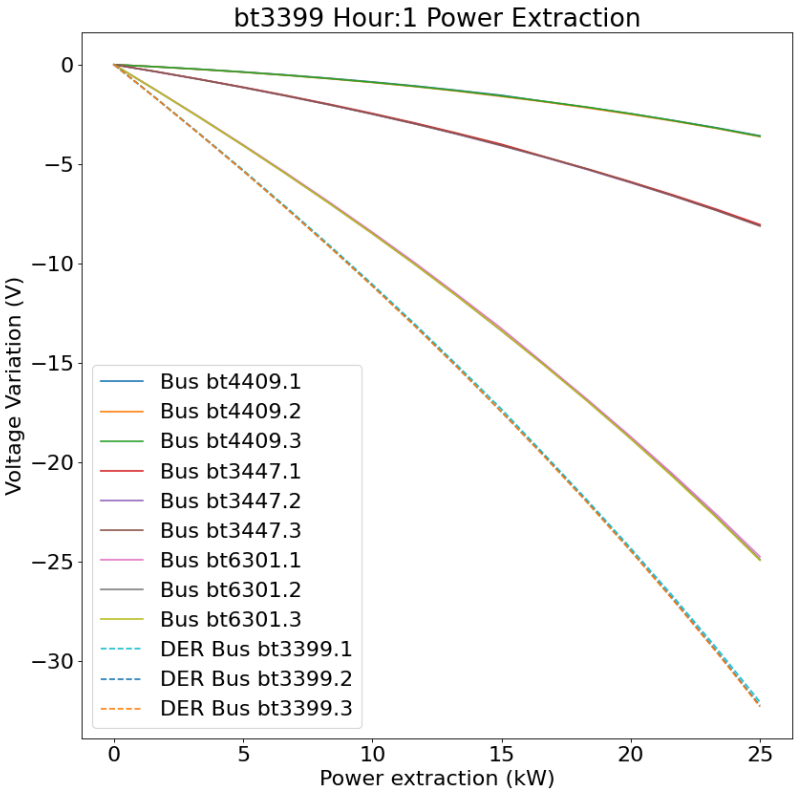

Figure 77 - Voltage variation for buses close to DER localization, with active power extraction

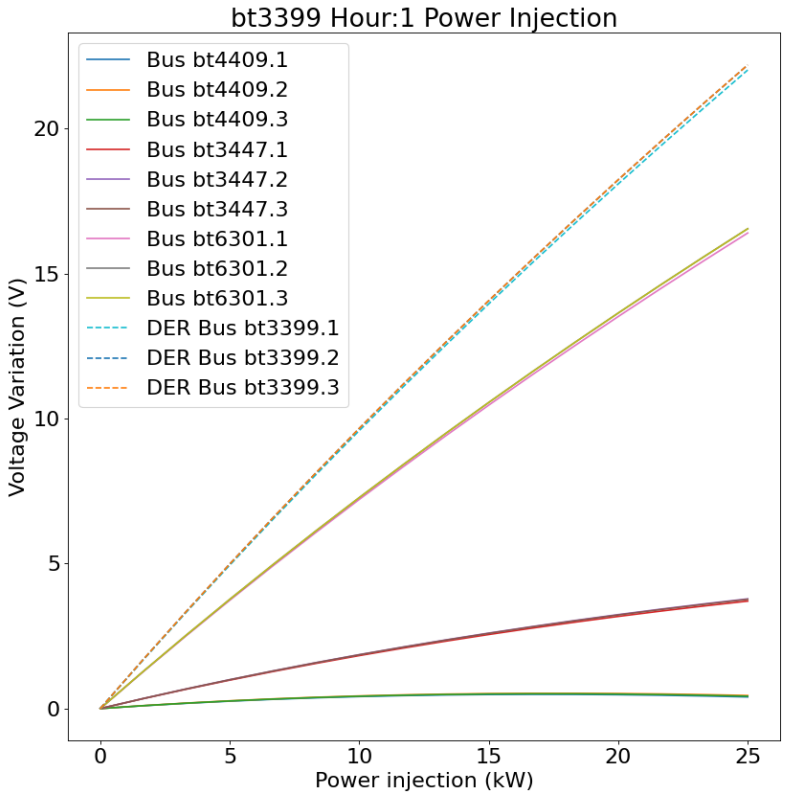

Figure 78 - Voltage variation for buses close to DER localization, with active power injection

Then, applying the optimization model with these new constraints, Figure 79 shows the result for BESS operation.

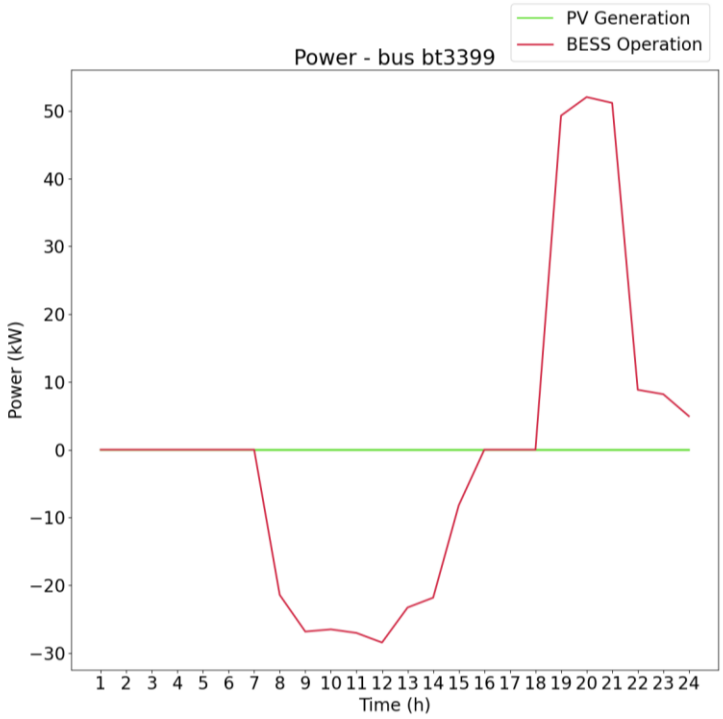

Figure 79 - BESS operation on bus bt6388, with voltage control for an entire region

Figures 80 to 82 present the voltage profile at the selected buses for voltage control before the BESS operation. It is noticed that there are no voltage violations on these buses, indicating that voltage control is not required in this case.

Figures 83 to 85 present the voltage profile at the same buses after the BESS operation. It is noticed that the operation alters the voltage profile at these locations.

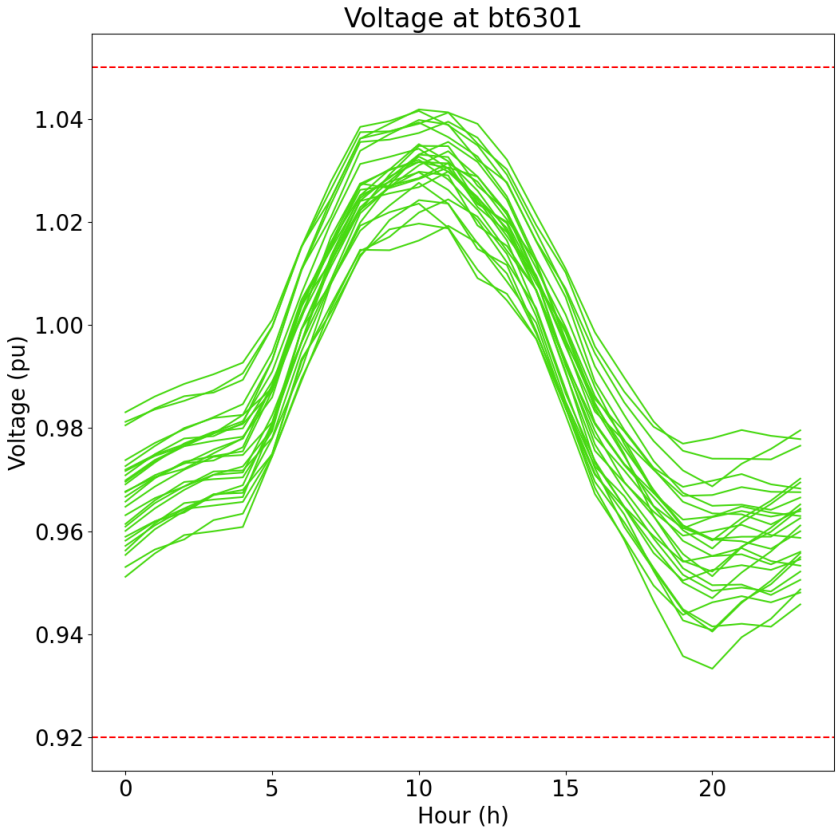

Figure 80 – Voltage at bus bt6301 before BESS operation (step 1)

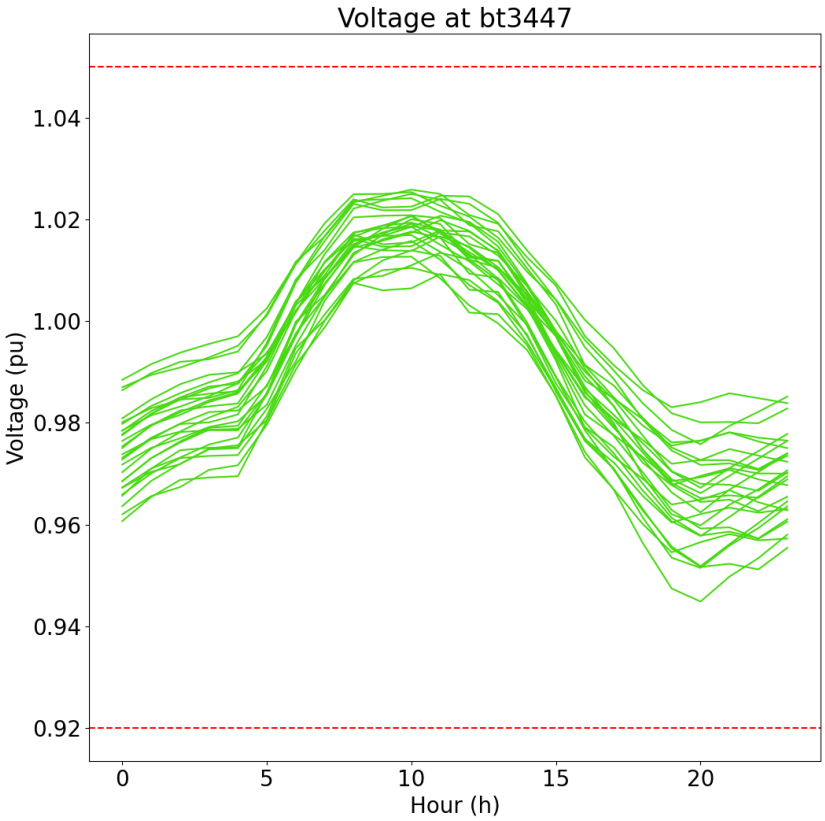

Figure 81 – Voltage at bus bt3447 before BESS operation (step 1)

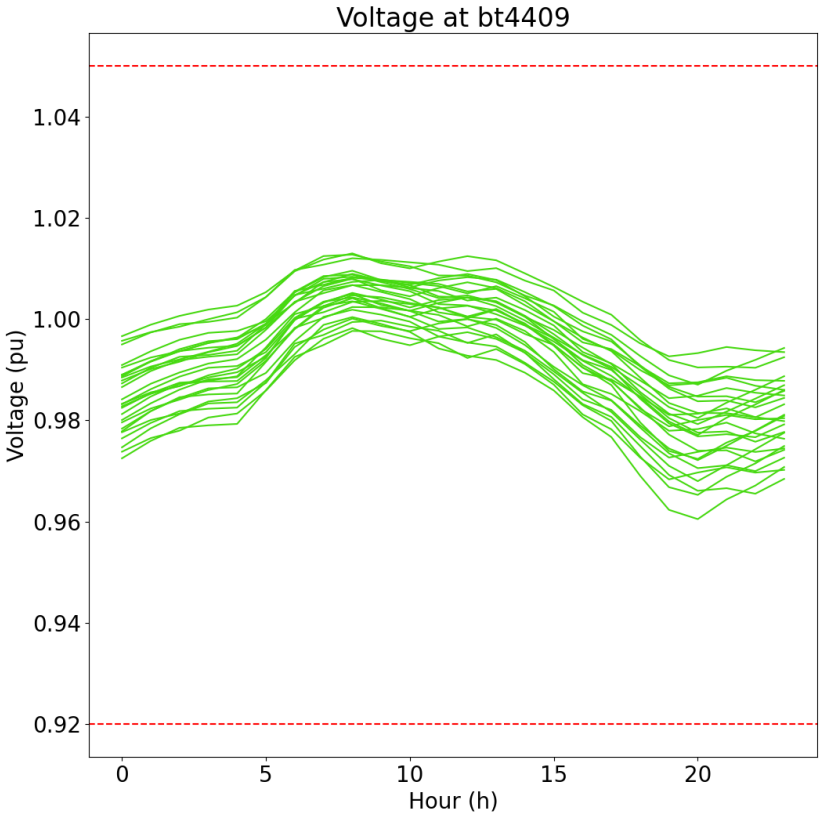

Figure 82 - Voltage at bus bt4409 before BESS operation (step 1)

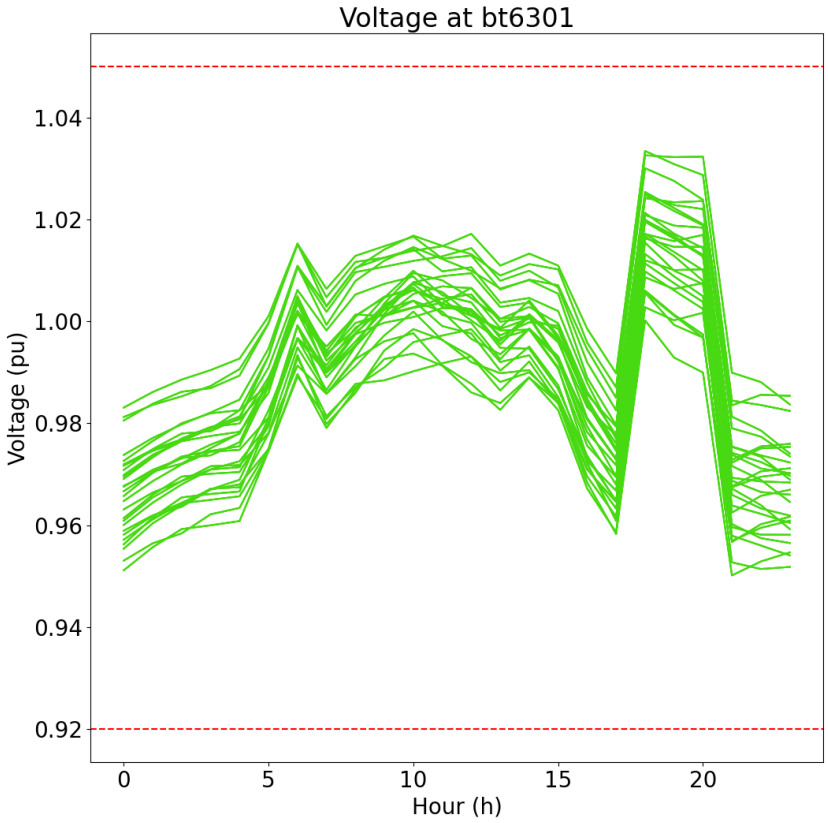

Figure 83 - Voltage on bus bt6301 after BESS operation (step 2)

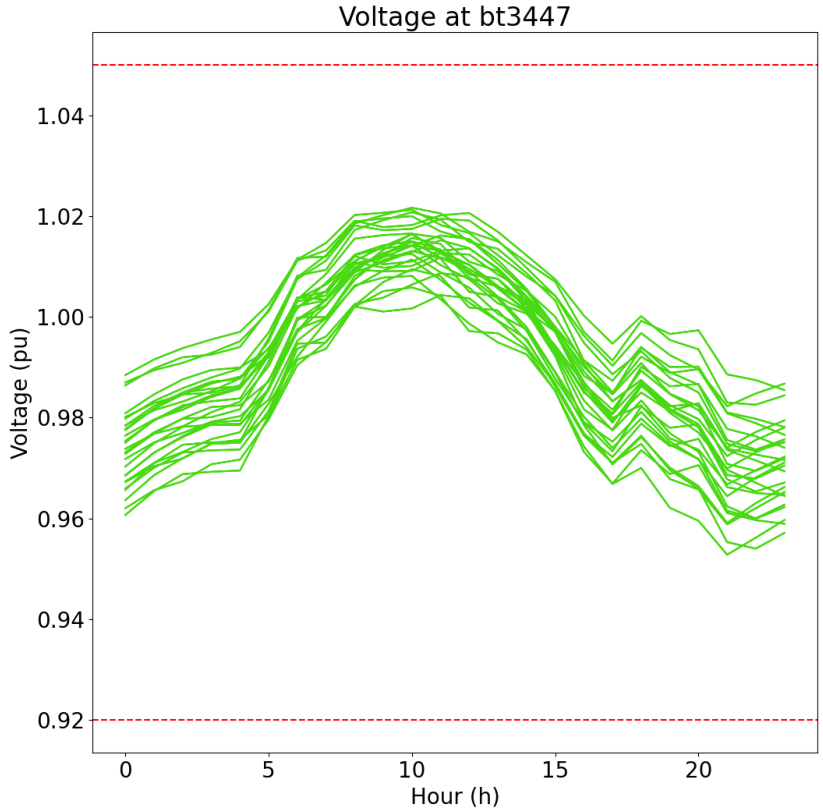

Figure 84 - Voltage on bus bt3447 after BESS operation (step 2)

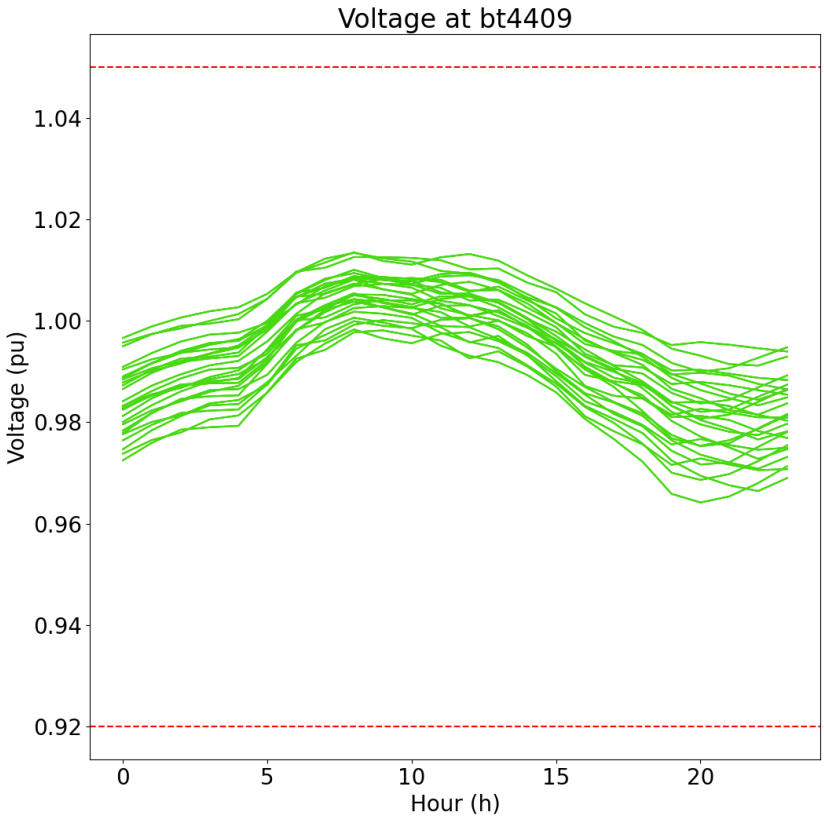

Figure 85 - Voltage on bus bt4409 after BESS operation (step 2)

Appendix E
Economic Viability

Net Present Value (NPV) is a metric used to evaluate the return on an investment. NPV is calculated by subtracting the initial investment from the sum of projected cash flows over the project's operational period, discounted to present value, as expressed in equation (72).

$$NPV = -I + \sum_{n=1}^{N} \frac{CF_n}{(1 + IRR)^n}, n = 1,2, \dots, N \quad (72)$$

Where:

- I is the initial investment
- CF_n is the Cash Flow in year n
- k is the discount rate
- N is the project lifetime (in years)

A positive NPV indicates that the project is economically viable, as the investments will generate more value than it costs. A negative NPV implies that the investment will not be recovered, making the project unfeasible. If NPV equals zero, the project breaks even, generating neither profit nor loss.

In the context of the proposed model, the cash flow in each year represented by the revenue generated by the VPP, as defined in equation (73). The initial investment is the total investment cost of the project.

$$CF_n = R_e^{p,n} + R_e^{op,n} + R_e^{int,n} + C_{LOSS}^n + C_{SE}^n + C_{Lifespan}^n + C_{replacement}^n \quad (73)$$

These annualized revenues and costs are computed according to equation (74).

$$R_n^a = \left(1 - \left(CM + FR\right)\right) \cdot \Delta P \cdot T_e \cdot (1 + EI)^{n+1} \quad (74)$$

Where:

- R^a the revenue or any cost associated with ancillary service
- CM is the customer margin
- FR is the frustration rate
- ΔP is the energy variation between case base and VPP operation (step 1)
- T_e is the tariff associated with the energy revenue or ancillary service
- EI is the electric inflation

$$NPV_{project} = -C_{INV} + \sum_{n=1}^{N} \frac{CF_n}{(1+k)^n}, n = 1,2,\dots,N \quad (75)$$

Where:

- $NPV_{project}$ is the NPV for this project
- C_{INV} is the initial investment on this project brought to present value

The Internal Rate of Return (IRR) is another financial indicator used to assess investment profitability. It is defined as the discount rate that results in a zero NPV.

Payback is an additional metric used to support investment decisions. It represents the number of periods (in months or year) required for the accumulated discounted cash flow to recover the initial investment. That is, it shows how long it takes for the project to start generating net positive returns.

The implementation of the VPP operations involves costs related to the acquisition of equipment. Table 17 presents the cost of each type of DER, including the inverters' costs.

Furthermore, Table 17 also presents the total investment cost for the VPP project, amounting to R$ 12,336,362.34.

Table 17 - Initial Investment

DER	Unit Cost	Quantity	Total Cost
PV	R$ 267,662.60	4	R$ 1,070,650.40
BESS	R$ 1,788,397.79	2	R$ 3,576,795.58
HIB	R$ 3,844,458.18	2	R$ 7,688,916.36
Total	R$		12,336,362.34

To ensure a return on investment over a 20-years, the following were considered as revenue streams: energy credits, and avoided costs associated with ancillary services, including:

- Cost of electrical losses
- Replacement transformer cost
- Lifespan transformer cost
- Cost associated with maximum demand at the substation

Due to dataset having only nine days of simulation (three days for each month, and three months), all the revenue and costs were annualized, following.

$$R_{annualized} = R_{dataset} \cdot \frac{365}{N_{dataset}} \tag{76}$$

Where:

- $R_{annualized}$ is the revenue or cost annualized
- $R_{dataset}$ is the revenue or cost from all days in dataset
- $N_{dataset}$ is the quantity of days in dataset

Table 18 presents the annualized revenue from energy credit and ancillary services.

Table 18 - Annualized revenue and associated costs for ancillary services

	Revenue (R$)	Losses Cost(R$)	Peak Demand SE (R$)	Lifespan Transformer (R$)	Replacement Transformer (R$)
Total	R$ 1,050,449	R$ 624,334	R$ 168,932	R$ 7,955	R$ 3,631,361

The Economic viability of this project was assessed using (NPV) and Internal Rate of Return (IRR) metrics, considering a 20-year operating period for the VPP. A discount rate of 6% was adopted, according to (Energy Research Company - EPE, 2023), and an electrical inflation rate of 16% were considered, based on (Brazilian Association of Energy Traders - ABREACEEL, 2023). Table 19 presents the input parameters used in economic feasibility analysis.

Figure 86 presents the NPV and IRR over the project lifespan. The NPV becomes positive only in the 11th year, which corresponds to the payback for this project.

Based on this data, the NPV of the project is R$64,362,280.33, indicating that the project is economically viable.

Table 19 – Input parameters

Customer Margin	10%
Frustration Rate	10%
Initial Degradation	2%
Annual Degradation	1%
Discount Rate	6%
Days	365
Years	20
Electric inflation	16%

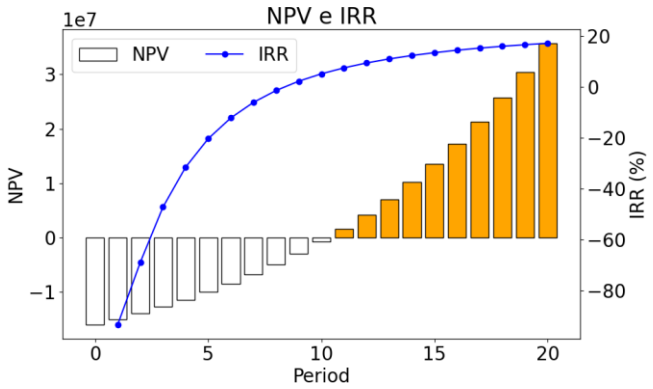

Figure 86 - NPV and IRR over this project